Oligoporphyrin Arrays Conjugated to [60]Fullerene: Preparation, NMR Analysis, and Photophysical and Electrochemical Properties

by **Davide Bonifazi**[a]), **Gianluca Accorsi**[c]), **Nicola Armaroli***[c]), **Fayi Song**[b]), **Amit Palkar**[b]), **Luis Echegoyen***[b]), **Markus Scholl**[a]), **Paul Seiler**[a]), **Bernhard Jaun**[a]), and **François Diederich***[a])

[a]) Laboratorium für Organische Chemie, ETH-Hönggerberg, CH-8093 Zürich (e-mail: diederich@org.chem.ethz.ch)

[b]) Department of Chemistry, Clemson University, 219 Hunter Laboratories, Clemson SC 29634, USA (e-mail: luis@clemson.edu)

[c]) Istituto per la Sintesi Organica e la Fotoreattività, Laboratorio di Fotochimica, Consiglio Nazionale delle Ricerche, I-40129 Bologna (e-mail: armaroli@isof.cnr.it)

Dedicated to Professor Dr. *Rolf Huisgen* on the occasion of his 85th birthday

We report the synthesis and physical properties of novel fullerene–oligoporphyrin dyads. In these systems, the C-spheres are singly linked to the terminal tetrapyrrolic macrocycles of rod-like *meso,meso*-linked or triply-linked oligoporphyrin arrays. Monofullerene–mono(Zn^{II} porphyrin) conjugate **3** was synthesized to establish a general protocol for the preparation of the target molecules (*Scheme 1*). The synthesis of the *meso,meso*-linked oligopophyrin–bisfullerene conjugates **4**–**6**, extending in size up to 4.1 nm (**6**), was accomplished by functionalization (iodination followed by *Suzuki* cross-coupling) of the two free *meso*-positions in oligomers **21**–**23** (*Schemes 2* and *3*). The attractive interactions between a fullerene and a Zn^{II} porphyrin chromophore in these dyads was quantified as $\Delta G = -3.3$ kcal mol^{-1} by variable-temperature (VT) ^{1}H-NMR spectroscopy (*Table 1*). As a result of this interaction, the C-spheres adopt a close tangential orientation relative to the plane of the adjacent porphyrin nucleus, as was unambiguously established by ^{1}H- and ^{13}C-NMR (*Figs. 9* and *10*), and UV/VIS spectroscopy (*Figs. 13–15*). The synthesis of triply-linked diporphyrin–bis[60]fullerene conjugate **8** was accomplished by *Bingel* cyclopropanation of bis-malonate **45** with two C_{60} molecules (*Scheme 5*). Contrary to the *meso,meso*-linked systems **4**–**6**, only a weak chromophoric interaction was observed for **8** by UV/VIS spectroscopy (*Fig. 16* and *Table 2*), and the ^{1}H-NMR spectra did not provide any evidence for distinct orientational preferences of the C-spheres. Comprehensive steady-state and time-resolved UV/VIS absorption and emission studies demonstrated that the photophysical properties of **8** differ completely from those of **4**–**6** and the many other known porphyrin–fullerene dyads: photoexcitation of the methano[60]fullerene moieties results in quantitative sensitization of the lowest singlet level of the porphyrin tape, which is low-lying and very short lived. The *meso,meso*-linked oligoporphyrins exhibit $^1O_2$ sensitization capability, whereas the triply-fused systems are unable to sensitize the formation of $^1O_2$ because of the low energy content of their lowest excited states (*Fig. 18*). Electrochemical investigations (*Table 3*, and *Figs. 19* and *20*) revealed that all oligoporphyrin arrays, with or without appended methano[60]fullerene moieties, have an exceptional multicharge storage capacity due to the large number of electrons that can be reversibly exchanged. Some of the Zn^{II} porphyrins prepared in this study form infinite, one-dimensional supramolecular networks in the solid state, in which the macrocycles interact with each other either through H-bonding or metal ion coordination (*Figs. 6* and *7*).

1. Introduction. – The assembly of molecular chromophoric entities into multi-component arrays may provide artificial systems capable of mimicking the basic characteristics of photosynthesis, such as stepwise, photoinduced energy- and electron-transfer processes. To generate such properties, it is essential to choose suitable chromophoric fragments exhibiting specific electrochemical and spectroscopic proper-

ties and assemble them in a well-defined spatial arrangement [1]. With its strong electron-accepting properties and remarkably small reorganization energy (*ca.* 0.23 eV [2]), C_{60} is one of the most popular chromophores that have been incorporated into multicomponent molecular architectures [3]. Following the first reports on a fullerene-containing donor–acceptor dyad [4] and a fullerene–porphyrin conjugate [5], a myriad of fullerene–porphyrin hybrids have been prepared and studied [6]. Our work on photoactive, fullerene-containing donor–acceptor dyads started with the preparation and photophysical investigation of Cu^{I}-complexed rotaxanes with fullerene stoppers [7]. This early work was followed by the use of porphyrin tethers to accomplish the regioselective *trans*-1 bisfunctionalization of C_{60} [8a].

Comprehensive investigations revealed that the photophysical and electrochemical properties of conjugate **1** (*Fig. 1*), with two [60]fullerene moieties attached by single linkers to the porphyrin macrocycle, were similar to those of **2** in which a single fullerene is doubly bridged in a cyclophane-type fashion [8b]. Upon photoexcitation of both dyads, the fullerene- and porphyrin-centered excited states are deactivated to a low-lying charge-transfer (CT) state emitting in the near-infrared (NIR). The spectroscopic observations suggested that a tight facing between fullerene and porphyrin moieties does not require double cyclophane-type bridging, but can also be established in singly-linked conjugates by taking advantage of attractive donor–acceptor interactions both in the ground and the excited state [8]. This was the starting point for the preparation and spectroscopic characterization of the novel monoporphyrin **3** and the linear oligoporphyrin arrays **4**–**8** with one or two appended [60]fullerene moieties (for preliminary communications on parts of this work, see [9][10]). Two types of porphyrin arrays were considered in this investigation: in one series, **4**–**7**, the tetrapyrrolic macrocycles are singly linked to each other (*meso*,*meso*-linked), whereas they are triply linked in conjugate **8**. Although a large body of elegant synthetic studies on the two types of oligoporphyrins has been published by *Osuka* and co-workers [11–14], only a limited number of physical studies has been undertaken to elucidate their electronic and photophysical characteristics [15–18]. In particular, their chemical derivatization with other redox- and/or photoactive molecular species and subsequent physical investigations remain largely unexplored [19].

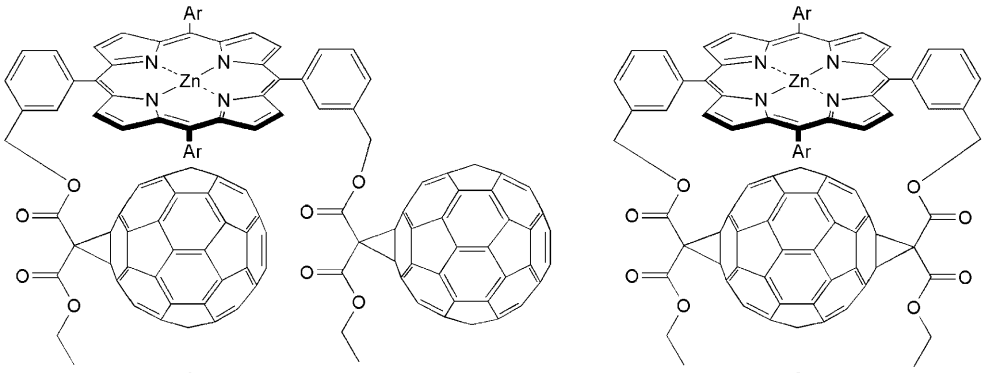

Fig. 1. *Original [60]fullerene–porphyrin conjugates* **1** *and* **2** *reported by* Diederich *and co-workers* [8]

Here, we show that these multicomponent arrays prefer distinct conformations as a result of strong intermolecular fullerene–porphyrin interactions that could be quantified by means of variable-temperature (VT) NMR measurements. The first full electrochemical studies on triply-linked porphyrin dimers revealed that such compounds are capable of undergoing as many as eight reversible electron-transfer processes. Covalent conjugation with two fullerene moieties increases the number of the electron-transfer processes to 15, which is unprecedented in non-dendritic structures. Moreover, a comprehensive photophysical study showed that, despite the exceptional electron-donating properties of triple-fused porphyrins, the low-lying and very short-lived (4.5 ps) [10][15] singlet level offers an extremely competitive deactivation pathway and thus acts as a sink for the higher-energy electronic states of the covalently linked [60]fullerene moieties.

2. Results and Discussion. – 2.1. *Preparation of the [60]Fullerene–Porphyrin Conjugates.* 2.1.1. *Synthesis of Fullerene–Porphyrin Dyad* **3**. A large number of protocols for the synthesis of 'asymmetrically' *meso*-substituted porphyrins has been reported [20]. Mixed macrocyclizations of pyrroles [21] or *meso*-substituted dipyrrylmethanes [22] with appropriate aromatic aldehydes afford tris- and tetrakis-*meso*-substituted porphyrins, whereas other approaches take advantage of selective *meso*-functionalization of preformed 5,15-disubstituted porphyrin scaffolds [23][24].

We opted for the latter variant to prepare the tris-*meso*-substituted precursors **9** and **10** on the way to conjugate **3** (*Scheme 1*). Thus, 5,15-diarylporphyrin **11** was readily obtained by condensation of dipyrrylmethane **12** [25] with aldehyde **13** [26] (TFA, CH_2Cl_2, for abbreviations, see the captions of *Scheme 1* or *Exper. Part*), followed by oxidation (DDQ, CH_2Cl_2). Metallation ($Zn(OAc)_2$, MeOH) afforded Zn^{II} porphyrin **14**. For the introduction of the third *meso*-aryl ring by Pd-catalyzed cross-coupling [24][27], **14** was brominated with NBS [28]; however, an unseparable mixture of *meso*- and β-brominated porphyrin derivatives was obtained. In contrast, iodination (1 equiv. I_2, $AgPF_6$, $CHCl_3$/pyridine) selectively afforded mono-*meso*-iodoporphyrin **15** (63%) besides only traces of diiodo derivative **16** [29]. Close monitoring of the reaction by TLC (SiO_2; cyclohexane/CH_2Cl_2 1:1) was necessary to prevent extensive decomposition of the porphyrin substrate. Separation of **15** and **16** was achieved by repeated column chromatography (SiO_2; cyclohexane/CH_2Cl_2 1:1). Larger-scale reactions afforded mixtures of **14**, **15**, and **16** from which the monoiodo derivative **15** was isolated in yields $\leq 40\%$.

In parallel, (*t*-Bu)Me_2Si(TBDMS)-protected **17** was obtained in 95% yield by reaction of benzyl alcohol **18** with (*t*-Bu)Me_2SiCl (DMAP, THF). Boronate **19** was subsequently formed by using 4,4,4′,4′,5,5,5′,5′-octamethyl-2,2′-bi(1,3,2-dioxaborolane) in the presence of $[PdCl_2(dppf)_2]$ and AcOK. In view of its limited stability, it was used in the next transformation without further purification (*ca.* 90% pure according to ^{1}H-NMR analysis). *Suzuki* cross-coupling [30] between **15** and **19** ($[Pd(PPh_3)_4]$, Cs_2CO_3) afforded 5,10,15-trisubstituted porphyrin **10** in good yield (67%).

Removal of the (*t*-Bu)Me_2Si protecting group with Bu_4NF in THF (with a few drops of H_2O added) yielded alcohol **20**. The deprotection was carefully monitored by TLC (SiO_2; cyclohexane/CH_2Cl_2 1:1) to avoid extensive decomposition of **10**. Subsequent conversion of **20** with $ClCOCH_2CO_2Et$ in the presence of Et_3N provided malonate-

Scheme 1. *Synthesis of [60]Fullerene – Porphyrin Adduct* **3**

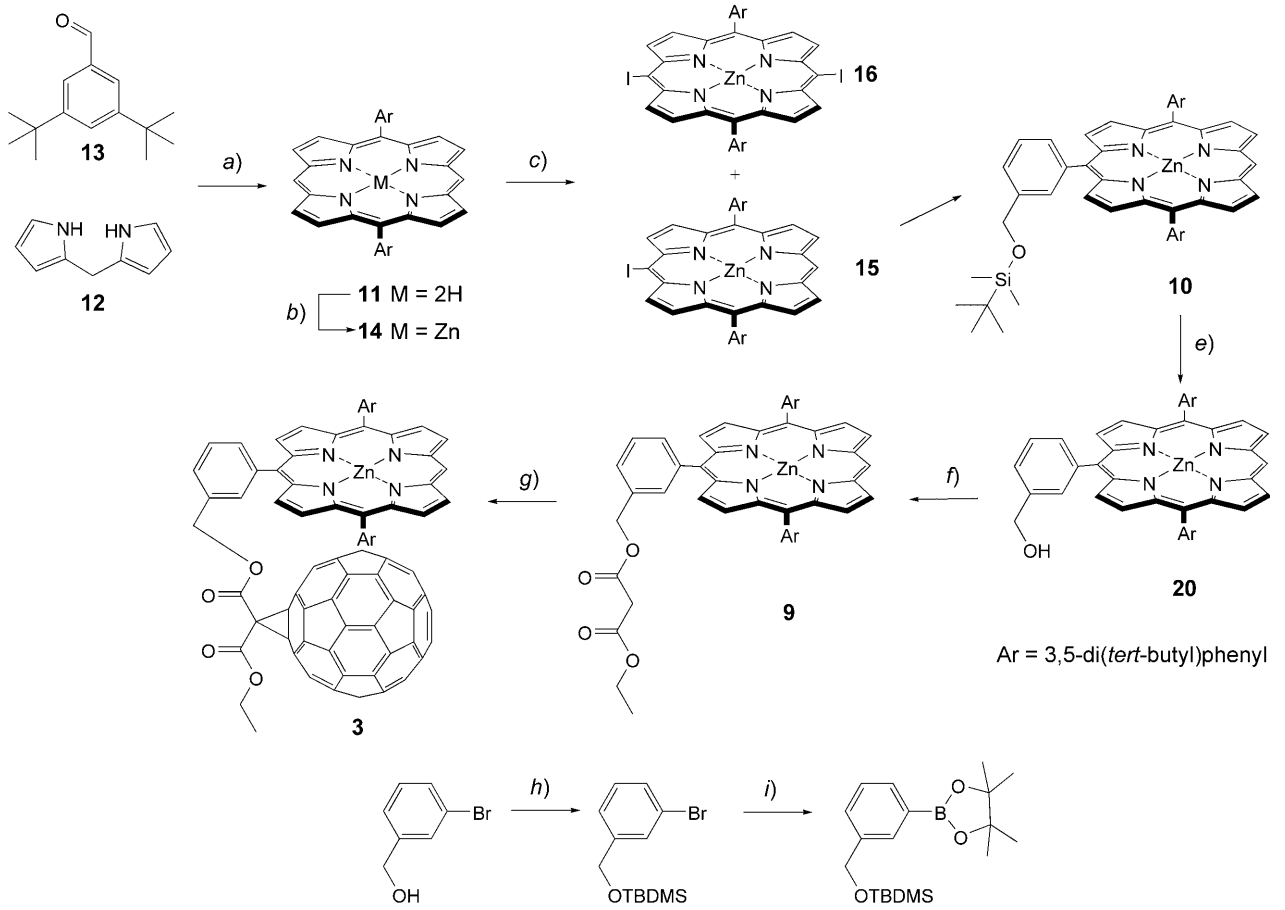

a) TFA, CH_2Cl_2, 25°, 16 h then *p*-chloranil, 70°, 2 h; 55%. *b*) $Zn(OAc)_2$, $MeOH/CH_2Cl_2$ 1:1, 25°, 2 h; 91%. *c*) I_2 (1 equiv.), $AgPF_6$ (1 equiv.), $Py/CHCl_3$ 1:30, 25°, 13 min; 63%. *d*) **19**, Cs_2CO_3, $[Pd(PPh_3)_4]$, PhMe, 140°, 18 h; 67%. *e*) Bu_4NF, THF, 0° (30 min) → 25° (1 h); 80%. *f*) $ClCOCH_2CO_2Et$, Et_3N, CH_2Cl_2, 0° (15 min) → 25° (1 h); 90%. *g*) C_{60}, I_2, DBU, PhMe, 25°, 1.5 h; 45%. *h*) *t*-$BuMe_2SiCl$ (TBDMSCl), DMAP, THF, 25°, 24 h; 95%. *i*) 4,4,4′,4′,5,5,5′,5′-Octamethyl-2,2′-bi(1,3,2-dioxaborolanyl), $[PdCl_2(dppf)_2] \cdot CH_2Cl_2$, AcOK, Me_2SO, 100°, 16 h; 55%. TFA = CF_3COOH; Py = pyridine; DBU = 1,8-diazabicyclo[5.4.0]undec-7-ene; DMAP = 4-(dimethylamino)pyridine; dppf = 1,1′-bis(diphenylphosphino)ferrocene.

appended porphyrin **9**. *Bingel* reaction of **9** with C_{60} (I_2, DBU, PhMe) afforded the desired dyad **3** as a brown solid in 45% yield. HR-FT-ICR-MALDI-TOF mass spectra (matrix: DCTB) of **3** displayed the molecular ion as the only peak at *m*/*z* 1686.4048 (M^+, $C_{120}H_{62}N_4O_4Zn^+$; calc. 1686.4057).

2.1.2. *Synthesis of Bis[60]fullerene–Oligoporphyrin Conjugates* **4**–**6**. Compounds **4**–**6** were prepared by the same synthetic route as described for **3**. First, the *meso*,*meso*-linked oligoporphyrin scaffolds with two, three, and four porphyrin units, **21**–**23**, respectively, were synthesized by oxidative coupling ($AgPF_6$) of **14**, according to *Osuka* and co-workers (*Scheme 2*) [13]. Increasing the amount of $AgPF_6$ from 0.5 to 0.8 equiv. improved the conversion of the starting porphyrin monomer.

Scheme 2. *Ag^I-Promoted Oligomerization of Porphyrin* **14**

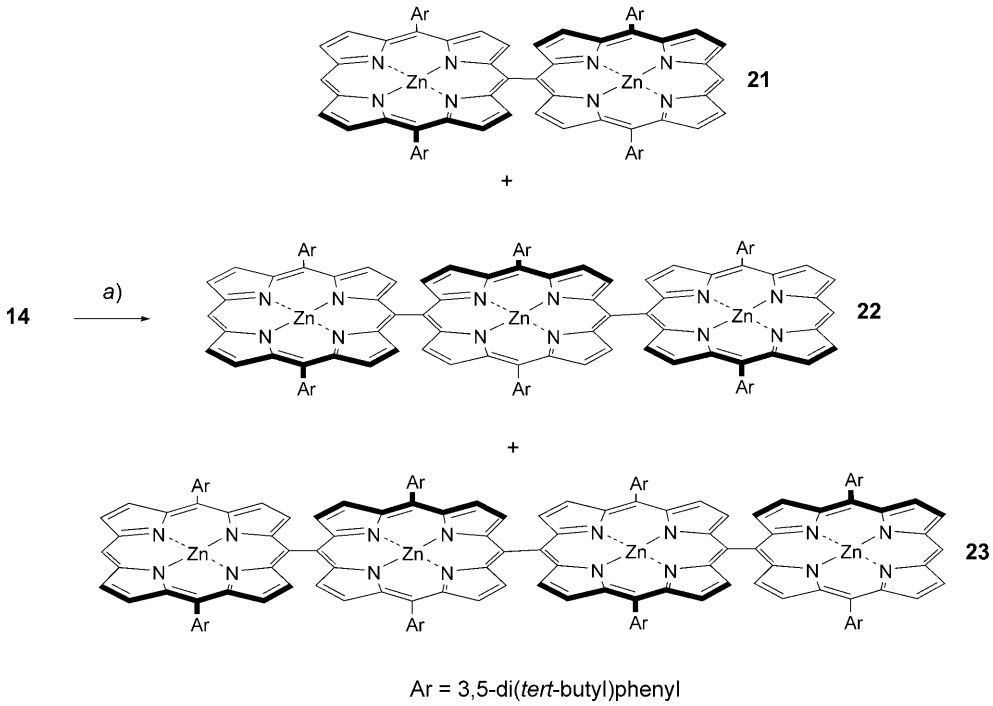

a) $AgPF_6$ (0.8 equiv.), MeCN/$CHCl_3$ 1:4, 25°, 16 h; 44% (**14**); 25% (**21**); 11% (**22**); 7% (**23**).

A small dark-red crystal of dimer **21**, suitable for X-ray diffraction, was obtained by vapor diffusion of aqueous MeOH into a solution of **21** in $CHCl_3$. The asymmetric unit of the crystal structure contains one molecule of **21** and five MeOH molecules. The molecular structure, depicted in *Fig. 2*,*a*, nicely reveals the nearly orthogonal arrangement of the two porphyrins with an interplanar angle of *ca.* 84°. Both Zn^{II} ions deviate by *ca.* 0.2 Å from the plane of the four surrounding pyrrolic N-atoms and, interestingly, show two different coordination motifs. While Zn(2) is in contact with one MeOH molecule ($Zn(2)\cdots O(300) = 2.25$ Å) to give a penta-coordinated species, Zn(1) is in contact with two MeOH molecules ($Zn(1)\cdots O(200) = 2.30$ Å, $Zn(1)\cdots O(500) =$

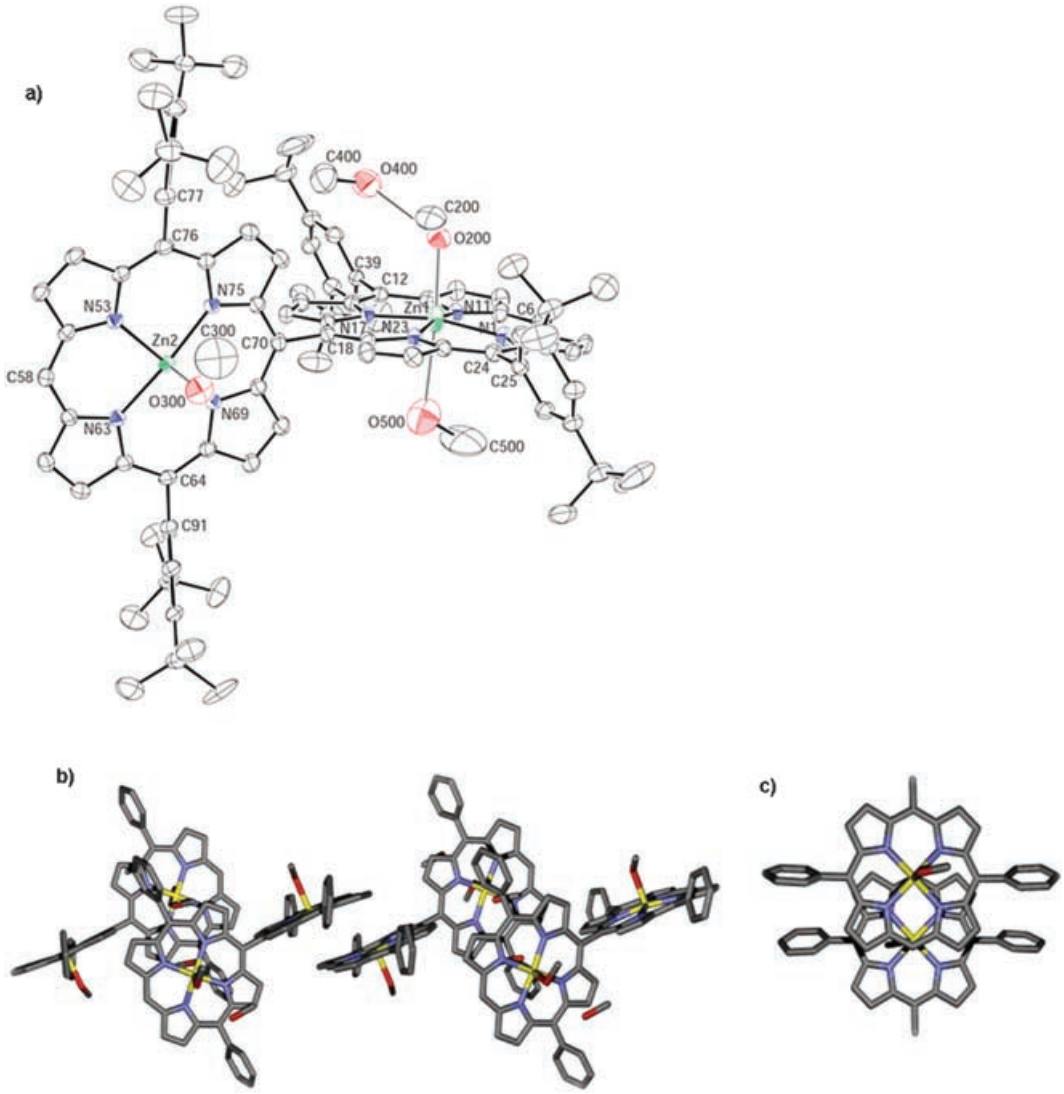

Fig. 2. a) *ORTEP Representation of porphyrin dimer* **21** *together with four MeOH molecules as determined by X-ray-diffraction analysis.* Arbitrary numbering. Atomic displacement parameters, obtained at 223 K, are drawn at the 30% probability level. Intermolecular contacts [Å]: O(200)···Zn(1) = 2.30; O(300)···Zn(2) = 2.25; O(500)···Zn(1) = 2.83; O(200)···O(400) = 2.92. The absolute values of the interplanar angles about the C(porph)–C(aryl) bonds are 64.5° (C(12)–C(36)), 66.1° (C(24)–C(25)), 72.1° (C(64)–C(91)), 66.1° (C(76)–C(77)), and 83.6° (C(porph)–C(porph, C(18)–C(70)). The interplanar angles are based on the least-square planes through the corresponding phenyl and porphyrin rings. A disordered MeOH molecule is not shown. b) *Relative arrangement of dimer* **21** *in the crystal packing clearly showing the π-π interactions between the porphyrins.* The *t*-Bu substituents on the phenyl moieties and the disordered MeOH molecules have been omitted. c) *Top view of the π-π interacting porphyrin pairs showing their relative orientation and offset*. Some substituents on the porphyrin rings have been omitted. Atom colors: blue N, red O, yellow Zn, gray C.

2.83 Å) leading to hexa-coordination. In addition, O(200) is connected to another MeOH (O(200)···O(400) = 2.92 Å), while the remaining disordered MeOH is not involved in any close contacts. The crystal packing (*Fig. 2,b*) shows an infinite network in which each of the Zn^{II} porphyrins displaying penta-coordination is involved in an attractive π-π stacking interaction with an adjacent dimer. The π-systems of two neighboring porphyrins are approximately parallel with an interplanar separation of *ca.* 3.37–3.66 Å. The distance between the two planes of N-atoms is close to 3.6 Å. One porphyrin is shifted relative to its neighbor (parallel to the intramolecular axis C(58)···C(70)) by *ca.* 3.45 Å (*Fig. 2,c*). It can be postulated that the presence of the bulky 3,5-di(*tert*-butyl)phenyl substituents prevents a shorter interplanar distance and an optimal porphyrin–porphyrin arrangement in which the π-electrons of a pyrrole sit on top of the metal center [31]. The fact that both Zn^{II} porphyrins involved in the π-π interaction are still coordinated to a MeOH molecule provides evidence for only a weak electrostatic interaction between the positive charge on the Zn-atom (local charge on Zn can be estimated to be *ca.* $+0.4\ e^-$ [31]) in one porphyrin unit and the π-electrons in the other one, which preserves the *Lewis* acidity of the metal centers [32].

Iodination of **21**–**23** (2 equiv. I_2, $AgPF_6$, $CHCl_3$/pyridine) afforded, within 15 min, diiodo derivatives **24**–**26** with complete selectivity for the *meso*-positions (>70% yield; *Scheme 3*). *Suzuki* cross-coupling of **24**–**26** with arylboronic ester **19** provided the arylated porphyrins **27**–**29**. Although the yields were good, some starting oligomers **21**–**23** and monosubstituted oligomers were obtained as side-products resulting from reductive dehalogenation. While the purification of **27** proceeded smoothly by a single column chromatography on SiO_2, the separation of **28** and **29** from the undesired by-products was unsuccessful, and the crude mixtures were directly used, without further purification, in the next synthetic steps.

Cleavage of the (*t*-Bu)Me_2Si protecting groups was performed in quantitative yield with Bu_4NF in THF, and the resulting diols **30**–**32** were easily purified by column chromatography (SiO_2; PhMe). Acylation with $ClCOCH_2CO_2Et$ in CH_2Cl_2/Et_3N 4:1 provided bis-malonates **33**–**35** in yields of *ca.* 70%. Some demetallation of the Zn^{II} porphyrins was occasionally detected during the *Suzuki* cross-coupling and/or acylation steps. In those cases, a remetallation of the tetrapyrrolic ligands with $Zn(OAc)_2$ was necessary. Cyclopropanation of C_{60} with **33**–**35** under modified *Bingel* conditions afforded, after column chromatography (SiO_2-H; PhMe), the targeted fullerene–porphyrin conjugates **4**–**6** (*Scheme 3*). The molecular mass of each compound was unambiguously established by HR-FT-ICR-MALDI-MS (DCTB), which displayed as prominent peak the molecular ion of each fullerene–porphyrin conjugate: *m*/*z* 3370.7940 (**4**; M^+, $C_{240}H_{122}N_8O_8Zn_2^+$; calc. 3370.7963), 4117.1200 (**5**; M^+, $C_{288}H_{172}N_{12}O_8Zn_3^+$; calc. 4117.1290), and 4864.4307 (**6**; MH^+, $C_{336}H_{223}N_{16}O_8Zn_4^+$; calc. 4864.4701). As a typical example, the spectrum of **6** is shown in *Fig. 3*. The structural assignments of **4**–**6** were also supported by their ^1H- and ^{13}C-NMR spectra. All fullerene–porphyrin conjugates were found to be brown solids, displaying good solubility in common organic solvents.

2.1.3. *Synthesis of Mono[60]fullerene–Diporphyrin Conjugate* **7**. The synthesis of **7** started with the iodination of *meso*,*meso*-linked diporphyrin **21** (1 equiv. I_2, $AgPF_6$) to give the mono-iodo derivative, which was transformed into alcohol **36** by *Suzuki* cross-coupling with **19** and deprotection (*Scheme 4*). Crude products of the iodination and

Scheme 3. *Synthesis of Bis[60]fullerene–Oligoporphyrin Arrays* **4**–**6**

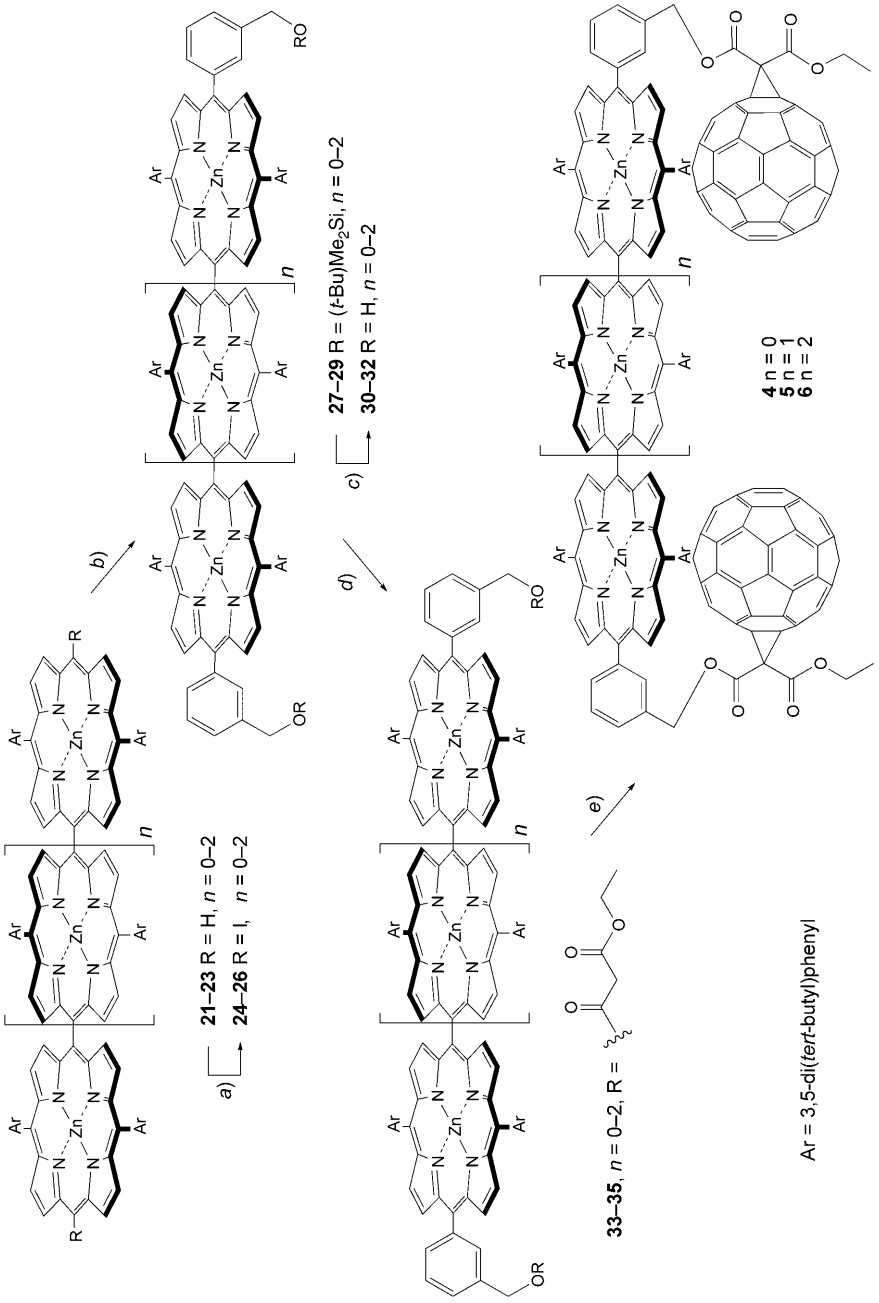

a) I_2 (2 equiv.), $AgPF_6$ (2 equiv.), Py/$CHCl_3$ 1:30, 25°, 11 min; 88% (**24**); 85% (**25**); 70% (**26**). *b*) **19**, Cs_2CO_3, [$Pd(PPh_3)_4$], PhMe, 140°, 18 h; 70% (**27**). *c*) Bu_4NF, THF, 0° (30 min) → 25° (1 h); 84% (**30** from **27**); 60% (**31,** from **25**); 55% (**32,** from **26**). *d*) $ClCOCH_2CO_2Et$, Et_3N, CH_2Cl_2, 0° (15 min) → 25° (1 h); 67% (**33**); 71% (**34**); 70% (**35**). *d*) C_{60}, I_2, DBU, PhMe, 25°, 1.5 h; 55% (**4**); 60% (**5**); 45% (**6**).

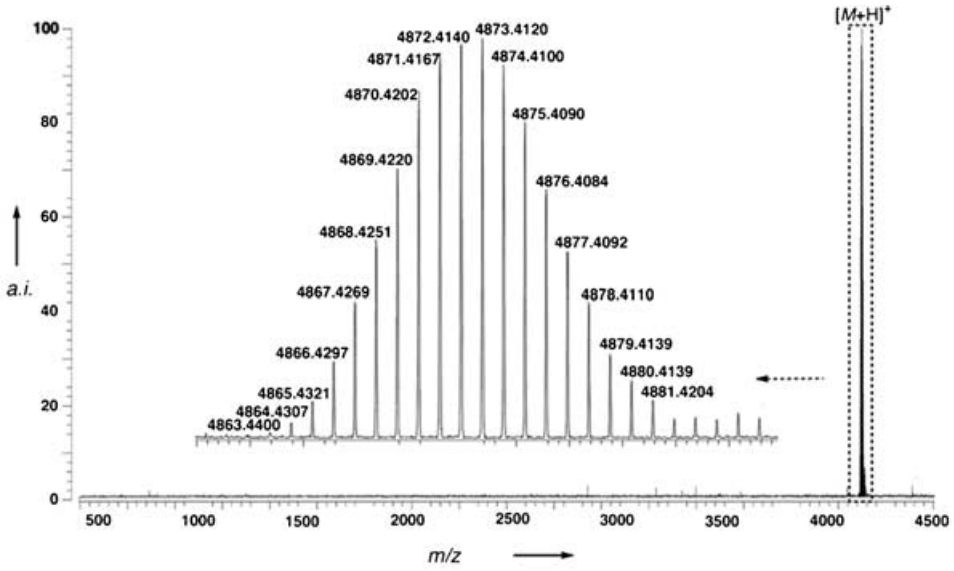

Fig. 3. *HR-FT-ICR-MALDI Mass spectrum of bis[60]fullerene – oligoporphyrin conjugate* **6** *in the positive-ion mode* (matrix: DCTB, N_2 laser: 337 nm).

desilylation reactions were used in the subsequent transformations, due to difficulties with the purification. Acylation (**36** → **37**) and *Bingel* addition afforded the desired C_s-symmetric conjugate **7** which was fully characterized.

2.1.4. *Synthesis of the Triply-Linked Diporphyrin – C_{60} Conjugate* **8**. The intermediate **38** on the way to **8** was obtained following two routes (*Scheme 5*). In the first one, Pd-catalyzed cross-coupling between **24** and phenylboronic ester **39** [33] afforded, after chromatographic separation (SiO_2; cyclohexane/CH_2Cl_2 1:1), compounds **40** (20%), **41** (69%), and **21** (11%). According to the protocol (DDQ, $Sc(OTf)_3$, PhMe) reported by *Tsuda* and *Osuka* for oxidative ring closure [11], biaryl-type dimer **41** was converted into the triply-linked derivative **38** in almost quantitative yield. In the second route, *Suzuki* cross-coupling between **15** and **39** gave, after column chromatography (SiO_2; cyclohexane/CH_2Cl_2 1:1), carbonitrile **42** (67%) and porphyrin **14** (23%; from reductive dehalogenation). Homo-coupling of **42** under the above-mentioned oxidative conditions provided, after several chromatographic purifications, the triply-linked dimer **38** in 89% yield. While the first route afforded **38** in four steps starting from **14** with an overall yield of 11%, the second route led to **38** in three steps in 39% yield (from **14**). The chemical structure of **38** was confirmed by HR-FT-ICR-MALDI mass spectrometry, ^{1}H-, ^{13}C-, and DQF-COSY NMR spectroscopies.

Reduction of **38** with DIBAL-H at 0° gave dicarbaldehyde **43** in 94% yield (*Scheme 5*). Subsequent reduction, again with DIBAL-H, afforded bis(benzyl alcohol) **44** (55%), which was transformed in 88% yield into bismalonate **45** (*Scheme 5*). Modified *Bingel* cyclopropanation of C_{60} with **45** provided dyad **8** in 41% yield, after filtration over a short plug (Al_2O_3; PhMe) and repeated precipitations from hexane, followed by washings with hexane, MeOH, and Et_2O. The compound is rather unstable in concentrated solution.

Scheme 4. *Synthesis of Mono[60]fullerene–Diporphyrin* **7**

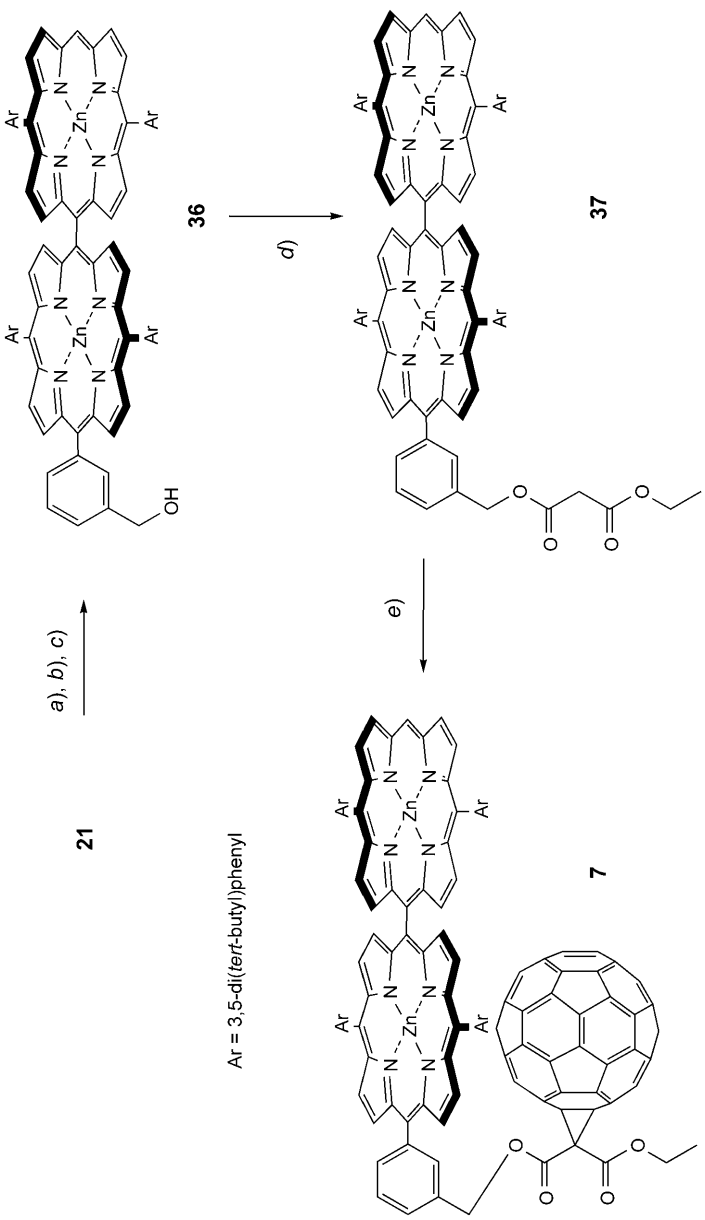

a) I_2 (1 equiv.), $AgPF_6$ (1 equiv.), Py/$CHCl_3$ 1:30, 25°, 15 min. *b*) **19**, Cs_2CO_3, $[Pd(PPh_3)_4]$, PhMe, 18 h. *c*) Bu_4NF, THF, 0° (30 min) → 25° (1 h); 40% (**36**, from **21**). *d*) $ClCOCH_2CO_2Et$, Et_3N, CH_2Cl_2, 0° (30 min), then 25° (1 h); 90%. *e*) C_{60}, I_2, DBU, PhMe, 25°, 1 h; 40%.

In the HR-FT-ICR-MALDI mass spectrum (matrix: DCTB) of conjugate **8**, the prominent peak corresponds to the molecular ion at *m/z* 3371.7749 (M^+, $C_{240}H_{118}N_8O_8Zn_2^+$; calc. 3371.7698). The ^{1}H- and ^{13}C-NMR, and UV/VIS spectra further support the chemical structure of **8**. Thus, the ^{13}C-NMR spectrum of **8** displays the following characteristic resonances: 163.57 and 163.42 ppm ($2 \times C{=}O$), overlapping and broad signals in the range of 154.06–117.12 ppm ($C(sp^2)$ of fullerene and diporphyrin), 70.86 ppm (fullerene $C(sp^3)$-atom), 68.35 ppm (benzylic $C(sp^3)$-atom), 52.74 ppm (methano bridge C-atom), and 63.46 and 14.22 ppm (ethoxy $C(sp^3)$-atoms).

2.2. *Supramolecular Networks in the Solid-State Structures of Monomeric Porphyrins.* Porphyrins **46** and **47** were prepared as controls for the planned physical studies, according to synthetic strategies similar to those reported for **41** in *Scheme 5* (**46**) and for **20** in *Scheme 1* (**47**). Both compounds as well as intermediate **42** show interesting supramolecular network structures in the solid state.

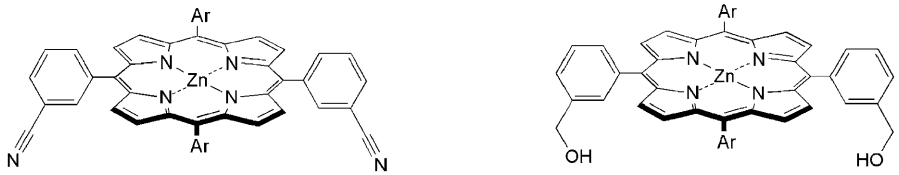

Ar = 3,5-di(*tert*-butyl)phenyl

Dark-red crystals of **42** and **46** were grown as solvates by slow diffusion of H_2O into solutions of the porphyrins in MeOH/$CHCl_3$ 5 : 1. The ORTEP drawing of **42** is shown in *Fig. 4* (the crystal structure of **46** had been reported in [34]).

Compound **42** crystallizes in the monoclinic space group $P2_1/n$ and **46** in the othorhombic space group *Pbca*. In both molecules, the four pyrrolic N-atoms coordinating to Zn^{II} form a distorted square plane, and each Zn^{II} ion is involved in a short intermolecular contact to a neighboring MeOH molecule ($Zn(1)\cdots O(61) = 2.19$ Å for **42** and $Zn(1)\cdots O(69) = 2.14$ Å for **46**). In both porphyrin complexes, the penta-coordinated Zn^{II} ions exhibit a square-pyramidal coordination geometry, with the metal ion deviating from the mean plane of the four pyrrole N-atoms towards the axial MeOH ligand by *ca.* 0.28 Å (**42**) and 0.25 Å (**46**), respectively. In **42**, the average Zn–N distance is 2.07 Å, and the angles N(1)–Zn(1)–N(17), N(11)–Zn(1)–N(23) are 165.2° and 163.2° (mean 164.2°). In **46**, the corresponding values are 2.06 Å, 164.8°, and 167.6° (mean 166.2°). In the crystal packing, both compounds **42** and **46** are arranged as infinite rod-like polymers in which the porphyrin units are connected to each other through H-bonding interaction between a MeOH molecule coordinated to a Zn^{II} ion and a C≡N group (*Figs. 5* and *6*). For porphyrin **42**, the $C{\equiv}N\cdots O$ distance is 2.88 Å (N(46)···O(61)) and the $N\cdots H{-}O$ angle 163° (N(46)···H–O(61)), for **46** the corresponding values are 2.86 Å (N(68)···O(69)) and 169° (N(68)···H–O(69)), respectively. As a consequence of the intermolecular H-bonding networks, the coordinative $Zn\cdots O$ bonds are shorter than those reported for a number of penta-coordinated porphyrinato Zn^{II} complexes with a metal-ion-coordinated MeOH molecule [35].

Scheme 5. *Synthesis of Triply-Fused Diporphyrin–Fullerene Conjugate* **8**

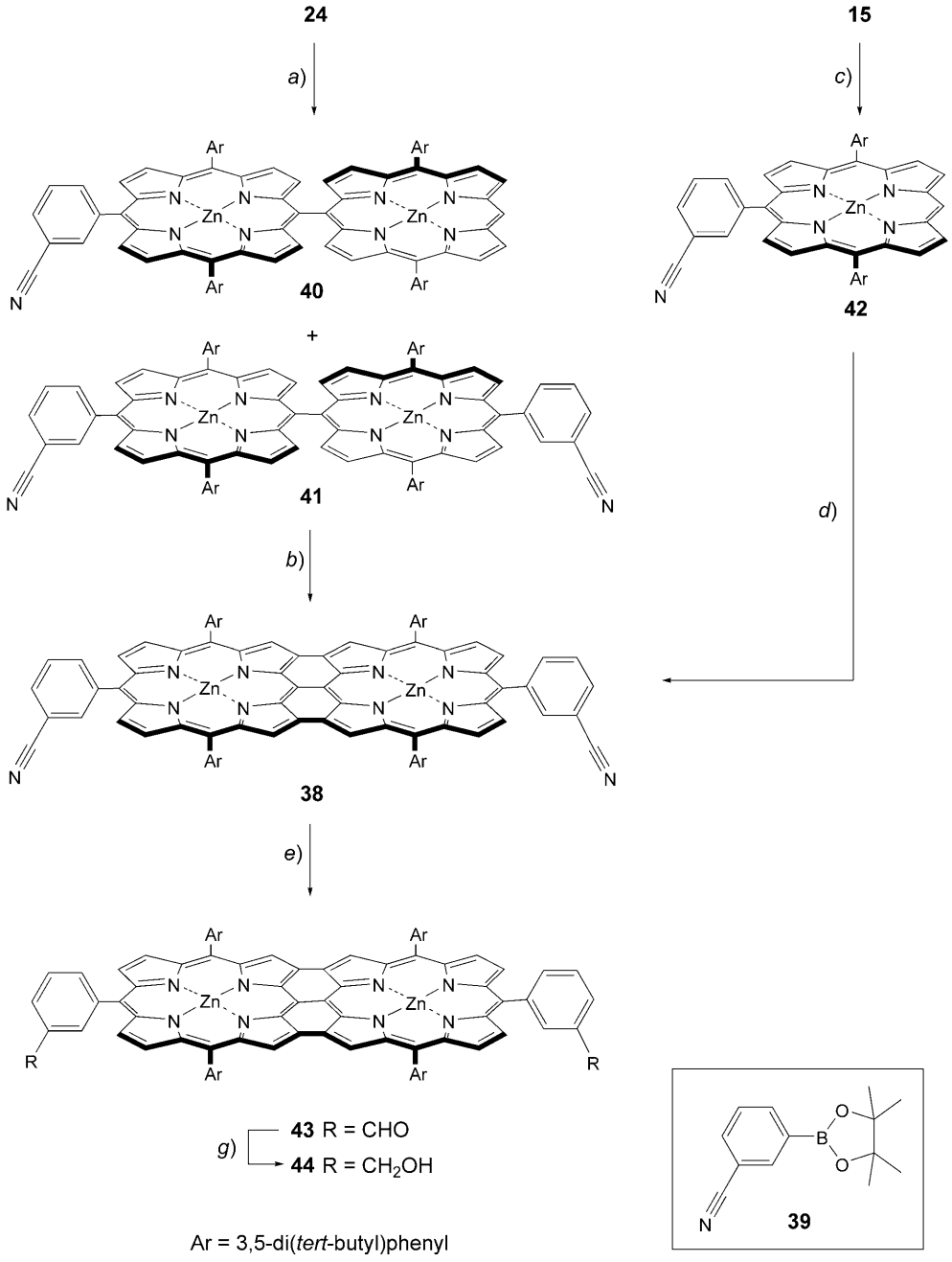

Scheme 5 (cont.)

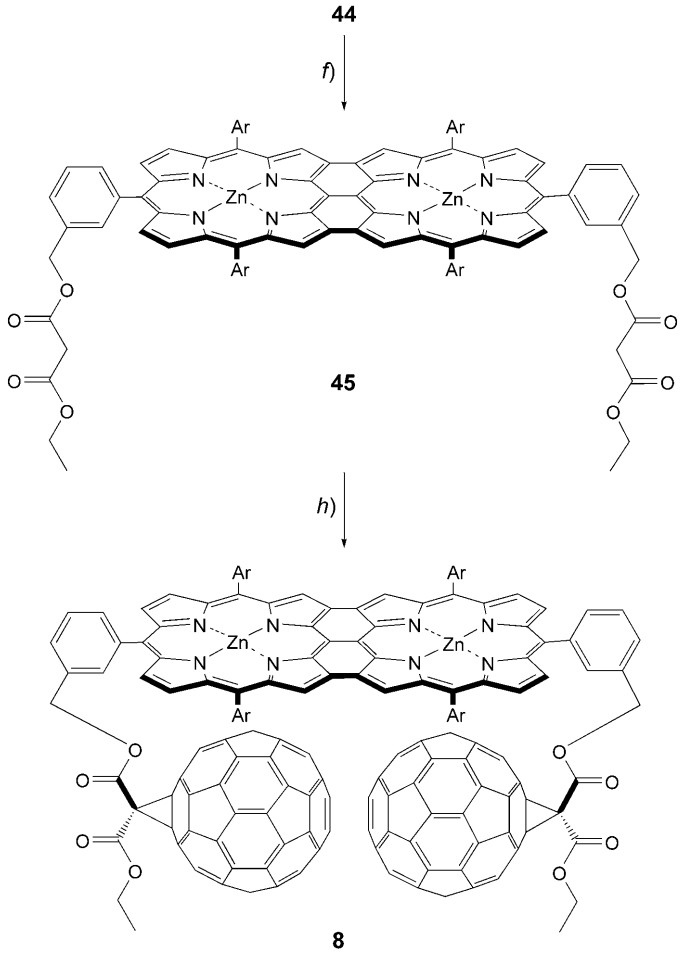

a) **39**, Cs_2CO_3, [$Pd(PPh_3)_4$], PhMe, 100°, 18 h; 20% (**40**); 69% (**41**). *b*) $Sc(OTf)_3$, DDQ, PhMe, 140°, 30 min; quant. *c*) **39**, Cs_2CO_3, [$Pd(PPh_3)_4$], PhMe, 100°, 18 h; 67%. *d*) $Sc(OTf)_3$, DDQ, PhMe, 140°, 30 min; 89%. *e*) DIBAL-H, CH_2Cl_2, −70° (2 h) → 25° (18 h); 94%. *f*) DIBAL-H, CH_2Cl_2, −70° (2 h) → 25° (18 h); 55%. *g*) $ClCOCH_2CO_2Et$, Et_3N, CH_2Cl_2 1:7, 0° (15 min) → 25° (16 h); 88%. *h*) C_{60}, I_2, DBU, PhMe, 0° → 25°, 1 h; 41%. DDQ = 2,3-Dichloro-5,6-dicyano-*p*-benzoquinone; DIBAL-H = diisobutylaluminum hydride.

Small dark-red crystals of **47** were obtained by slow vapor diffusion of H_2O into a solution of the porphyrin in MeOH. In the triclinic crystals (space group $P\bar{1}$), there are two independent molecules in the asymmetric unit (*Fig. 7*). While the porphyrin unit at the center (with primed (′) atoms) sits on a crystallographic center of symmetry, the tetrapyrrolic macrocycles left and right are related by the center of symmetry. In contrast to compounds **42** and **46**, which form infinite one-dimensional chains *via* H-bonded MeOH molecules, the self-assembly of porphyrin **47** is characterized by the

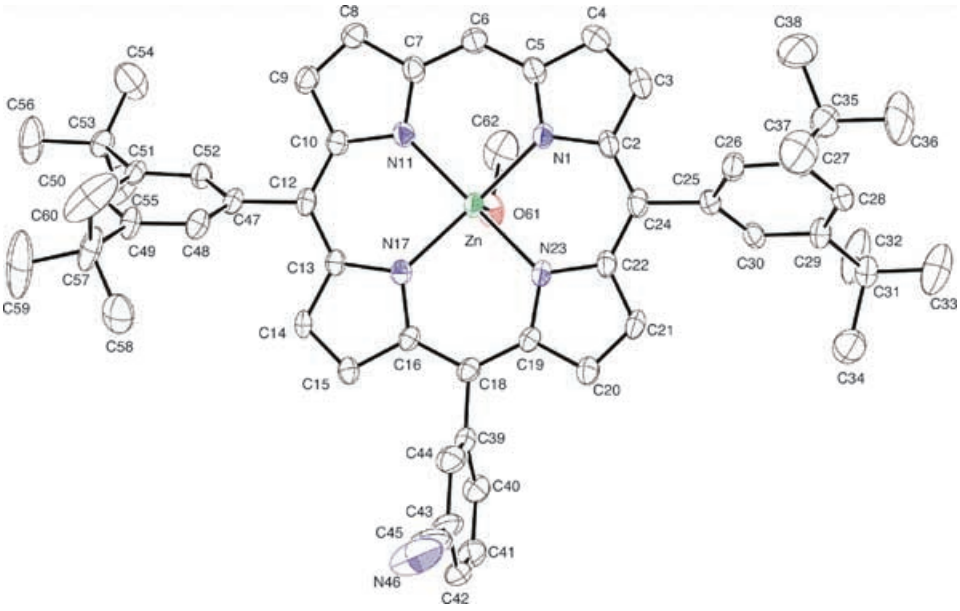

Fig. 4. *ORTEP Representation of porphyrin* **42** *with one MeOH molecule.* A second solvent molecule ($CHCl_3$) in the crystal is omitted for clarity. Arbitrary numbering. Atomic displacement parameters obtained at 173 K are drawn at the 30% probability level. Intermolecular distance O(61)···Zn(1) = 2.19 Å. The absolute values of the interplanar angles about the C(porph)–C(aryl) bonds are 60.4° (C(12)–C(47)), 84.2° (C(18)–C(39)), and 59.1° (C(24)–C(25)). The angles are based on the least-square planes through the corresponding phenyl and porphyrin rings. Atom colors: blue N, red O, green Zn, white C.

coordination of the CH_2OH residues to the metal centers of neighboring Zn^{II} porphyrins. *Fig. 7* shows that Zn(1) is penta-coordinated due to an intermolecular contact Zn(1)···O(68′) of 2.14 Å, while Zn(1′), involved in two symmetry-related contacts Zn(1′)···O(46) of 2.47 Å, exhibits an octahedral coordination. As expected, the Zn(1′)···O(46) distance is slightly larger than the distance Zn(1)···O(68′) measured for the penta-coordinate Zn(1). The penta-coordinated Zn(1) ion is displaced from the mean plane of the four pyrrolic N-atoms towards the coordinating O(68′)-atom by *ca.* 0.32 Å, and the angles N(1)–Zn(1)–N(17) and N(11)–Zn(1)–N(23) are decreased to 162.7° and 163.6°, respectively. Due to symmetry, Zn(1′) sits exactly in the plane of the four N-atoms. Notably, O(68′) is H-bonded to a MeOH molecule, as shown by the characteristic short intermolecular O(71A)···O(68′) contact (2.72 Å).

2.3. *NMR-Spectroscopic Conformational Analysis.* In dyads **3**–**7**, the C-spheres rest atop the porphyrin plane. The tangential position of the fullerene moiety with respect to the porphyrin ring was unambiguously established by ^{1}H- and ^{13}C-NMR spectroscopy. This conformational preference is characterized by the non-equivalence of the *ortho* and *t*-Bu H-atoms on the 3,5-di(*tert*-butyl)phenyl substituents, since phenyl rotation, which exchanges the fullerene from one to the other porphyrin face, is slow on the NMR time scale (*Fig. 8*). The geometrical preference is a consequence of the strong attractive interaction between the two chromophores [8][9][36].

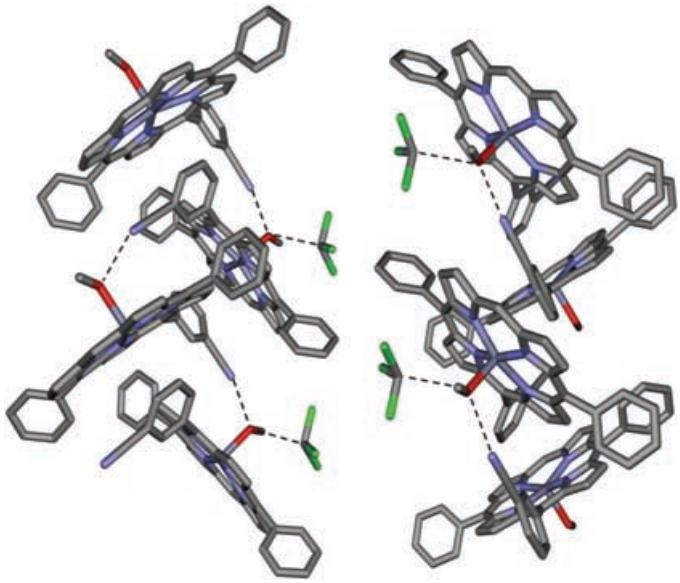

Fig. 5. *One-dimensional, MeOH-mediated supramolecular network of porphyrin* **42** *illustrating the short intermolecular N···O contacts* (2.88 Å, dashed line) *extending along the crystallographic* b *axis.* The $CHCl_3$ solvent molecules between two adjacent H-bonded columnar porphyrin arrays are also in close (C–H···O) contact with the coordinated MeOH (C(100)···O(61) = 3.24 Å). The *t*-Bu substituents have been omitted. Atom colors: blue N, red O, gray Zn, gray C, and green Cl.

In accordance with this reasoning, the ^{1}H-NMR spectrum (500 MHz, $CDCl_3$, 298 K) of **3** shows two *triplets* for the *ortho* H-atoms (H_a, H_b in *Fig. 8*) and two *singlets* for the *t*-Bu H-atoms of its 3,5-di(*tert*-butyl)phenyl substituents. A 500-MHz homonuclear DQF-COSY spectrum allowed the unambiguous assignment of the resonances of these residues. The ^{13}C-NMR (125 MHz, $CDCl_3$, 298 K) spectrum depicts, as expected, nine resonances for the C(sp^3)-atoms and, due to some overlap, 52 out of the 56 expected resonances for the C(sp^2)-atoms. Such signal pattern is in agreement with the postulated C_s-symmetric conformation in which the two porphyrin faces are non-equivalent.

Similarly, in **4** the two fullerenes also lie on a porphyrin plane but, as a consequence of the orthogonal position of the two porphyrin planes, the dyad adopts a C_2-symmetric conformation (*Fig. 9*). The ^{1}H-NMR (500 MHz, $C_2D_2Cl_4$, 298 K) spectrum of **4** displays two and four *triplets* for H–C(4) and H–C(2), respectively, and four *singlets* for the *t*-Bu H-atoms. The ^{13}C-NMR (125 MHz, $CDCl_3$, 298 K) spectrum displays 13 resonances for the C(sp^3)-atoms and 79 expected resonances for the C(sp^2)-atoms. The 500-MHz homonuclear DQF-COSY spectrum confirmed the assignment of the ^{1}H resonances. Analogous considerations are also valid for **6** which preferentially adopts a C_2-symmetric conformation with the two C-spheres nesting on the outer porphyrins. In principle, such a conformation should be preferred by all oligomers of this type having an even number of porphyrin units.

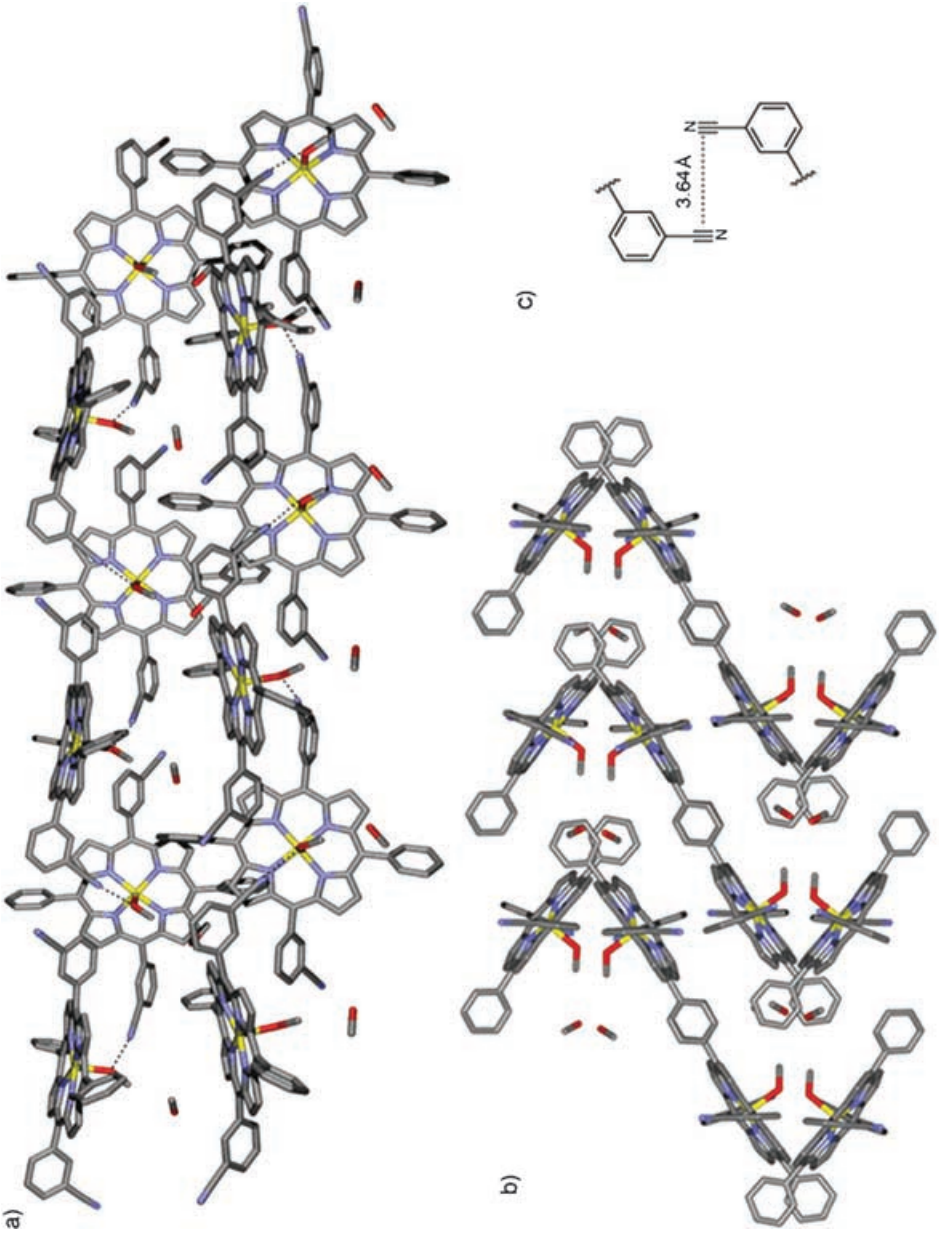

Fig. 6. a) *View of the (0 1 0) plane of the crystal packing of porphyrin* **46** *illustrating the one-dimensional MeOH-mediated supramolecular network.* The short intermolecular N···O contacts are indicated (dashed line). b) *View of the corresponding (1 0 0) plane of the crystal packing.* c) *Arrangement of C≡N groups not involved in H-bonding.* Neighboring intercolumnar, non-H-bonded terminal C≡N groups interact pairwise by dipolar forces (the distance between two C≡N groups is 3.64 Å). The *t*-Bu substituents have been omitted. Atom colors: blue N, red O, yellow Zn, gray C.

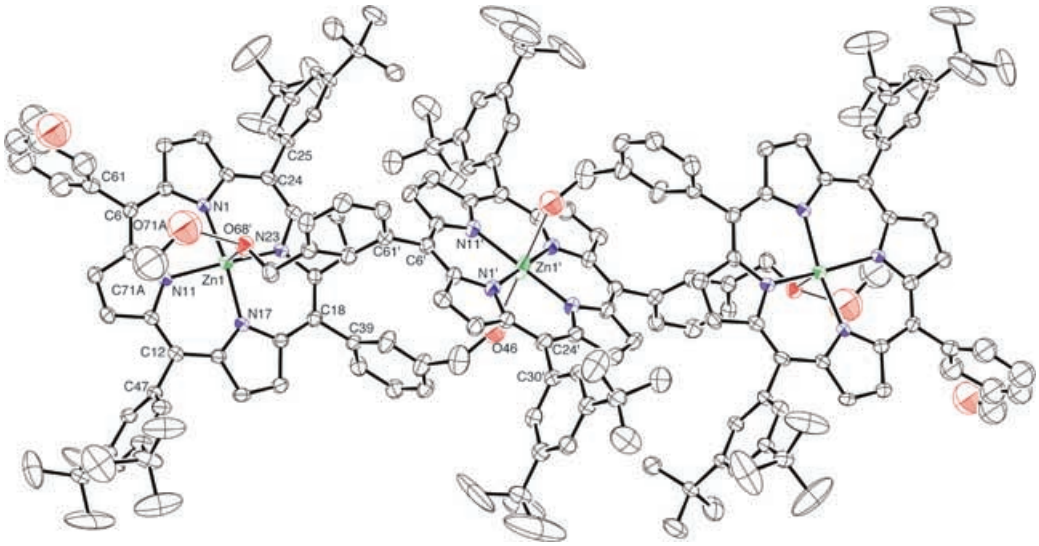

Fig. 7. *Crystal structure of porphyrin* **47** *showing the intermolecular contacts between two independent molecules of* **47** *and two MeOH molecules.* The molecule at the center (with primed (′) atoms) sits on an inversion center, the molecules left and on the right are in general positions and related by the inversion center. Atomic displacement parameters obtained at 203 K are drawn at the 30% probability level. Intermolecular contacts [Å]: O(68′)···Zn(1) = 2.14; O(46)···Zn(1′) = 2.46; O(68′)···O(71A) = 2.72. The absolute values of the interplanar angles about the C(porph)–C(aryl) bonds are 79.7° (C(12)–C(47)), 82.7° (C(6)–C(61)), 78.9° (C(24)–C(25)), 82.7° (C(18)–C(39)), 81.1° (C(6′)–C(61′)), and 81.6° (C(24′)–C(30′)). The angles are based on the least-square planes through the corresponding phenyl and porphyrin rings. A disordered MeOH molecule is not shown. Atom colors: blue N, red O, green Zn, white C.

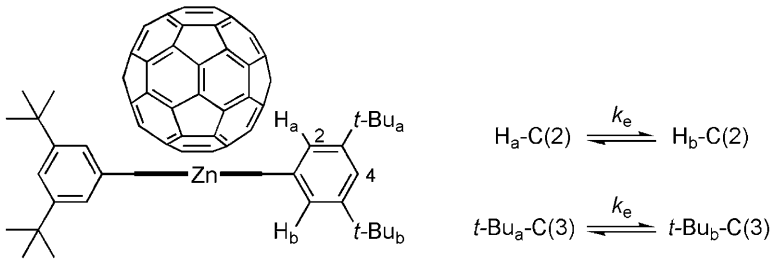

Fig. 8. *Schematic view of the face-to-face conformation adopted by the porphyrin–fullerene conjugates* (k_e = rate constant of exchange)

Two conformers of **5** can be distinguished by NMR spectroscopy. The two C-spheres can either be in a *syn* (C_{2v}-symmetry) or an *anti* (C_{2h}-symmetry) arrangement. This hypothesis was confirmed by ^{1}H- and ^{13}C-NMR ($CDCl_3$) analysis of conjugate **5** at 25°, which revealed the presence of the two conformers in a 1:1 ratio (*Fig. 10*). Whereas the two phenyl H–C(4′) protons are equivalent in the *anti* conformer, they show non-equivalence in the *syn*-conformer. As expected, three *triplets* with relative intensities 1:2:1 are observed at 7.76, 7.67, and 7.58 ppm, respectively, for the H–C(4′)

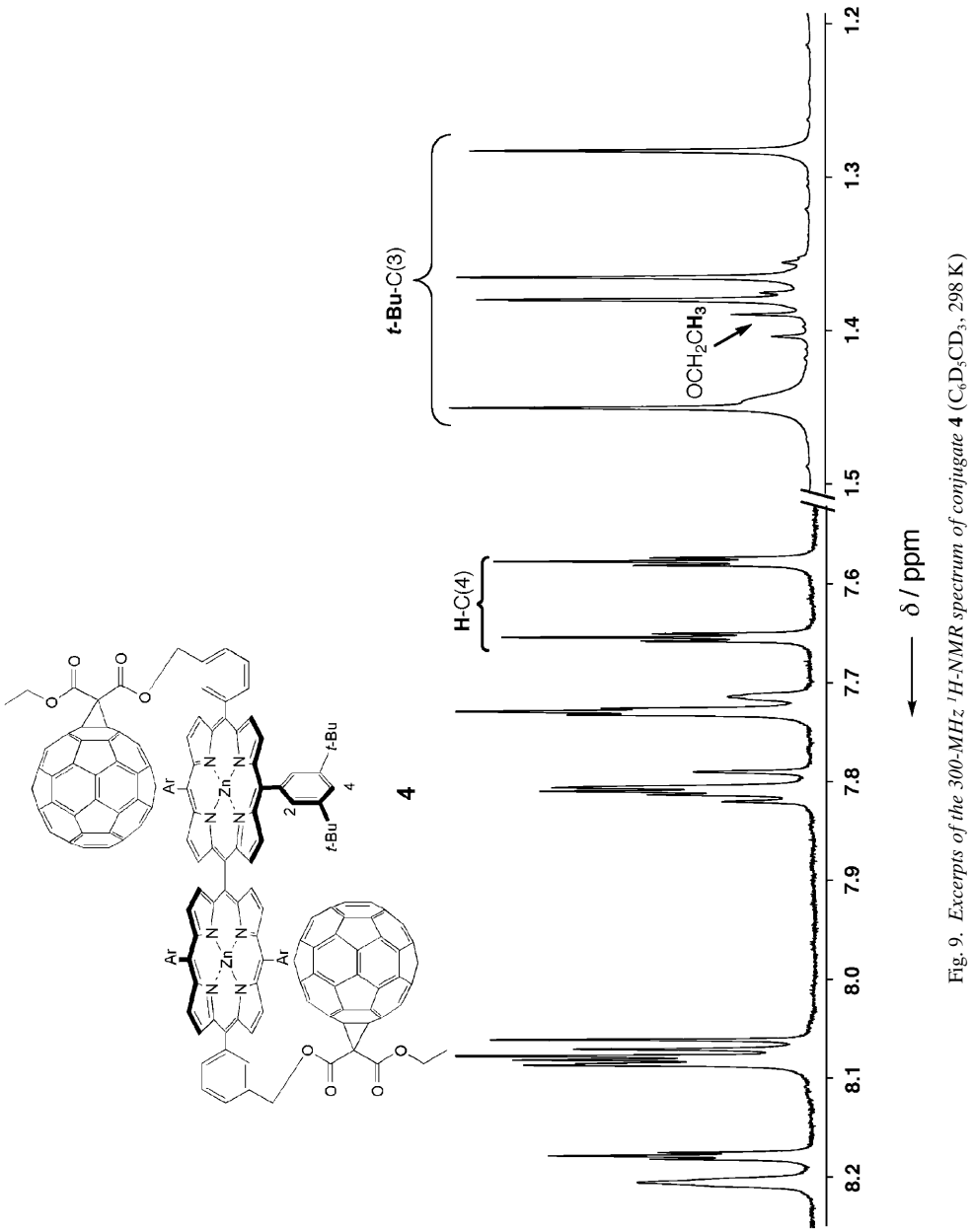

Fig. 9. *Excerpts of the 300-MHz ^{1}H-NMR spectrum of conjugate* **4** ($C_6D_5CD_3$, 298 K)

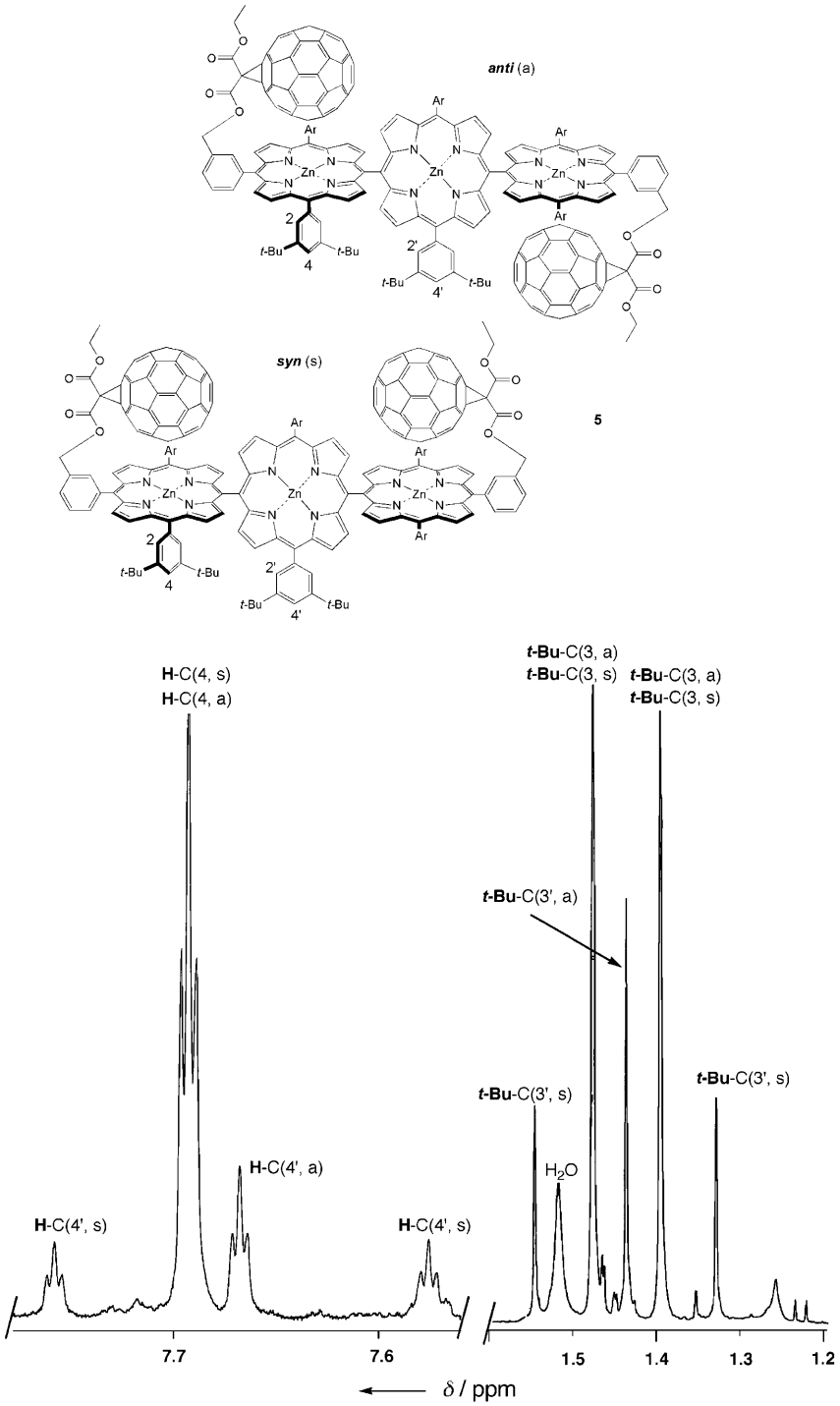

Fig. 10. *Excerpts of the 500-MHz ^{1}H-NMR spectrum of conjugate* **5** ($CDCl_3$, 298 K)

protons in the 1:1 mixture of conformers. The same ^{1}H-NMR pattern was also observed for the *t*-Bu–C(3′) protons. The latter are equivalent in the *anti*-conformer (1.44 ppm), but split into two *singlets* in the *syn*-conformer (1.33 and 1.55 ppm). Furthermore, the eight *t*-Bu–C(3) groups on the phenyl substituents of the outer porphyrin ring form equivalent pairs in both conformers and the expected two *singlets* are clearly observed (1.40 and 1.47 ppm) in the ^{1}H-NMR spectrum (*Fig. 10*). Again, both *syn*- and *anti*-conformations should also be adopted by higher oligomers of this class with odd numbers of tetrapyrrolic macrocycles.

In sharp contrast, no evidence for a face-to-face interaction between the C-spheres and the triply-fused porphyrins of **8** could be detected by NMR spectroscopy. In the ^{1}H-NMR (500 MHz, $CDCl_3$, 298 K) spectrum, the *t*-Bu H-atoms only display one *singlet*, and in the ^{13}C-NMR spectrum (125 MHz, $CDCl_3$, 298 K), only two resonances are attributed to the *t*-Bu groups (one to the quaternary C(sp^3)-atom (34.87 ppm) and one to the primary C(sp^3)-atom (31.70 ppm)). This finding suggests that the interchromophoric interactions in **8** are much weaker than in **4**. As a consequence, the conformation of **8** depicted in *Scheme 5* is only one of many possible; conformers with the C-spheres nesting on opposite faces of the triply-linked porphyrin dimer or turned away from the macrocycle are equally probable.

By means of variable-temperature (VT) ^{1}H-NMR measurements, two conformational motions were observed (*Fig. 11*): *i*) *Rotation 1* around the single bond between the terminal porphyrin rings and the 3,5-di(*tert*-butyl)phenyl moieties, which could be monitored in all dyads **3**–**7** following the temperature-induced shifts of the H–C(2) and *t*-Bu proton resonances, and *ii*) *Rotation 2* around the single bond between the porphyrin and the *meso*-phenyl ring to which the fullerene moiety (or the silyl ether residue in **27**) is attached. This motion was monitored in dyad **4** by following the temperature dependence of the resonances $H_\beta(1)$ and $H_\beta(2)$ (*Fig. 11*). The activation parameters ($\Delta H^{\ddagger}$, $\Delta S^{\ddagger}$, and $\Delta G^{\ddagger}$ at 298 K) correlated to these rotations were subsequently determined and are reported in *Table 1*. Since the coalescence temperatures of the ^{1}H resonances could not be reached due to boiling point limitations of the used deuterated solvents, the activation parameters for the rotations in **3** and **4** were

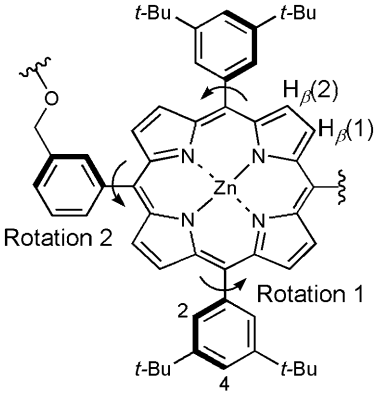

Fig. 11. *Rotatory motions observed for fullerene–porphyrin conjugates* **3**–**7** *by VT-NMR spectroscopy*

estimated using the method reported by *Sandström* [37], and applied to porphyrins by *Eaton* and *Eaton* [38]. As an example, the *Eyring* plot obtained for **3** is shown in *Fig. 12*.

Very similar results were obtained for the two independently monitored resonances of H–C(2) and *t*-Bu–C(3). At 298 K, $\Delta G^{\neq}$ for *Rotation 1* in **3** was found to be *ca.* 19.2 kcal mol^{-1}, whereas the according values for *Rotation 2* in **4** and **27** are *ca.* 21.4 and 18.1 kcal mol^{-1}, respectively.

Table 1. *Rotatory Motions in Fullerene–Porphyrin Conjugates*[a])

Compound	Solvent	H-Atom	*Rotation*[b])	$\Delta H^{\neq}$ [kcal · mol^{-1}]	$\Delta S^{\neq}$ [cal · mol^{-1} · K^{-1}]	$\Delta G^{\neq}_{298}$ [kcal · mol^{-1}]
3	$C_6D_5CD_3$ ($\varepsilon = 2.38$)	H–C(2)	*1*	18.5	– 1.6	18.9
		t-Bu–C(3)	*1*	18.8	– 1.5	19.2
3	$C_2D_2Cl_4$ ($\varepsilon = 10.36$)	H–C(2)	*1*	13.4	– 15.8	18.1
		t-Bu–C(3)	*1*	13.6	– 16.0	18.1
3	(D_8)Dioxane ($\varepsilon = 2.25$)	H–C(2)	*1*	15.3	– 10.9	18.5
		t-Bu–C(3)	*1*	14.9	– 11.7	18.4
4	$C_6D_5CD_3$	*t*-Bu–C(3)	*1*	–	–	18.7
		H–C(4)	*2*	20.7	2.3	21.4
27	$C_6D_5CD_3$	H_β–C(2)	*2*	13.5	– 15.3	18.1

[a]) Experimental uncertainty ± 1.5 kcal mol^{-1} ($\Delta H^{\neq}$) and ± 3 cal mol^{-1} K^{-1} ($\Delta S^{\neq}$). [b]) For the definition of the rotations, see *Fig. 11*.

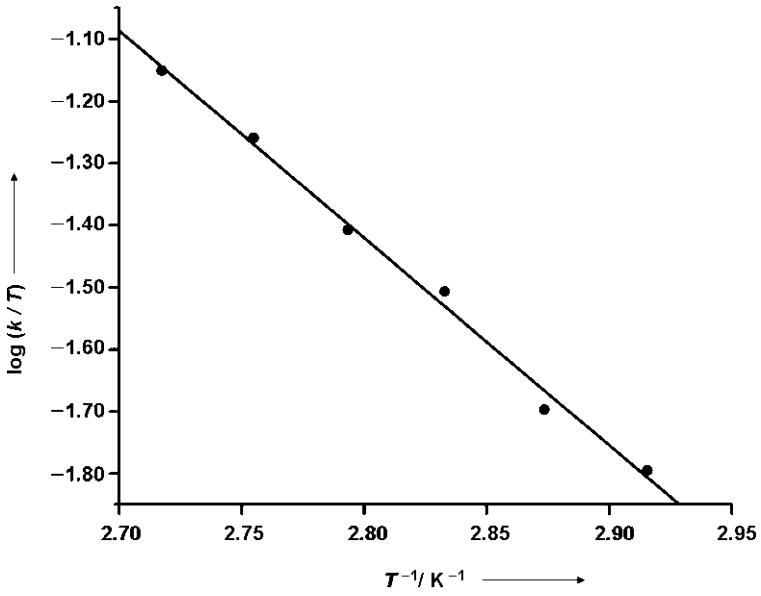

Fig. 12. Eyring *plot and activation parameters from calculated rate constants* (k_e) *for the phenyl rotation of conjugate* **3** *in* (D_8)*dioxane*

Assuming that there are no significant interactions between the (*t*-Bu)Me_2Si groups and the porphyrin rings in **27**, we can conclude that the attractive interactions between the fullerene and the tangential porphyrin in **4** increase the activation free enthalpy for *Rotation 2* by *ca.* 3.3 kcal mol^{-1}. In light of the flexibility of the malonate linker bearing the fullerene moiety, it is reasonable to assume that this increase in $\Delta G^{\ddagger}_{298}$ largely reflects the magnitude of the ground-state interactions between the two chromophores in $C_6D_5CD_3$.

The good solubility of dyad **3** in a wide range of solvents allowed the study of the rotary motion in other solvents such as (D_8)dioxane and $C_2D_2Cl_4$ (measurements carried out in THF led to inaccurate results due to the limited accessible temperature range). While $\Delta G^{\ddagger}_{298}$ stays substantially unchanged (within the error range of the measurement), $\Delta H^{\ddagger}$ and $\Delta S^{\ddagger}$ are strongly affected by the nature of the solvent. $\Delta H^{\ddagger}$ increases in the order $C_2D_2Cl_4 <$ (D_8)dioxane $< C_6D_5CD_3$, whereas $\Delta S^{\ddagger}$ decreases in the same order. At present, we do not have a good explanation for these observations.

2.4. *Photophysical Analysis.* 2.4.1. *Steady-State UV/VIS Absorption Spectra Analysis.* The electronic absorption spectra of the *meso*,*meso*-linked bis[60]fullerene–oligoporphyrin arrays in PhMe at 298 ± 2 K together with those of reference compounds **14** and **21**–**23** are shown in *Table 2* and *Fig. 13*. In the UV window, the fullerene-centered absorption is stronger than that of the porphyrin, whereas in the VIS-spectral region an opposite trend is observed. The spectra of the five conjugates **3**–**7** differ dramatically. In particular, a splitting of the *Soret* band (S_2 state) due to exciton coupling is observed for **4**–**7**, relative to the parent monomer **3** (for UV/VIS studies in the solid state, see [39]). Both bands show a progressive enhancement of the molar absorption coefficient values (ε) with increasing number of porphyrin moieties. While the higher-energy *Soret*-type band negligibly shifts, the lower-energy feature moves to higher wavelength upon elongation of the porphyrin backbone [18]. Band

Table 2. *UV/VIS Data of Fullerene–Porphyrin Conjugates* **3**–**7** *in Comparison with the Porphyrin Derivatives* **14** *and* **21**–**23**. Spectra recorded at 298 ± 2 K in PhMe.

Compound	λ_{max}/nm [eV] (ε/M^{-1} cm^{-1})					
3	328 [3.78] (41900)	421 [2.95] (23300)	508 [2.44] (3540)	546 [2.27] (14300)	582 [2.13] (2860)	682 [1.82] (640)
4	331 [3.75] (83300)	426 [2.91] (123100)	465 [2.67] (143300)	562 [2.21] (36500)	600 [2.21] (6930)	682 [1.82] (640)
5	335 [3.70] (102100)	420 [2.95] (61100)	481 [2.58] (61300)	568 [2.18] (23200)	–	682 [1.82] (760)
6	333 [3.72] (165000)	419 [2.96] (256500)	489 [2.54] (286300)	572 [2.17] (121200)	–	682 [1.82] (2160)
7	333 [3.72] (70100)	418 [2.97] (158700)	458 [2.71] (176100)	558 [2.22] (43400)	594 [2.09] (7680)	682 [1.82] (760)
14	309[4.01] (8030)	412 [3.01] (237400)	539 [2.30] (11100)	575 [2.16] (1410)	–	–
21	309 [4.01] (21900)	415 [2.99] (180400)	451 [2.75] (167800)	554 [2.24] (41500)	591 [2.10] (4310)	–
22	309 [4.01] (36100)	412 [3.01] (279000)	474 [2.62] (234600)	564 [2.20] (72800)	600 [2.07] (9020)	–
23	305 [4.07] (48500)	413 [3.00] (346700)	485 [2.56] (303100)	569 [2.18] (11600)	606 [2.05] (16700)	–

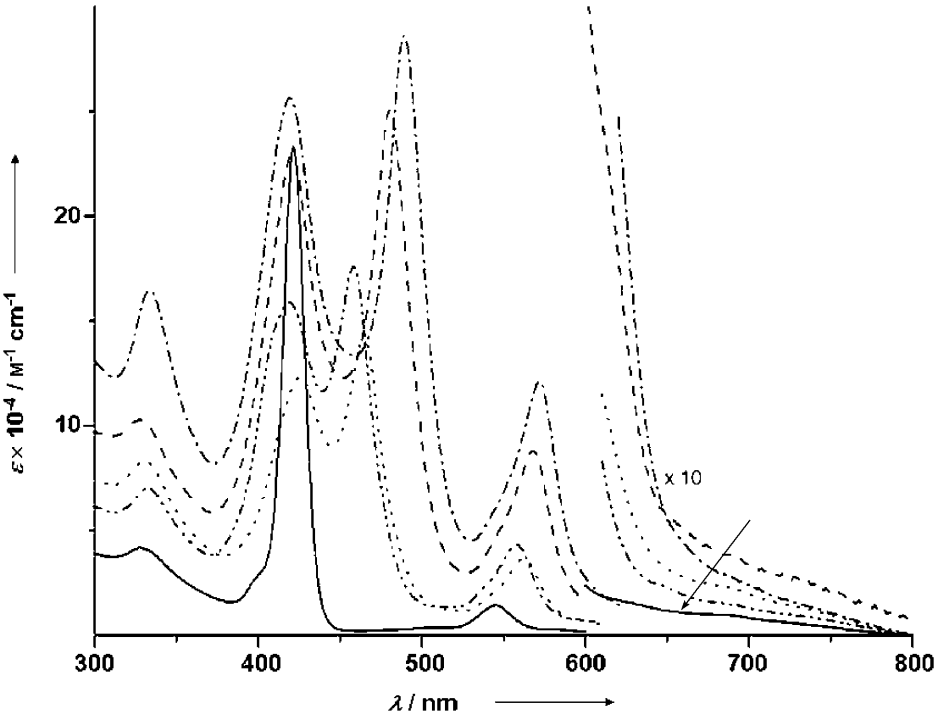

Fig. 13. *UV/VIS Spectra of conjugates* **3** (—), **4** (····), **5** (—), **6** (-·-·-), *and* **7** (-··-··) *in PhMe at 298 K*. The arrow indicates the CS-state-centered absorption.

maxima shift from 558 (**7**), to 562 (**4**), to 568 (**5**), and to 572 nm (**6**). Similar red shifts are also observed for the *Q* band above 540 nm (for a comprehensive photophysical study of the bis([60]fullerene)–porphyrin conjugates, see [40]).

Fig. 14 displays the absorption spectrum of conjugate **4** compared to the sum of the spectra of its component units, taking both **21** and **27** as porphyrin and compound **48** as fullerene reference fragments. In neither case, good overlapping is obtained, and this indicates specific porphyrin–fullerene interactions in the multicomponent system **4**, related to tight face-to-face vicinity between the two chromophores. This is also

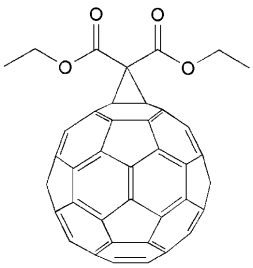

48

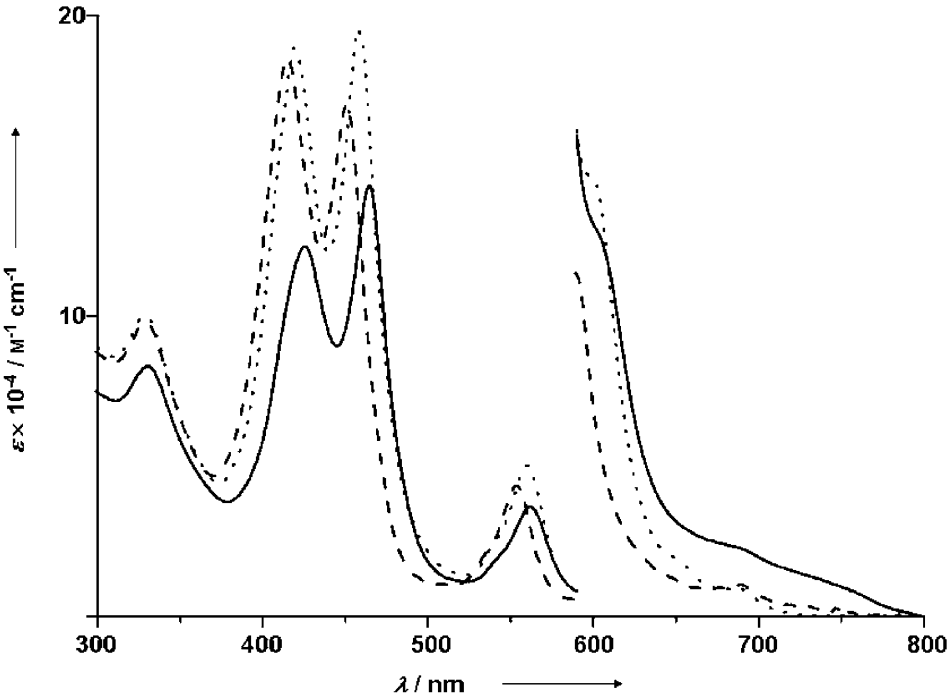

Fig. 14. *UV/VIS Spectra of compounds* **4** (—), *2* × **48** + **21** (---), *and 2* × **48** + **27** (····) *recorded in PhMe at 298 K*

signalled by the strong decrease and slight red shift of the higher energy *Soret* feature, accompanied by the new absorption detected above 700 nm and attributed to low-energy charge-transfer (CT) transitions [8][10]. The strong interchromophoric interactions and the peculiarity of the specific porphyrin backbone are also exemplified in the comparison depicted in *Fig. 15*. The experimental spectrum of *meso,meso*-linked tetraporphyrin **6** bears no similarity with the profile obtained by summing a porphyrin dimer (**21**, central core) and two terminal fullerene–porphyrin dyads **3**.

Fig. 16 depicts the UV/VIS spectra of bis[60]fullerene–diporphyrin conjugates **4** and **8**. Interestingly, while the higher-energy *Soret*-type band is centered almost at the same wavelength in both dyads (426 and 423 nm for **8** and **4**, resp.), the lower-energy band in **8** undergoes a significant bathochromic shift (*ca.* 100 nm) as compared to **4**. The exciton splitting energies are *ca.* 0.24 and 0.75 eV for **4** and **8**, respectively.

2.3.2. *Emission-Spectra Analysis of* **8**. At any excitation wavelength, **45** exhibits an emission band in the NIR region ($\lambda_{max} = 1080$ nm) [10]. This is a mirror image of the *Q*-band profile, and is unambiguously assigned to emission from the lowest singlet-excited state. Upon selective excitation of the porphyrin chromophore (420 or 585 nm), the NIR emission band is observed also for **8** ($C_{60}-{}^1(Zn\cdot P{\equiv}P\cdot Zn)^*-C_{60}$). This band is shifted by 12 nm ($\lambda_{max} = 1092$ nm) relative to **45**, in line with the absorption trend. Upon excitation (*ca.* 80%) of the fullerene moiety of **8** at 330 nm, a strong quenching of the fullerene fluorescence, relative to reference compound **48**, is detected. Fullerene

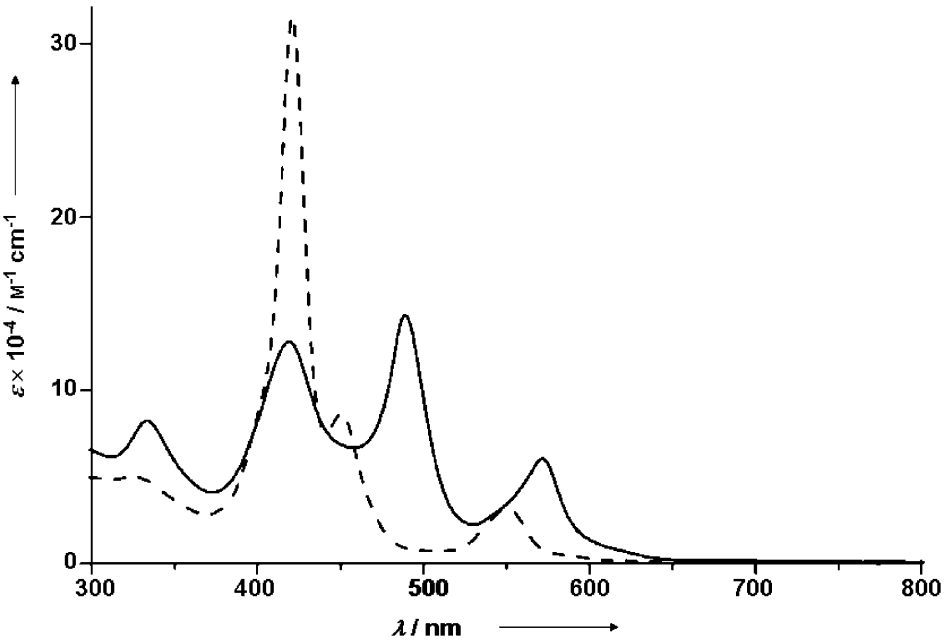

Fig. 15. *UV/VIS Spectra of a* $2 \times$ **3** $+$ **21** *mixture* (- - -) *and conjugate* **6** (—) *recorded in PhMe at 298 K*

quenching is accompanied by sensitization of the porphyrin fluorescence in the NIR region. The population of the porphyrin singlet level ($C_{60}-{}^1(Zn\cdot P{\equiv}P\cdot Zn)^*-C_{60}$) is quantitative and, by comparison with **45**, no quenching of this excited state is detected from fluorescence intensity measurements. The above results clearly indicate the occurrence of photoinduced singlet energy transfer from the fullerene unit to the porphyrin core ($^1C_{60}^*-(Zn\cdot P{\equiv}P\cdot Zn)-C_{60}\rightarrow C_{60}-{}^1(Zn\cdot P{\equiv}P\cdot Zn)^*-C_{60}$), and that electron transfer to the lowest-lying charge-separated state ($C_{60}-(Zn\cdot P{\equiv}P\cdot Zn)-C_{60}\rightarrow C_{60}-(Zn\cdot P{\equiv}P\cdot Zn)^{\cdot+}-C_{60}^{\cdot-}$) is not competitive with ultrafast deactivation of the porphyrin singlet ($\tau_F = 4.5$ ps) back to the ground state ($C_{60}-{}^1(Zn\cdot P{\equiv}P\cdot Zn)^*-C_{60}\rightarrow C_{60}-(Zn\cdot P{\equiv}P\cdot Zn)-C_{60}$; *Fig. 17*) [16].

The quenching factor (Q_F) of fullerene fluorescence relative to that for model compound **48** is *ca.* 10, and a rate constant k_{EN} of *ca.* 6×10^9 s^{-1} can be estimated for the energy transfer process from *Eqn. 1*[1]):

$$k_{EN} = (Q_F - 1)/\tau_F \tag{1}$$

where τ_F (1.6 ns) is the singlet lifetime of **48** [8].

---

[1]) This equation can be used to evaluate the quenching rate of a luminescent moiety and is obtained from $k_Q = 1/\tau - 1/\tau_0$, taking into account that $\Phi/\Phi_0 = \tau/\tau_0$, where Φ (emission quantum yield) and τ (excited-state lifetime) refer to the quenched unit, and Φ and τ refer to an unquenched reference model compound; see [41].

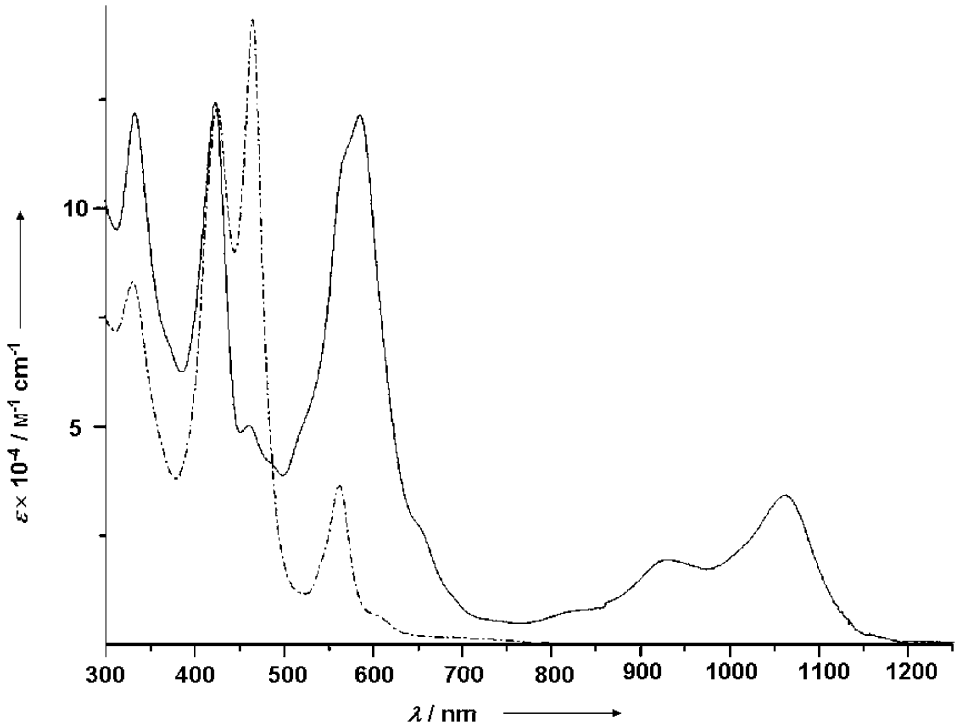

Fig. 16. *UV/VIS Spectra of compounds* **4** (---) *and* **8** (—) *recorded in PhMe at 298 K*

Formation of the fullerene triplet is ruled out by monitoring the NIR luminescence of singlet O_2 ($^1O_2$), a convenient marker for fullerene triplets (*Fig. 18*) [42]. The steady-state VIS-NIR luminescence spectrum of **48** in air-equilibrated PhMe solution exhibits the diagnostic $^1O_2$ luminescence peak at 1270 nm, which is no longer observed after removal of O_2 from the solution. This treatment has no effect on the emission spectrum of **8**, confirming that no $^1O_2$ (*i.e.*, no fullerene triplet) is produced under fullerene excitation at 330 nm. Notably, also the porphyrin reference compound **45** does not show any $^1O_2$ emission signal, at any excitation wavelength. Given the energy position of the lowest singlet state of **45** (1.15 eV), it is likely that the corresponding triplet level is lower in energy than that of the excited singlet state of molecular oxygen ($^1\Delta_g(^1O_2) = 0.98$ eV), thus rendering thermodynamically forbidden the triplet-singlet energy transfer sensitization process responsible for $^1O_2$ generation [43].

Electronic delocalization in porphyrin tapes allows progressive lowering of the electronic levels with increasing molecular length [11]. From the lack of $^1O_2$ sensitization of the smallest (dimer) tape that has been observed here, one may anticipate that all porphyrin tapes are unable to produce $^1O_2$, unlike 'regular' porphyrin molecules, which are among the best and most widely investigated photosensitizers of $^1O_2$ [43]. In this regard, we note that the relative $^1O_2$ sensitization yield of porphyrin monomer **14** and *meso,meso*-linked oligoporphyrins **21**–**23** in air-equilibrated PhMe solutions turned out to be identical within the experimental error.

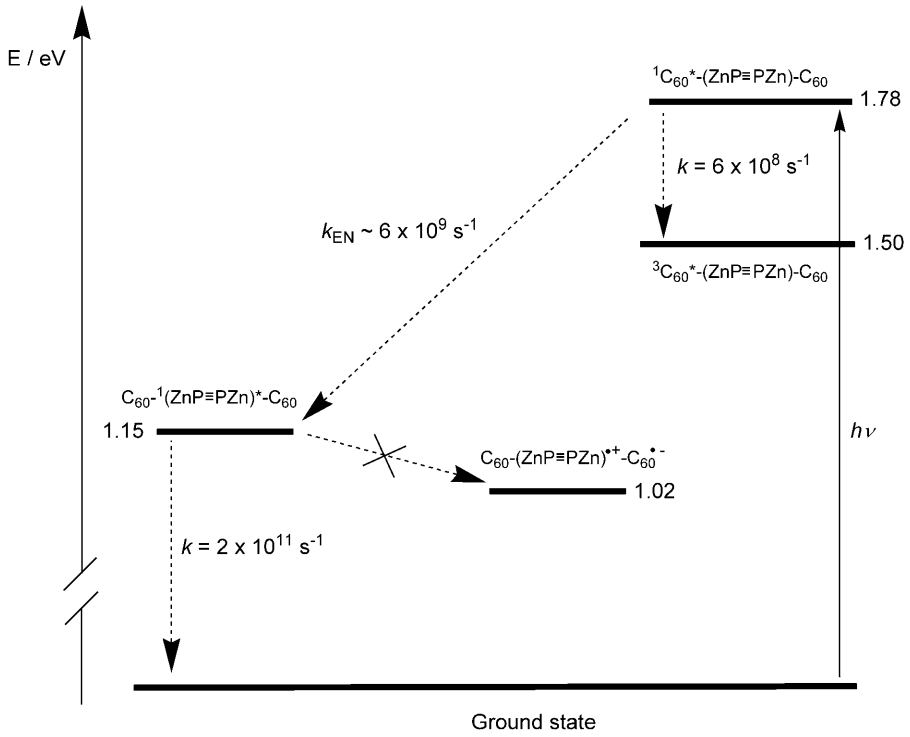

Fig. 17. *Energy-level diagram* (PhMe) *and intercomponent processes following photoexcitation of the methano[60]fullerene residue of triply-fused diporphyrin–fullerene conjugate* **8** (C_{60}–(Zn·P≡P·Zn)–C_{60}). The lowest electronic excited states located on each moiety and the intramolecular charge-separated state are reported. The excited-state energies localized on the fullerene and porphyrin units were calculated from absorption and luminescence spectra, except for that of C_{60}–$(Zn \cdot P \equiv P \cdot Zn)^{\cdot+}$–$C_{60}^{\cdot-}$ which was estimated from electrochemical data (*Table 3*).

2.4. *Electrochemical Investigations.* The redox characteristic of all new compounds listed in *Table 3* were studied by cyclic (CV) and differential pulse (DPV) voltammetry in CH_2Cl_2 (+0.1M Bu_4NPF_6) at 293 ± 2 K. All potentials are referenced to the ferrocene/ferricinium (Fc/Fc^+) couple, used as internal standard. Tetrakis(*meso*-arylated) **46** displayed very similar electrochemical behavior to that of bis(*meso*-arylated) **14**. The typical DPV of **46** (*Fig. 19*, curve *c*) showed four redox peaks with a potential difference of 0.29 V ($Zn \cdot P^{1+}/Zn \cdot P^{2+} - Zn \cdot P/Zn \cdot P^{1+}$) and 0.38 V ($Zn \cdot P^{1-}/Zn \cdot P^{2-} - Zn \cdot P/Zn \cdot P^{1-}$) between the two oxidation and the two reduction steps, respectively. Comparison of these electrochemical data with those of **14** revealed some anodic shifts for both the two reduction and the first oxidation peaks. This can be explained by the presence of two electron-withdrawing 3-cyanophenyl substituents at positions 5 and 15 of the porphyrin macrocycle. Compound **41** (*Fig. 19*, curve *b*) displayed very similar electrochemical behavior to **21**, except for a small difference in the reduction peak potentials. The biaryl-type dimer **41** showed two partially overlapping reduction peaks at −1.72 and −1.83 V with a difference of 0.11 V. The

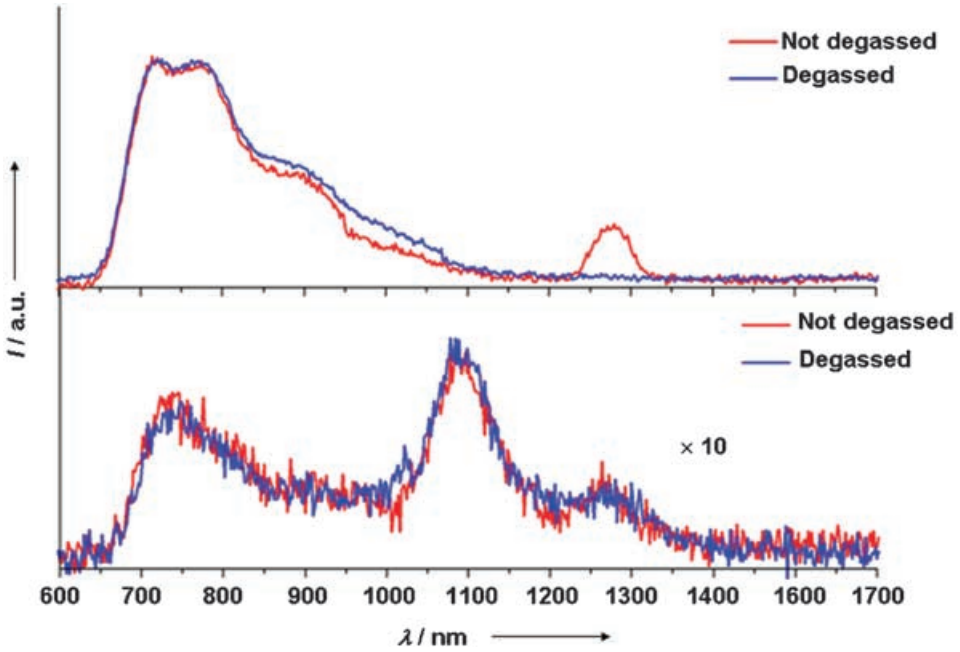

Fig. 18. *Sensitized* $^1O_2$ *luminescence spectra of compounds* **48** (top) *and* **8** (bottom) *in air-equilibrated* (red) *and air-free* (blue) *solutions in PhMe.* $A = 0.600$ for all samples, $\lambda_{exc} = 330$ nm. For compound **8**, light absorption partitioning between C_{60} and porphyrin moieties is 4 : 1. The peak with a maximum at *ca.* 720 nm corresponds to some residual signal fullerene-centered fluorescence (quenching factor of 10 relative to **48**)

first one-e$^-$ oxidations of the two porphyrin moieties appeared as separate peaks at 0.33 and 0.47 V. Similarly, the second oxidation of both rings gives two couples as well, at 0.77 and 1.07 V. In comparison with compound **46**, each peak is split into two and the reduction peak potentials are negatively shifted by 40–110 mV (*Table 3*). The potential gap between the first oxidation and reduction potentials ($E^{1/2}_{ox,1} - E^{1/2}_{red,1}$) in the CV is *ca.* 2.13 V, which is almost identical to that of monomer **46** (2.15 V).

The electrochemical behavior of triply-linked porphyrin dimer **38** (Zn·P≡P·Zn) differs dramatically from those of monomeric porphyrin **46** and *meso*,*meso*-dimer **41** (*Table 3*). As shown in *Fig. 19* (curve *a*), seven redox peaks in CH_2Cl_2 with identical peak current were observed for the triply-linked porphyrin dimer **38**. The first (Zn·P≡P·Zn/Zn·P≡P·Zn^{1-}, −0.97 V) and second (Zn·P≡P·Zn^{1-}/Zn·P^{1-}≡P·Zn^{1-}, −1.23 V) reduction peaks correspond to two one-e$^-$ processes, formally equivalent to one-e$^-$ reductions for each porphyrin ring. Likewise, the first (Zn·P≡P·Zn/Zn·P≡P·Zn^{1+}, 0.08 V) and the second (Zn·P≡P·Zn^{1+}/Zn·P^{1+}≡P·Zn^{1+}, 0.35 V) oxidation peaks correspond each to a one-e$^-$ process, one per porphyrin ring. The third (Zn·P^{1+}≡P·Zn^{1+}/Zn·P^{1+}≡P·Zn^{2+}, 0.81 V) and fourth (Zn·P^{1+}≡P·Zn^{2+}/Zn·P^{2+}≡P·Zn^{2+}, 1.08 V) oxidation peaks represent the two second one-e$^-$ oxidation processes. Relative to **46**, the first one-e$^-$ reduction potential of **38** is anodically shifted by 0.71 V (CH_2Cl_2), whereas the first one-e$^-$ oxidation potential is negatively shifted by 0.34 V (CH_2Cl_2). Unfortunately, the fourth one-e$^-$ reduction step could not be identified in the

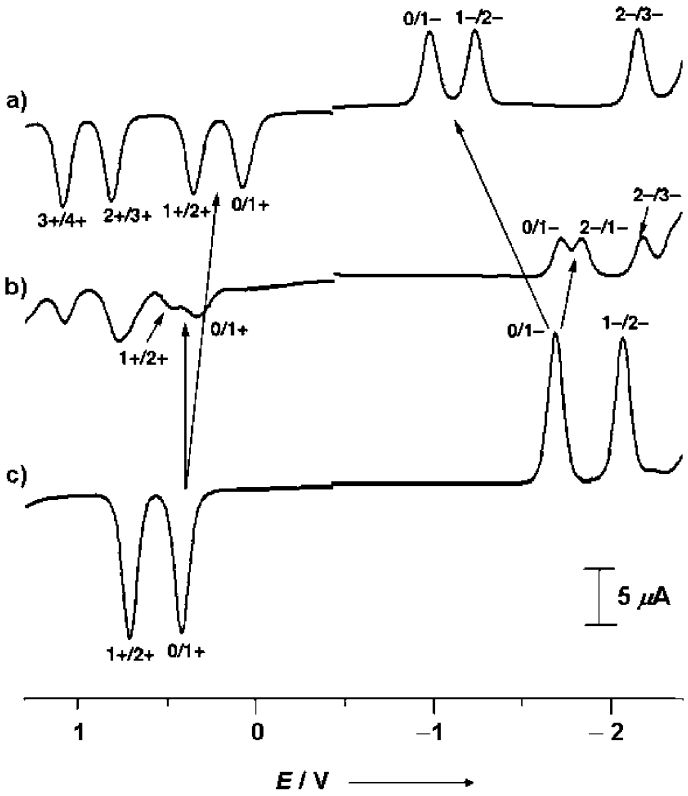

Fig. 19. *Differential pulse voltammogram of porphyrins* **38** (*a*), **41** (*b*), *and* **46** (*c*) *in* CH_2Cl_2 *at 293 K*

cyclic voltammogram of **38** in CH_2Cl_2 because of the limited potential window which did not permit a scan to potential values more negative than -2.5 V.

CV and DPV measurements performed in THF, allowed the detection of the fourth reduction peak for triply-linked dimer **38** (-2.56 V, THF; see *Table 3*), confirming that each redox process of **46** splits into two processes in the case of **38**. The reduction peaks shifted negatively by 50–200 mV, while the oxidation peaks shifted positively by *ca.* 100 mV, and the peak-to-peak separations increased by *ca.* 20–50 mV, as compared to those observed when the DPVs were performed in CH_2Cl_2.

To unambiguously confirm that each peak observed in the CV and DPV of **38** corresponds to a one-e^- transfer process centered on the zinc–porphyrin units, CV measurements of **38** and **46** were performed at different concentrations. The current intensity observed in the voltammogram of a 0.2 mM solution of **46** in CH_2Cl_2 was found to be exactly twice as high as that of a 0.1 mM solution of **38**. The normalized peak current (peak current/concentration ratio) for **38** was, as expected, identical to that of **46**. It can be noted that the difference in potential between the first and second reduction peaks for **38** (0.25 V, CH_2Cl_2) is almost identical to those between the first and second (0.28 V, CH_2Cl_2), and the third and fourth oxidation peaks (0.27 V, CH_2Cl_2). The potential difference between the first oxidation and the first reduction

Table 3. *Redox Potentials of Triply-Linked Porphyrin Derivatives* **8**, **38**, *and* **45**, *and Reference Compounds* **41**, **45**, *and* **46** *in Ar-Purged CH_2Cl_2. $T = 298 \pm 2$ K, 0.1M Bu_4NPF_6 as supporting electrolyte; potentials vs.* Fc/Fc^+.

Compound	CV[a]) [V]							
	$E^{1/2}_{red,1}$ [ΔE_{pp}]	$E^{1/2}_{red,2}$ [ΔE_{pp}]	$E^{1/2}_{red,3}$ [ΔE_{pp}]	$E^{1/2}_{red,4}$ [ΔE_{pp}]	$E^{1/2}_{ox,1}$ [ΔE_{pp}]	$E^{1/2}_{ox,2}$ [ΔE_{pp}]	$E^{1/2}_{ox,3}$ [ΔE_{pp}]	$E^{1/2}_{ox,4}$ [ΔE_{pp}]
8	– 0.99/ – 1.09 [60]	– 1.40 [80]	– 1.87 [108]	– 2.29 [80]	0.03 [60]	0.34 [68]	0.82 [80]	1.09 [70]
38[c])	– 1.06 [80]	– 1.40 [90]	– 2.29 [90]	– 2.59 [110]	0.15 [68]	0.47 [75]	0.92 [110]	-
38	– 1.01 [62]	– 1.26 [60]	– 2.18 [66]	–	0.09 [60]	0.37 [60]	0.83 [62]	1.10 [64]
41	– 1.75 [60]	– 1.86 [60]	– 2.20 [80]	–	0.38 [62]	0.51 [62]	0.78 [128]	1.10 [60]
45	– 1.12 [62]	– 1.36 [60]	–	–	– 0.01 [60]	0.29 [60]	0.77 [50]	1.03 [60]
46	– 1.71 [68]	– 2.09 [80]	–	–	0.44 [62]	0.74 [70]	–	–
	DPV[b]) [V]							
	$E^p_{red,1}$	$E^p_{red,2}$	$E^p_{red,3}$	$E^p_{red,4}$	$E^p_{ox,1}$	$E^p_{ox,2}$	$E^p_{ox,3}$	$E^p_{ox,4}$
8	– 0.97/ – 1.06 ($3e^-$)	– 1.38 ($3e^-$)	– 1.84 ($2e^-$)	– 2.28 ($3e^-$)	– 0.01 ($1e^-$)	0.3 ($1e^-$)	0.79 ($1e^-$)	1.06 ($1e^-$)
38[c])	– 1.05 ($1e^-$)	– 1.38 ($1e^-$)	– 2.26 ($1e^-$)	– 2.56 ($1e^-$)	0.12 ($1e^-$)	0.45 ($1e^-$)	0.88 ($1e^-$)	–
38	– 0.97 ($1e^-$)	– 1.23 ($1e^-$)	– 2.15 ($1e^-$)	–	0.08 ($1e^-$)	0.35 ($1e^-$)	0.81 ($1e^-$)	1.08 ($1e^-$)
41	– 1.72 ($1e^-$)	– 1.83 ($1e^-$)	– 2.18 ($1e^-$)	–	0.33 ($1e^-$)	0.47 ($1e^-$)	0.77 ($1e^-$)	1.07 ($1e^-$)
45	– 1.04 ($1e^-$)	– 1.28 ($1e^-$)	–	–	0.05 ($1e^-$)	0.26 ($1e^-$)	0.74 ($1e^-$)	1.00 ($1e^-$)
46	– 1.68 ($1e^-$)	– 2.06 ($1e^-$)	–	–	0.42 ($1e^-$)	0.71 ($1e^-$)	–	–

[a]) Scan rate: 0.1 mV s^{-1}; $E^{1/2} = (E_{pa} + E_{pc})/2$, where E_{pc} and E_{pa} are the cathodic and anodic peak potentials, respectively; $\Delta E_{pp} = E_{pa} - E_{pc}$. [b]) Scan rate: 0.4 mV s^{-1}, amplitude: 50 mV, pulse width: 0.05 s^{-1}; E^p is the peak potential. [c]) Data recorded in THF.

($E^{1/2}_{ox,1} - E^{1/2}_{red,1}$, CH_2Cl_2) decreases significantly upon changing from porphyrin **46** (2.15 V) and biaryl-type diporphyrin **41** (2.13 V) to the planar porphyrin dimer **38** (1.10 V). This decrease of the electrochemical HOMO-LUMO gap is the result of the extension of the π-conjugation between the porphyrin moieties. Hence, all differences in the electrochemical behavior between **38**, **41**, and **46** can be explained in terms of extension of the π-conjugation between the two fused Zn^{II} tetrapyrrole rings.

Functionalization of the triply-linked porphyrin dimer with two methano[60]fullerene moieties (**8**) introduces eight additional redox processes as shown in *Fig. 20* (curves *a* and *b*), thus leading to an electrochemical fingerprint with a total of fifteen electrons per molecule in the investigated potential range (– 2.5 to 1.25 V, CH_2Cl_2). The four oxidation peaks correspond to the four one-e^- oxidation steps centered on the porphyrin units, the first oxidation ($C_{60}-Zn\cdot P{\equiv}P\cdot Zn-C_{60}/C_{60}-Zn\cdot P{\equiv}P\cdot Zn^{1+}-C_{60}$) peak being cathodically shifted by 60 mV relative to that of **38** ($Zn\cdot P{\equiv}P\cdot Zn/Zn\cdot P{\equiv}P\cdot Zn^{1+}$; *Table 3*). The two partially overlapping peaks at – 1.0 V correspond to the first fullerene- and porphyrin-centered reductions ($C_{60}-Zn\cdot P{\equiv}P\cdot Zn-C_{60}/C^{1-}_{60}-Zn\cdot P{\equiv}P\cdot Zn^{1-}-C^{1-}_{60}$, a three-$e^-$ process). Similarly, the peak ($C^{1-}_{60}-Zn\cdot P{\equiv}P\cdot Zn^{1-}-C^{1-}_{60}/C^{2-}_{60}-Zn\cdot P^{1-}{\equiv}P\cdot Zn^{1-}-C^{2-}_{60}$) at – 1.38 V corresponds to the second fullerene- and porphyrin-centered reductions (once more, a total of three e^- are involved). The peak at – 1.84 V is attributed to the third one-e^- reduction ($C^{2-}_{60}-Zn\cdot P^{1-}{\equiv}P\cdot Zn^{1-}-C^{2-}_{60}/C^{3-}_{60}-Zn\cdot P^{1-}{\equiv}P\cdot Zn^{1-}-C^{3-}_{60}$, a two-$e^-$ process) of the two fullerene moieties. This interpretation is based on the lower peak current when compared to those at – 1.0 and – 1.4 V. The peak at – 2.28 V corresponds to the fourth one-e^- reduction of the fullerene moieties and to the third one-e^- reduction ($C^{3-}_{60}-Zn\cdot P^{1-}{\equiv}P\cdot Zn^{1-}-C^{3-}_{60}/C^{4-}_{60}-Zn\cdot P^{1-}{\equiv}P\cdot Zn^{2-}-C^{4-}_{60}$, a three-$e^-$ process) of the diporphyrin units.

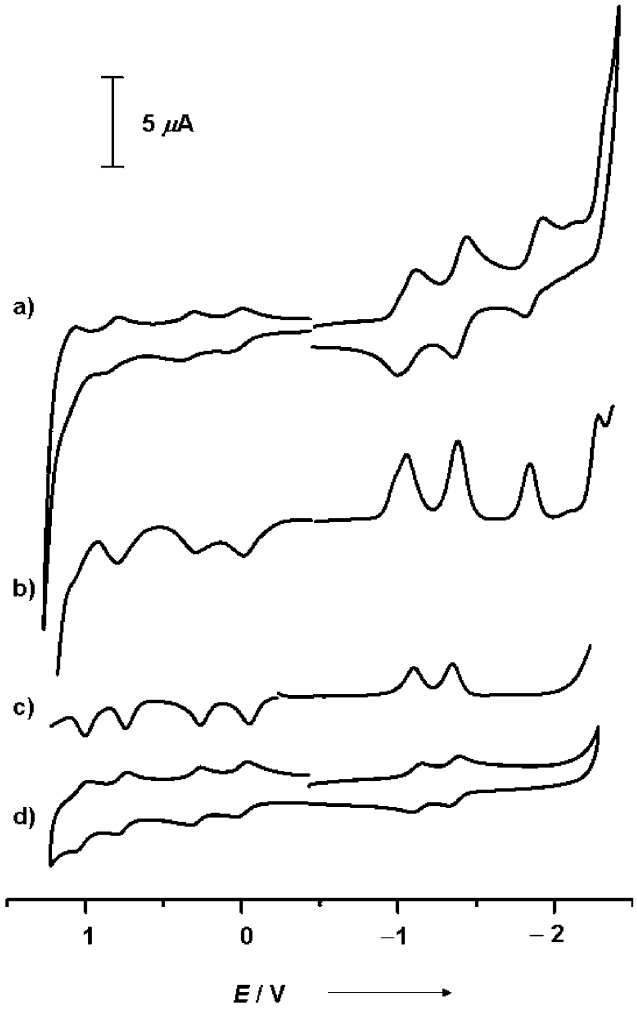

Fig. 20. *Typical cyclic and differential pulse voltammograms of compounds* **8** (curves *a* and *b*, resp.) *and* **45** (curves *c* and *d*, resp.) *in* CH_2Cl_2 *at 293 K*

For comparison, CVs and DPVs of **45** were also measured in CH_2Cl_2. The results are illustrated in *Fig. 20* (curves *c* and *d*). These experiments revealed a similar electrochemical behavior for the diporphyrin unit as in the case of derivative **8**. In general, all porphyrin-centered redox peaks in **8** were found at more positive potentials in comparison to those of **45** (*Table 3*), suggesting that the oxidation of the tetrapyrrolic macrocycles in **8** is more difficult whereas the reductions are easier. Comparing the first oxidation potential of **45** with that of **8**, a cathodic shift of 40 mV was observed while the effect on the second and third oxidations is somewhat larger (*ca.* 50 mV). Although the shifts are small, these results are similar to those reported [10][40] for the *meso*,*meso*-linked bis[60]fullerene – oligoporphyrin conjugates de-

scribed above, suggesting the existence of a mutual electronic influence between the fullerene and the porphyrin moieties within **8**. The measured $E^{1/2}_{ox,1} - E^{1/2}_{red,1}$ gap in CH_2Cl_2 was 1.13 V for **45** which is slightly larger than that of **8** (1.02 V).

3. Conclusion. – A series of fullerene–oligo(Zn^{II} porphyrin) conjugates were prepared with the aim to investigate in detail the chromophoric interaction between the C-spheres and the tetrapyrrolic macrocycles both in solution and on surfaces [34]. Two rod-like porphyrin architectures were selected for this study: biaryl-type *meso,meso*-linked and sheet-like triply-linked porphyrin arrays initially introduced by *Osuka* and co-workers [11–18]. Some of the Zn^{II} porphyrins, prepared as intermediates and as control compounds, were found to form infinite one-dimensional supramolecular networks in the solid state, in which the porphyrin moieties interact with each other either through H-bonding or metal ion coordination. ^{1}H- and ^{13}C-NMR spectroscopy established that the C-spheres appended to the *meso,meso*-linked arrays adopt a close tangential orientation relative to the plane of the adjacent tetrapyrrolic macrocycles although they are only singly linked to the porphyrin backbone. As a result of the interchromophoric attraction, dyads **4**–**6** feature distinct conformational preferences. By VT-NMR measurements, the ground-state fullerene–Zn^{II} porphyrin interaction in these hybrid systems was quantified as $\Delta G = -3.3$ kcal mol^{-1} (PhMe, 298 K). In contrast, the chromophoric interaction between the triply-fused diporphyrin sheet and the two appended fullerenes in **8** is weak, and no orientational preference of the C-spheres was observed by NMR. Photophysical studies confirmed the strong ground-state interchromophoric interactions in the *meso,meso*-linked oligoporphyrin–bis[60]fullerene conjugates **4**–**6**. In other work, we had demonstrated efficient photoinduced electron transfer from the oligoporphyrin donors to the fullerene acceptors in these systems [40]. By contrast, the triply-fused dimer **8** exhibits unprecedented fullerene → porphyrin photoinduced energy transfer, resulting in quantitative sensitization of the low-lying, short-lived singlet excited state of the latter [10]. *meso,meso*-Linked diporphyrins exhibit $^1O_2$ sensitization capability, whereas the triply-fused systems are unable to sensitize the formation of $^1O_2$ because of the low-energy content of their lowest singlet (1.15 eV) and triplet excited states. The electrochemical studies clearly demonstrate the presence of an electronic interaction between porphyrin and fullerene moieties in all conjugates reported here. This interaction shifts the potentials of the first fullerene-centered one-electron reduction and the porphyrin-centered oxidation/reduction steps. The experimental results also show that all oligoporphyrin arrays, with or without appended methano[60]fullerene moieties, have an exceptional multicharge storage capacity due to the large number of electrons that can be reversibly exchanged.

F. D. and *D. B.* acknowledge the financial support by the *Swiss National Science Foundation* and the *NCCR 'Nanoscience'*. *N. A.* and *G. A.* thank the *Italian CNR* and *MIUR* (contract *FIRB RBNE019 H9K*, Molecular Manipulation for Nanometric Machines), and the *EU* (*RTN* Contract *'FAMOUS', HPRN-CT-2002-00171*) for support. *L. E.* and *F. S.* thank the *US NSF*, grant *CHE-0135786*, for financial support. We are grateful to Dr. *Carlo Thilgen* and Dr. *Vladimir Azov* for helpful discussions as well as for help with the nomenclature (*C. Thilgen*).

Experimental Part

General. Reagents and solvents were purchased reagent-grade and used without further purification. CH_2Cl_2 was dried over CaH_2, and PhMe and THF over Na. Compounds **21** (X-ray; see *Fig. 2*), **22**, and **33** were prepared as reported in [13]. All reactions were performed in standard oven-dried glassware under N_2. Evaporation and concentration were done at water-aspirator pressure, and compounds were dried at 10^{-2} Torr. Column chromatographic (CC) purification refers to flash chromatography (FC) on SiO_2-*60* (230–400 mesh), *Fluka*, with elution at a maximum pressure of 0.1 bar. TLC: *Alugram SIL G/UV*$_{254}$, *Macherey-Nagel*, visualization by UV light at 254 nm. M.p.: *Büchi B-540* apparatus, uncorrected. UV/VIS Spectra (λ_{max} in nm (ε [l mol^{-1} cm^{-1}])): *Varian Cary 5* spectrometer. IR Spectra [cm^{-1}]: *Perkin-Elmer Spektrum BX II*. NMR Spectra: *Bruker AM 500* and *Varian Gemini 300* at 300 K, with solvent peaks as internal references. MS (*m*/*z* (%)); *EI VC Tribrid* mass spectrometer at 70 eV ionization energy; high-resolution *Fourier*-transform ion-cyclotron-resonance matrix-assisted laser-desorption ionization (HR-FT-ICR-MALDI): *Ion Spec Ultima FT-ICR-MS VG ZAB 2SEQ* (337-nm N_2-laser system) instrument; 2,5-dihydroxybenzoic acid (DHB) or {(2*E*)-3-[4-(*tert*-butyl)phenyl]-2-methylprop-2-enylidene}malonitrile (DCTB) as matrix. Elemental analyses were performed by the Mikrolabor at the Laboratorium für Organische Chemie, ETH-Zürich.

Determination of the Kinetic Parameters for the Barriers to Rotation by ^{1}H-NMR Spectroscopy. Deuterated solvents were used as internal references: $C_2D_2Cl_6$ (residual proton signal: 5.91 ppm), $C_6D_5CD_3$ (6.98 ppm), (D_8)dioxane (3.53 ppm). Variable-temp. (VT) ^{1}H-NMR was performed on a *Varian Mercury 300* spectrometer. The temp. was calibrated with MeOH ($T \leq 313$ K) or $CH_2(OH)-CH_2OH$ ($T \geq 313$ K) reference samples. Temp. regulation was stable within 0.5° between 273 and 383 K. Fitting of the NMR spectra was performed with the *gNMR v3.6 for Macintosh* program (*Cherwell Scientific Publishing, Ltd.*, Oxford, UK). The rate constant k_e was determined for five–six temp. in the interval between 273 and 373 K by comparison of the global shape of the experimental spectrum with the simulated one. Determination of the activation enthalpy and entropy was based on *Eqn. 2* (*Eyring* plot):

$$\log(k_e/T) = -\Delta H^{\neq}/aT + \Delta S^{\neq}/a + 10.319 \quad (2)$$

where k_e [Hz] is an exchange constant obtained from spectral fitting, T the temperature in Kelvin, and $a = 1.914\ 10^{-1}$ for $\Delta H^{\neq}$ in kcal mol^{-1} and $\Delta S^{\neq}$ in kcal mol^{-1} K^{-1}. Determination of the free enthalpy of activation was based on *Eqn. 3:*

$$\Delta G^{\neq} = \Delta H^{\neq} - T\Delta S^{\neq} \quad (3)$$

where T is the temp. in Kelvin (298 K).

Photophysical Measurements. The solvent used is spectrofluorimetric-grade PhMe from *Carlo Erba*. The instrumentation for UV/VIS/NIR steady-state and time-resolved absorption and emission spectroscopy was described in [40][44]. O_2 was removed from PhMe solns. by at least four *freeze-pump-thaw* cycles with a diffusive vacuum pump at 10^{-6} Torr.

Electrochemical Measurements. All electrochemical measurements were performed with the *CHI 440 Electrochemical Workstation* (*CH Instruments Inc.*, Austin, Texas). 0.1M Bu_4NPF_6, from *Fluka*) in CH_2Cl_2 (redistilled) was used as the supporting electrolyte (degassed with Ar). Pt Wire was employed as the counter electrode. An aq. Ag/AgCl electrode, separated by a 0.1M Bu_4NPF_6 salt-bridge, was used as the reference. Ferrocene (Fc) was added as an internal reference, and all potentials were referenced relative to the Fc/Fc^+ couple. A glassy C electrode (*CHI*, 3 mm in diameter), polished with 1.0–03 μm Al paste and ultrasonicated in deionized H_2O and a CH_2Cl_2 bath, was used as the working electrode. The scan rates for cyclic voltammetry (CV) and differential pulse voltammetry (DPV) were 100 and 4 mV/s, resp. For the DPV measurements, the amplitude was 50 mV and the pulse width was 0.05 s. All experiments were performed at 293 ± 2 K.

*[(3-Bromobenzyl)oxy](*tert*-butyl)(dimethyl)silane* (**17**). In a dry 50-ml round-bottomed flask, DMAP (2.71 g, 22.2 mmol) was slowly added to a soln. of (3-bromophenyl)methanol (2.8 g, 15.0 mmol) and (*t*-Bu)Me_2SiCl (3.3 g, 21.0 mmol) in dry THF at 0°. The mixture was stirred for 24 h at 25°. A white precipitate was filtered off and washed with cold THF. Evaporation of the solvent *in vacuo* afforded a pale yellow oil, which was submitted to a short plug (SiO_2; CH_2Cl_2) to give **17** (4.20 g, 95%). Colorless oil. IR (neat): 2953*w*, 2928*w*, 2884*w*, 2857*w*, 1599*w*, 1572*w*, 1472*w*, 1462*w*, 1428*w*, 1366*w*, 1253*m*, 1198*w*, 1105*m*, 1078*m*, 1067*m*, 1006*w*, 938*w*, 834*s*, 814*m*, 774*s*, 681*w*, 666*w*. ^{1}H-NMR ($CDCl_3$, 300 MHz): 7.48 (*s*, 1 H); 7.38–7.34 (*m*, 1 H); 7.25–7.15 (*m*, 2 H); 4.70 (*s*, 2 H); 0.95 (*s*, 9 H); 0.11 (*s*, 6 H). ^{13}C-NMR ($CDCl_3$, 75 MHz): 143.67; 129.80; 129.67; 128.91; 124.34; 122.31;

64.19; 26.03; 18.50; −5.12. EI-MS: 302.1 (MH^+), 245.0 ($[M-CMe_3]^+$), 215.0 ($[M-2\ Me-CMe_3]^+$), 169.0 ($[M-OSiMe_2CMe_3]^+$). Anal. calc. for $C_{13}H_{21}OSiBr$ (301.30): C 51.82, H 7.02, Br 26.52; found: C 52.00, H 6.96, Br 26.40.

*2-[3-(([(*tert*-Butyl)(dimethyl)silyl]oxy}methyl)phenyl]-4,4,5,5-tetramethyl-1,3,2-dioxaborolane* (**19**). To a 50-ml round-bottomed flask, a soln. of **17** (500 mg, 1.66 mmol), 4,4,4′,4′,5,5,5′,5′-octamethyl-[2,2′]bis([1,3,2]-dioxaborolanyl) (510 mg, 2 mmol), AcOK (500 mg, 5 mmol), and $[PdCl_2(dppf)_2]\cdot CH_2Cl_2$ (10 mg, 0.012 mmol) in Me_2SO (20 ml) was added. The resulting mixture was deoxygenated *via* three *freeze-pump-thaw* cycles with N_2 and stirred at 100° for 16 h. After cooling to 25°, the mixture was diluted with $CHCl_3$ (20 ml), filtered through *Celite*, and washed with H_2O (3 × 100 ml) and sat. aq. NaCl soln. (3 × 100 ml). The org. phase was dried ($MgSO_4$), and the solvent was removed *in vacuo*. A quick plug filtration (Al_2O_3 act. III; cyclohexane/CH_2Cl_2 6:4) yielded **19** (300 mg, 55%). Colorless oil. IR (neat): 2954*w*, 2929*w*, 2885*w*, 2857*w*, 1704*m*, 1607*w*, 1590*w*, 1472*w*, 1462*w*, 1360*w*, 1314*w*, 1253*m*, 1201*w*, 1142*m*, 1103*m*, 1076*m*, 1006*w*, 964*w*, 938*w*, 887*w*, 834*s*, 815*w*, 776*s*, 708*w*, 685*w*, 669*w*, 652*w*. ^{1}H-NMR ($CDCl_3$, 300 MHz): 7.73–7.7 (*m*, 1 H); 7.54–7.51 (*m*, 1 H); 7.04–7.35 (*m*, 2 H); 4.77 (*s*, 2 H); 1.37 (*s*, 12 H); 0.97 (*s*, 9 H); 0.12 (*s*, 6 H). ^{13}C-NMR ($CDCl_3$, 75 MHz): 140.38; 133.12; 132.19; 128.96; 127.55; 83.58; 64.85; 25.97; 24.86; 18.47; −5.17; one peak is missing. Not stable under EI, MALDI, and FAB mass-spectrometric conditions.

*5,15-Bis[3,5-di(*tert*-butyl)phenyl]porphyrin* (**11**). In a oven-dried 4-l three-necked round-bottomed flask purged with N_2, a soln. of **12** (2.4 g, 16.5 mmol) and **13** (3.8 g, 17 mmol) in CH_2Cl_2 (4 l) was deoxygenated by bubbling N_2 through for 1 h. TFA (432 mg, 3.66 mmol) was added dropwise, and the mixture was vigorously stirred in the dark for 16 h at 25°. *p*-Chloranil (12.32 g, 50.1 mmol) was added, and the mixture was heated to 70° for 2 h. The mixture was then concentrated, and stirred with 0.1M aq. $Na_2S_2O_3$ soln. and MeOH (200 ml) until all *p*-chloranil was consumed. The org. phase was separated and washed with H_2O (3 × 250 ml), dried (Na_2SO_4), and the solvent was evaporated *in vacuo*. FC (SiO_2; cyclohexane/CH_2Cl_2 1:1, 1% (*v*/*v*) Et_3N) and precipitation from CH_2Cl_2 upon addition of MeOH yielded **11** (3.12 g, 55%). Violet solid. M.p. >300°. UV/VIS ($CHCl_3$): λ_{max} 296 (10300), 410 (298800), 505 (11700). IR (neat): 2953*w*, 1590*w*, 1475*w*, 1410*w*, 1362*w*, 1247*m*, 1062*w*, 1046*w*, 962*m*, 916*m*, 897*w*, 882*w*, 846*m*, 804*m*, 791*s*, 759*m*, 739*s*, 714*m*, 688*s*, 636*w*. ^{1}H-NMR ($CDCl_3$, 300 MHz): 10.31 (*s*, 2 H); 9.41 (*d*, *J* = 4.5, 4 H); 9.15 (*d*, *J* = 4.5, 4 H); 8.16 (*d*, *J* = 2.0, 4 H); 7.85 (*t*, *J* = 2.0, 2 H); 1.59 (*s*, 36 H); −3.00 (*s*, 2 H). ^{13}C-NMR ($CDCl_3$, 75 MHz): 148.99; 147.34; 144.91; 140.26; 131.41; 131.19; 130.13; 121.02; 120.41; 105.04; 35.22; 31.89. ESI-MS: 687.2 (MH^+). Anal. calc. for $C_{48}H_{54}N_4$ (686.43): C 83.92, H 7.92, N 8.16; found: C 83.89, H 8.08, N 8.11.

*{5,15-Bis[3,5-di(*tert*-butyl)phenyl]porphyrinato(2−)-κN^{21},κN^{22},κN^{23},κN^{24}}zinc(II)* (**14**). To a vigorously stirred soln. of **11** (2.6 g, 3.79 mmol) in $CHCl_3$ (150 ml), a soln. of $Zn(OAc)_2$ (8.32 g 37.9 mmol) in MeOH (150 ml) was added in the dark at 25°. After 2 h, the org. phase was washed with H_2O (3 × 100 ml), dried (Na_2SO_4), and the solvent was evaporated *in vacuo*. FC (SiO_2; cyclohexane/CH_2Cl_2 5:5. 1% (*v*/*v*) Et_3N) and precipitation from CH_2Cl_2 upon addition of MeOH provided **14** (2.48 g, 91%). Red powder. M.p. >300°. UV/VIS ($CHCl_3$): λ_{max} 540 (11300), 414 (260100), 294 (10000). IR (neat): 2953*m*, 1591*m*, 1476*w*, 1391*m*, 1362*w*, 1296*w*, 1246*m*, 1220*w*, 1060*w*, 994*s*, 926*m*, 899*w*, 881*w*, 851*m*, 822*m*, 784*s*, 764*w*, 728*w*, 714*m*, 699*m*, 614*w*. ^{1}H-NMR ($CDCl_3$, 300 MHz): 10.34 (*s*, 2 H); 9.46 (*d*, *J* = 4.5, 4 H); 9.21 (*d*, *J* = 4.5, 4 H); 8.15 (*d*, *J* = 2.0, 4 H); 7.85 (*t*, *J* = 2.0, 2 H); 1.58 (*s*, 36 H). ^{13}C-NMR ($CDCl_3$, 75 MHz): 150.27; 149.27; 148.55; 141.39; 132.71; 131.50; 129.83; 121.41; 120.75; 106.06; 35.16; 31.87. HR-FT-ICR-MALDI-MS (DHB): 748.3480 (M^+, $C_{48}H_{52}N_4Zn^+$; calc. 748.3478). Anal. calc. for $C_{48}H_{52}N_4Zn\cdot H_2O$ (766.36): C 75.03, H 7.08, N 7.29; found: C 74.76, H 6.99, N 7.24.

*{5,15-Bis[3,5-di(*tert*-butyl)phenyl]-10-iodoporphyrinato(2−)-κN^{21},κN^{22},κN^{23},κN^{24}}zinc(II)* (**15**). To a 100-ml round-bottomed flask charged with a soln. of **14** (630 mg, 0.87 mmol) and I_2 (220 mg, 0.87 mmol) in $CHCl_3$/pyridine 30:1 (65 ml), a soln. of $AgPF_6$ (223 mg, 0.87 mmol) in MeCN (5 ml) was added at 25°. The reaction, which was monitored by TLC (cyclohexane/CH_2Cl_2 1:1), was complete within 13 min; then H_2O (20 ml) was added. The org. layer was washed with H_2O (3 × 50 ml), dried (Na_2SO_4), and the solvent was evaporated *in vacuo*. FC (SiO_2; cyclohexane/CH_2Cl_2 1:1, 1% (*v*/*v*) Et_3N) yielded **15** (250 mg, 63%) and traces of **16**. Red solid. M.p. >300°. UV/VIS ($CHCl_3$): λ_{max} 312 (12600), 425 (294100), 557 (13100). IR (neat): 2961*m*, 1591*m*, 1519*w*, 1476*w*, 1424*w*, 1392*w*, 1381*w*, 1362*m*, 1320*w*, 1287*w*, 1246*m*, 1219*w*, 1080*w*, 1064*m*, 996*s*, 928*m*, 898*m*, 882*m*, 848*m*, 815*m*, 780*s*, 728*m*, 714*m*, 697*m*, 652*m*, 615*m*. ^{1}H-NMR (CS_2/$CDCl_3$ 1:1, 300 MHz): 10.22 (*s*, 1 H); 9.83 (*d*, *J* = 4.5, 2 H); 9.36 (*d*, *J* = 4.8, 2 H); 9.07 (*d*, *J* = 4.5, 2 H); 9.04 (*d*, *J* = 4.8, 2 H); 8.07 (*d*, *J* = 1.8, 4 H); 7.82 (*t*, *J* = 1.8, 2 H); 1.58 (*s*, 36 H). ^{13}C-NMR (CS_2/$CDCl_3$ 1:1, 75 MHz): 151.54; 150.00; 148.46; 141.22; 137.73; 135.15; 133.66; 133.17; 132.00; 129.84; 122.61; 120.97; 106.89; 35.06; 31.90; two peaks are missing due to overlap. HR-FT-ICR-MALDI-MS (DHB): 874.2446 (M^+, $C_{48}H_{51}IN_4Zn^+$; calc. 874.2444), 748.3520 ($[M-I]^+$, $C_{48}H_{51}N_4Zn^+$; calc. 748.3478).

*{5,15-Bis[3,5-di(*tert*-butyl)phenyl]-10-[3-({[(*tert*-butyl)(dimethyl)silyl]oxy}methyl)phenyl]porphyrinato(2−)-*$\kappa N^{21},\kappa N^{22},\kappa N^{23},\kappa N^{24}$*}zinc(II)* (**10**). To a 250-ml round-bottomed flask charged with **15** (192 mg, 0.22 mmol) in dry PhMe (15 ml), **19** (229 mg, 0.66 mmol), [$Pd(Ph_3P)_4$] (25 mg, 0.022 mmol), Cs_2CO_3 (616 mg, 0.22 mmol), and three drops of H_2O were added. The mixture was deoxygenated by bubbling N_2 through and heated to 140° for 18 h. After cooling to 25°, the mixture was filtered through *Celite*, and the solvent was evaporated *in vacuo*. FC (SiO_2; cyclohexane/CH_2Cl_2 8:2, 1% (*v*/*v*) Et_3N) afforded two fractions corresponding to **14** and **10**. Precipitation of the chromatographic fractions from $CHCl_3$ upon addition of MeOH/H_2O 95:5 afforded **14** (37 mg, 23%) and **10** (142 mg, 67%). Red solid. M.p. 300°. UV/VIS ($CHCl_3$): λ_{max} 305 (15500), 419 (450700), 547 (19000). IR (neat): 2955*m*, 2858*w*, 1591*m*, 1523*w*, 1462*m*, 1426*m*, 1383*w*, 1362*m*, 1324*w*, 1290*w*, 1250*m*, 1209*w*, 1168*w*, 1105*m*, 1078*m*, 1064*m*, 994*m*, 928*m*, 914*w*, 899*w*, 882*w*, 836*s*, 795*s*, 777*s*, 738*s*, 722*m*, 702*m*, 668*m*, 620*w*. ^{1}H-NMR ($CDCl_3$, 300 MHz): 10.28 (*s*, 1 H); 9.43 (*d*, *J* = 4.6, 2 H); 9.17 (*d*, *J* = 4.6, 2 H); 9.05 (*d*, *J* = 4.5, 2 H); 8.99 (*d*, *J* = 4.5, 2 H); 8.17–8.01 (*m*, 6 H); 7.82 (*s*, 2 H); 7.89–7.70 (*m*, 2 H); 5.1 (*s*, 2 H); 1.56 (*s*, 36 H); 0.96 (*s*, 9 H); 0.17 (*s*, 6 H). ^{13}C-NMR ($CDCl_3$, 75 MHz): 150.32; 149.70; 149.64; 148.51; 142.76; 141.56; 139.50; 133.10; 132.82; 132.20; 132.05; 131.86; 131.51; 129.83 (2×); 126.31; 125.17; 121.94; 120.74; 105.74; 65.29; 35.17; 31.88; 27.02; 26.13; −4.90; one peak is missing, probably due to overlap. HR-FT-ICR-MALDI-MS (DHB): 968.4758 (M^+, $C_{61}H_{72}N_4OSiZn^+$; calc. 968.4761).

*{5,15-Bis[3,5-di(*tert*-butyl)phenyl]-10-[3-(hydroxymethyl)phenyl]porphyrinato(2−)-*$\kappa N^{21},\kappa N^{22},\kappa N^{23},\kappa N^{24}$*}-zinc(II)* (**20**). To a 50-ml round-bottomed flask charged with a soln. of **10** (40 mg, 4.1 10^{-2} mmol) in THF (10 ml), several drops of a 1M soln. of Bu_4NF in THF were added at 0°. The mixture was stirred for 30 min at 0° and 1 h at 25°. When all of **10** was consumed, $CHCl_3$ (10 ml) was added, followed by H_2O. The org. layer was washed with H_2O (3 × 50 ml) and sat. aq. NaCl soln. (3 × 50 ml), dried (Na_2SO_4), and the solvent was evaporated *in vacuo*. FC (SiO_2; cyclohexane/CH_2Cl_2 1:1, 1% (*v*/*v*) Et_3N) and precipitation from $CHCl_3$ upon addition of MeOH/H_2O 95:5 afforded **20** (28 mg, 80%). Red solid. M.p. > 300°. UV/VIS ($CHCl_3$): λ_{max} 303 (14400), 419 (425800), 546 (17300). IR (neat): 2959*m*, 1646*w*, 1590*m*, 1521*w*, 1475*m*, 1423*m*, 1382*w*, 1362*m*, 1289*w*, 1247*m*, 1219*m*, 1062*w*, 994*s*, 929*m*, 899*m*, 881*m*, 847*w*, 822*m*, 792*s*, 777*s*, 719*s*, 702*m*, 660*m*, 619*w*. ^{1}H-NMR ($CDCl_3$, 300 MHz): 10.28 (*s*, 1 H); 9.42 (*d*, *J* = 4.5, 2 H); 9.17 (*d*, *J* = 4.5, 2 H); 9.04 (*d*, *J* = 4.3, 2 H); 8.90 (*d*, *J* = 4.3, 2 H); 8.13–8.10 (*m*, *J* = 1.8, 5 H); 7.99 (*s*, 1 H); 7.83 (*t*, *J* = 1.8, 2 H); 7.66 (*t*, *J* = 7.8, 1 H); 7.51 (*d*, *J* = 7.8, 1 H); 4.57 (*s*, 2 H); 1.56 (*s*, 36 H); OH resonance is missing. ^{13}C-NMR ($CDCl_3$, 75 MHz): 150.31; 150.25; 149.68; 149.40; 148.46; 143.09; 141.53; 138.28; 133.51; 132.81; 132.58; 132.07; 131.63; 131.52; 129.78; 126.42; 125.61; 121.91; 120.71; 105.77; 64.93; 35.14; 31.86; one peak is missing probably due to overlap. HR-FT-ICR-MALDI-MS (DHB): 854.3890 (M^+, $C_{55}H_{58}N_4OZn^+$; calc. 854.3897). Anal. calc. for $C_{55}H_{58}N_4OZn \cdot 0.5$ MeOH (888.51): C 76.40, H 6.93, N 6.42; found: C 76.72, H 7.22, N 6.36

*{5,15-Bis[3,5-di(*tert*-butyl)phenyl]-10-(3-{[(3-ethoxy-3-oxopropanoyl)oxy]methyl}phenyl)porphyrinato(2−)-*$\kappa N^{21},\kappa N^{22},\kappa N^{23},\kappa N^{24}$*}zinc(II)* (**9**). To an oven-dried 50-ml round-bottomed flask charged with a soln. of **20** (18 mg, 6.3×10^{-2} mmol) and Et_3N (9 µl, 6.3×10^{-2} mmol) in dry CH_2Cl_2 (10 ml), $ClCOCH_2CO_2Et$ (8 µl, 6.3×10^{-2} mmol) was added at 0°, and the mixture was stirred for 1 h at 25°. When all starting material **20** was consumed (TLC control, SiO_2; cyclohexane/CH_2Cl_2 1:1), the mixture was diluted with $CHCl_3$ (10 ml) and quenched with H_2O. The org. layer was washed with H_2O (3 × 50 ml) and sat. aq. NaCl soln. (3 × 50 ml), dried (Na_2SO_4), and the solvent was evaporated *in vacuo*. FC (SiO_2; cyclohexane/CH_2Cl_2 1:1, 1% (*v*/*v*) Et_3N) and precipitation from $CHCl_3$ upon addition of MeOH/H_2O 9:1 afforded **9** (20 mg, 90%). Red solid. M.p. > 300°. IR (neat): 2956*s*, 2928*m*, 2870*m*, 1725*s*, 1591*m*, 1521*w*, 1459*m*, 1424*w*, 1382*w*, 1362*m*, 1268*s*, 1220*m*, 1208*m*, 1122*s*, 1070*s*, 1038*w*, 993*s*, 927*m*, 899*m*, 881*m*, 847*w*, 822*m*, 794*m*, 741*m*, 727*m*, 715*s*, 703*m*. ^{1}H-NMR ($CDCl_3$, 300 MHz): 10.24 (*s*, 1 H); 9.36 (*d*, *J* = 4.6, 2 H); 9.08 (*d*, *J* = 4.6, 2 H); 8.97 (*d*, *J* = 4.9, 2 H); 8.85 (*d*, *J* = 4.9, 2 H); 8.22–8.23 (*m*, 2 H); 8.12 (*d*, *J* = 1.8, 4 H); 7.83 (*t*, *J* = 1.8, 2 H); 7.77–7.80 (*m*, 2 H); 5.50 (*s*, 2 H); 4.11 (*q*, *J* = 7.0, 2 H); 3.48 (*s*, 2 H); 1.56 (*s*, 36 H); 1.12 (*t*, *J* = 7.0, 3 H). ^{13}C-NMR ($CDCl_3$, 75 MHz): 166.36; 166.19; 148.76; 147.04; 145.59; 143.03; 140.55; 134.22; 133.76; 133.51; 131.54; 131.07; 129.90; 128.67; 127.20; 126.67; 120.96; 119.32; 104.69; 67.25; 61.57; 41.73; 35.14; 31.82; 14.04; one peak is missing, probably due to overlap. HR-FT-ICR-MALDI-MS (DHB): 970.4243 (M^+, $C_{60}H_{64}N_4O_4Zn^+$; calc. 968.4219), 906.5008 ($[M - Zn]^+$, $C_{60}H_{66}N_4O_4^+$; calc. 906.5084).

*(5,15-Bis[3,5-di(*tert*-butyl)phenyl]-10-[3-({[3′-(ethoxycarbonyl)-3′*H*-cyclopropa[1,9](*C_{60}*-*I_h*)[5,6]fullerene-3′-yl]carbonyl}oxy)methyl]phenyl)porphyrinato(2−)-*$\kappa N^{21},\kappa N^{22},\kappa N^{23},\kappa N^{24}$*)zinc(II)* (**3**). To an oven-dried 200-ml round-bottomed flask charged with a soln. of **9** (90 mg, 9.6×10^{-2} mmol), C_{60} (137 mg, 0.19 mmol), and I_2 (25 mg, 0.1 mmol) in dry and deoxygenated PhMe (150 ml), DBU (42 µl, 0.29 mmol) was added dropwise. After 1.5 h, the mixture was filtered through a short plug (SiO_2; PhMe). The brown-red fraction was purified by FC (SiO_2; cyclohexane/PhMe 8:2 → PhMe, 1% (*v*/*v*) Et_3N) and the solvent evaporated *in vacuo*. Precipitation of the chromatographic fraction from $CHCl_3$ upon dropwise addition of MeOH afforded **3** (147 mg, 45%).

Brownish solid. M.p. $>300°$. UV/VIS ($CHCl_3$): λ_{max} 259 (227000), 329 (56900), 422 (374000), 549 (18800). IR (neat): 2960*s* 1747*s*, 1590*m*, 1524*w*, 1462*m*, 1428*m*, 1383*w*, 1362*m*, 1291*m*, 1266*m*, 1204*s*, 1184*s*, 1097*m*, 1061*m*, 996*s*, 928*m*, 900*w*, 881*m*, 848*w*, 824*m*, 794*s*, 780*m*, 737*w*, 714*s*, 701*s*, 668*w*. Fluorescence ($CHCl_3$; $\lambda_{exc}=422$ nm): λ_{max} 596, 644. ^{1}H-NMR ($CDCl_3$, 500 MHz): 10.25 (*s*, 1 H); 9.39 (*d*, $J=4.5$, 2 H); 9.09 (*d*, $J=4.5$, 2 H); 8.97 (*d*, $J=4.5$, 2 H); 8.85 (*d*, $J=4.5$, 2 H); 8.38–8.40 (*m*, 1 H); 8.18 (*t*, $J=1.8$, 2 H); 8.07 (*s*, 1 H); 7.84 (*t*, $J=1.8$, 2 H); 7.77–7.82 (*m*, 4 H); 5.89 (*s*, 2 H); 4.44 (*q*, $J=7.2$, 2 H); 1.55 (*s*, 18 H); 1.47 (*s*, 18 H); 1.36 (*t*, $J=7.2$, 3 H). ^{13}C-NMR ($CDCl_3$, 150 MHz): 163.47; 163.28; 150.43; 150.35; 149.37; 148.57; 144.58; 144.38; 144.34; 144.28; 144.09; 143.98; 143.92; 143.66; 143.53; 143.26; 143.18; 142.95; 142.42; 142.25; 142.17; 142.07; 141.77; 141.67; 141.59; 141.39; 141.34; 141.22; 141.19; 140.50; 140.35; 139.97; 139.65; 139.11; 139.10; 137.05; 134.05; 133.13; 132.95; 132.35; 131.72; 131.62; 129.80; 129.53; 126.76; 125.95; 122.05; 120.79; 120.25; 105.98; 70.86; 68.25; 63.42; 51.99; 35.05, 35.01; 31.80, 31.78; 14.17; one peak is missing probably due to overlap. HR-FT-ICR-MALDI-MS (DCTB): 1686.4048 (M^+, $C_{120}H_{62}N_4O_4Zn^+$; calc. 1686.4057).

Iodination of meso,meso-*Oligoporphyrin Arrays* **21**–**23**. To a 50-ml round-bottomed flask charged with the appropriate oligoporphyrin (1.7×10^{-2} mmol) and I_2 (3.4×10^{-2} mmol) in $CHCl_3$/pyridine 30:1 (10 ml), a soln. of $AgPF_6$ (3.4×10^{-2} mmol) in dry MeCN (3 ml) was added at 25°. The mixture was stirred for 11 min (TLC control, SiO_2; cyclohexane/CH_2Cl_2 1:1) and then quenched with H_2O (10 ml). The org. layer was diluted with $CHCl_3$ (10 ml), washed with H_2O (3×100 ml) and sat. aq. NaCl soln. (3×100 ml), dried (Na_2SO_4), and the solvent was evaporated *in vacuo*. FC (SiO_2; cyclohexane/CH_2Cl_2 7:3, 1% (*v*/*v*) Et_3N) and precipitation from CH_2Cl_2 upon addition of MeOH yielded the desired diiodoporphyrin as red solid.

(μ-[15,15′-Diiodo-10,10′,20,20′-tetrakis[3,5-di(tert-*butyl)phenyl]-5,5′-biporphyrinato(4−)-*κN^{21},κN^{22},κN^{23},κN^{24}:κN$^{21'}$,κN$^{22'}$,κN$^{23'}$,κN$^{24'}$*)dizinc(II)* (**24**; 26 mg, 88% from **21**). Red solid. M.p. $>300°$. UV/VIS ($CHCl_3$): λ_{max} 428 (240700), 463 (268000), 572 (52000), 614 (sh, 19100). IR (neat): 2960*m*, 2903*w*, 2867*w*, 2324*w*, 1806*w*, 1692*w*, 1592*m*, 1547*w*, 1519*w*, 1476*w*, 1426*w*, 1392*w*, 1362*m*, 1339*w*, 1314*m*, 1288*m*, 1265*w*, 1246*m*, 1220*w*, 1208*w*, 1069*w*, 994*s*, 929*m*, 899*w*, 882*w*, 817*m*, 802*w*, 790*s*, 782*m*, 726*s*, 715*m*, 701*m*, 696*w*. ^{1}H-NMR ($CDCl_3$/CS_2 1:1, 300 MHz): 9.89 (*d*, $J=4.9$, 4 H); 9.05 (d, $J=4.9$, 4 H); 8.65 (*d*, $J=4.8$, 4 H); 8.07 (*d*, $J=4.8$, 4 H); 8.04 (*d*, $J=1.5$, 8 H); 7.71 (*t*, $J=1.5$, 4 H); 1.44 (*s*, 72 H). ^{13}C-NMR ($CDCl_3$/CS_2 1:1, 75 MHz): 154.78; 151.93; 150.32; 148.36; 141.29; 137.88; 134.22; 133.67; 132.52; 129.66; 123.99; 120;97; 120.12; 34.99; 31.86; two peaks are missing probably due to overlap. HR-FT-ICR-MALDI-MS (DHB): 1750.4741 (M^+, $C_{96}H_{100}I_2N_8Zn_2^+$; calc. 1750.4726), 1624.5577 ($[M-I]^+$, $C_{96}H_{100}IN_8Zn_2^+$; calc. 1624.5675).

(μ$_3$-[10,10′,10″,20,20′,20″-Hexakis[3,5-di(tert-*butyl)phenyl]-15,15″-diiodo-5,5′:15′,5″-terporphyrinato*(6−)-*κN^{21},κN^{22},κN^{23},κN^{24}:κN$^{21'}$,κN$^{22'}$,κN$^{23'}$,κN$^{24'}$:κN$^{21''}$,κN$^{22''}$,κN$^{23''}$,κN$^{24''}$*)trizinc(II)* (**25**; 36 mg, 85% from **22**). Red solid. M.p. $>300°$. UV/VIS ($CHCl_3$): λ_{max} 351 (53600), 424 (292000), 478 (260700), 573 (83000), 615 (*sh*, 25300). IR (neat): 2959*m*, 1591*m*, 1519*w*, 1475*w*, 1393*w*, 1362*m*, 1339*w*, 1313*w*, 1288*m*, 1261*w*, 1246*w*, 1218*w*, 1070*m*, 997*s*, 980*m*, 963*w*, 928*m*, 914*w*, 882*w*, 844*w*, 824*m*, 791*m*, 782*m*, 758*s*, 727*s*, 716*m*, 697*m*, 665*w*, 609*w*. ^{1}H-NMR ($CDCl_3$/CS_2 1:1, 300 MHz): 9.91 (*d*, $J=4.6$, 4 H); 9.07 (*d*, $J=4.4$, 4 H); 8.73 (*d*, $J=4.4$, 4 H); 8.72 (*d*, $J=4.4$, 4 H); 8.22 (*d*, $J=4.4$, 4 H); 8.17 (*d*, $J=4.4$, 4 H); 8.10 (*d*, $J=1.7$, 8 H); 8.07 (*d*, $J=1.7$, 4 H); 7.76 (*t*, $J=1.7$, 4 H); 7.58 (*t*, $J=1.7$, 2 H); 1.50 (*s*, 72 H); 1.36 (*s*, 36 H). ^{13}C-NMR ($CDCl_3$/CS_2 1:1, 75 MHz): 154.95; 154.48; 151.92; 151.86; 150.38; 148.40; 148.24; 141.25; 141.37; 137.73; 134.24; 133.88; 133.63; 132.49; 132.16; 129.56; 129.37; 128.94; 128.14; 125.23; 124.05; 123.99; 120.92; 120.69; 120.51; 119.72; 35.03; 34.91; 31.81; 31.69. HR-FT-ICR-MALDI-MS (DHB): 2492.8090 (M^+, $C_{144}H_{150}I_2N_{12}Zn_3^+$; calc. 2492.8065).

(μ$_4$-[15,15‴-Diiodo-10,10′,10″,10‴,20,20′,20″,20‴-octakis[3,5-di(tert-*butyl)phenyl]-5,5′:15′,5″:15″,5‴-quaterporphyrinato(8−)-*κN^{21},κN^{22},κN^{23},κN^{24}:κN$^{21'}$,κN$^{22'}$,κN$^{23'}$,κN$^{24'}$:κN$^{21''}$,κN$^{22''}$,κN$^{23''}$,κN$^{24''}$:κN$^{21'''}$,κN$^{22'''}$,κN$^{23'''}$,κN$^{24'''}$*)tetrazinc(II)* (**26**; 39 mg, 70% from **23**). Red solid. M.p. $>300°$. IR (neat): 2957*m*, 1591*m*, 1518*w*, 1475*w*, 1392*w*, 1361*m*, 1339*w*, 1315*w*, 1246*w*, 1207*w*, 1144*w*, 1069*m*, 995*s*, 928*m*, 914*w*, 899*w*, 882*w*, 824*m*, 790*m*, 765*w*, 750*m*, 727*s*, 714*s*, 696*m*. ^{1}H-NMR ($CDCl_3$/CS_2 1:1, 500 MHz): 9.89 (*d*, $J=4.8$, 4 H); 9.05 (*d*, $J=4.8$, 4 H); 8.78 (*d*, $J=4.8$, 4 H); 8.73 (*d*, $J=4.8$, 4 H); 8.71 (*d*, $J=4.8$, 4 H); 8.30 (*d*, $J=4.8$, 4 H); 8.23 (*d*, $J=4.8$, 4 H); 8.17 (*d*, $J=4.8$, 4 H); 8.09 (*s*, 16 H); 7.73 (*s*, 4 H); 7.59 (*s*, 4 H); 1.48 (*s*, 72 H); 1.37 (*s*, 72 H). ^{13}C-NMR (CS_2/$CDCl_3$ 1:1, 125 MHz): 155.09; 154.77; 154.60; 154.49; 152.03; 151.97; 150.58; 150.50; 148.50; 148.35; 141.63; 141.58; 141.38; 137.80; 134.35; 134.08; 133.94; 133.69; 132.54; 132.20; 129.63; 129.44; 124.10; 124.04; 120.97; 120.76; 120.23; 119.73; 34.91; 34.80; 31.68; 31.59; one peak is missing probably due to overlap. HR-FT-ICR-MALDI-MS (DCTB): 3239.1201 (M^+, $C_{192}H_{200}I_2N_{16}Zn_4^+$; calc. 3239.1392).

General Procedure for the Pd-Catalyzed Cross-Coupling Reaction between Diiodo-oligoporphyrins **24**–**26** *and Boronate* **19**. To a 50-ml round-bottomed flask charged with the appropriate diiodo derivative (1.5×10^{-2} mmol) in dry PhMe (10 ml), **19** (0.12 mmol), [Pd(PPh_3)$_4$] (3×10^{-3} mmol), Cs_2CO_3 (0.24 mmol), and three drops of H_2O were added. The resulting mixture was deoxygenated by three *freeze-pump-thaw* cycles with N_2 and heated to reflux for 18 h. After cooling to 25°, the suspension was filtered through a *Celite* plug. The org.

layer was washed with H_2O (3×100 ml) and sat. aq. NaCl soln. (3×100 ml), dried (Na_2SO_4), and the solvent was evaporated *in vacuo*. FC (SiO_2; cyclohexane/CH_2Cl_2 8:2, 1% (*v*/*v*) Et_3N), and precipitation from $CHCl_3$ upon dropwise addition of MeOH/H_2O 9:1 yielded the desired oligoporphyrin derivative. Due to separation difficulties, **28** and **29** were submitted directly to the next transformation without purification. These compounds were characterized only by HR-FT-ICR-MALDI spectrometry:

*(μ3-[15,15″-Bis[3-([[(*tert*-butyl)(dimethyl)silyl]oxy}methyl)phenyl]-10,10′,10″,20,20′,20″-hexakis[3,5-di-(*tert*-butyl)phenyl-]-5,5′:15′,5″-terporphyrinato(6−)-κN21,κN22,κN23,κN24:κN21′,κN22′,κN23′,κN24′:κN21″,κN22″, κN23″,κN24″])trizinc(II)* (**28**). HR-FT-ICR-MALDI-MS (DCTB): 2682.2602 (MH^+, $C_{170}H_{193}N_{12}O_2Si_2Zn_3^+$; calc. 2682.2767);

*(μ4-[15,15‴-Bis[3-([[(*tert*-butyl)(dimethyl)silyl]oxy}methyl)phenyl]-10,10′,10″,10‴,20,20′,20″,20‴-octakis[3,5-di(*tert*-butyl)phenyl]-5,5′:15′,5″:15″,5‴-quarterporphyrinato(8−)-κN21,κN22,κN23,κN24:κN21′,κN22′, κN23′,κN24′:κN21″,κN22″,κN23″,κN24″:κN21‴,κN22‴,κN23‴,κN24‴])tetrazinc(II)* (**29**). HR-FT-ICR-MALDI-MS (DCTB): 3427.6026 (M^+, $C_{218}H_{242}N_{16}O_2Si_2Zn_4^+$; calc. 3427.6026).

*(μ-[15,15′-Bis[3-([[(*tert*-butyl)(dimethyl)silyl]oxy}methyl)phenyl]-10,10′,20,20′-tetrakis[3,5-di(*tert*-butyl)-phenyl]-5,5′-biporphyrinato(4−)-κN21,κN22,κN23,κN24:κN21′,κN22′,κN23′,κN24′])dizinc(II)* (**27**; 26 mg, 70% from **24**). Red solid. M.p. >300°. IR (neat): 2953*s*, 2926*w*, 2855*m*, 1592*m*, 1523*w*, 1462*m* (br.), 1426*w*, 1383*w*, 1362*m*, 1330*w*, 1290*w*, 1248*m*, 1209*w* (br.), 1168*w*, 1070*m* (br.), 1000*s*, 930*m*, 900*w*, 882*w*, 836*s*, 824*s*, 795*s*, 779*s*, 715*s*, 722*m*, 668*s*, 620*w*. ^{1}H-NMR ($CDCl_3$, 300 MHz): 9.04–9.01 (*m*, 8 H); 8.72 (*d*, *J* = 4.8, 2 H); 8.71 (*d*, *J* = 4.8, 2 H); 8.25 (*s*, 2 H); 8.23–8.21 (*m*, 2 H); 8.15 (*d*, *J* = 4.8, 2 H); 8.13 (*d*, *J* = 4.8, 2 H); 8.09 (*d*, *J* = 1.4, 8 H); 7.83–7.74 (*m*, 4 H); 7.69 (*t*, *J* = 1.4, 4 H); 5.10 (*s*, 4 H); 1.44 (*s*, 72 H); 0.99 (*s*, 18 H); 0.21 (*s*, 12 H). Both H–C(8) and H–C(9) split into *doublets* due to atropisomerism. ^{13}C-NMR ($CDCl_3$, 75 MHz): 154.65; 150.81; 149.90; 148.33; 142.72; 141.54; 139.60; 133.71; 133.10; 132.22; 132.13; 131.98; 131.89; 129.57; 126.40; 125.20; 123.18; 121.62; 120.64; 119.37; 65.30; 35.05; 31.76; 29.80; 26.14; −4.89; one peak is missing probably due to overlap. HR-FT-ICR-MALDI-MS (DHB): 1934.9361 (M^+, $C_{122}H_{142}N_8O_2Si_2Zn_2^+$; calc. 1934.9372).

General Procedure for the Cleavage of the (t-*Bu*)*Me*$_2$*Si Protecting Group.* To a 50-ml round-bottomed flask charged with a soln. of the appropriate (*t*-Bu)Me_2Si-protected alcohol in THF (10 ml), several drops of a 1M soln. of Bu_4NF in THF were added at 0°. The mixture was stirred for 30 min at 0° and 1 h at 25°. The reaction was monitored by TLC (SiO_2; cyclohexane/CH_2Cl_2 1:1). When all starting material had disappeared, the mixture was diluted with $CHCl_3$ (10 ml), and the reaction was quenched with H_2O. The org. layer was washed with H_2O (3×50 ml) and sat. aq. NaCl soln. (3×50 ml), dried (Na_2SO_4), and the solvent was evaporated *in vacuo*. FC (SiO_2; cyclohexane/CH_2Cl_2 1:1, 1% (*v*/*v*) Et_3N) and precipitation from $CHCl_3$ upon addition of MeOH/H_2O 9:1 afforded the desired bis-alcohol as red powder. Small amounts of monohydroxy derivatives and oligoporphyrins **21**–**23** were also isolated.

*(μ-[15,15′-Bis[3-(hydroxymethyl)phenyl]-10,10′,20,20′-tetrakis[3,5-di(*tert*-butyl)phenyl]-5,5′-biporphyrinato-(4−)-κN21,κN22,κN23,κN24:κN21′,κN22′,κN23′,κN24′])dizinc(II)* (**30**; 24 mg, 84% from **27**). Red solid. M.p. <300°. UV/VIS ($CHCl_3$): λ_{max} 305 (21000), 423 (145700), 459 (138000), 564 (30900). IR (neat): 2956*m*, 1590*m*, 1519*w*, 1476*m*, 1423*w*, 1392*w*, 1362*m*, 1330*w*, 1287*m*, 1247*m*, 1207*m*, 1160*w*, 1068*m*, 998*s*, 929*m*, 899*w*, 881*m*, 822*m*, 794*s*, 724*s*, 715*s*, 660*m*. ^{1}H-NMR ($CDCl_3$, 500 MHz): 9.01 (*d*, *J* = 4.7, 4 H); 8.97 (*d*, *J* = 4.7, 4 H); 8.71 (*d*, *J* = 4.7, 2 H); 8.70 (*d*, *J* = 4.7, 2 H); 8.23–8.17 (*m*, 4 H); 8.14 (*d*, *J* = 4.7, 2 H); 8.13 (*d*, *J* = 4.7, 2 H); 8.09 (*d*, *J* = 1.9, 8 H); 7.78–7.73 (*m*, 4 H); 7.69 (*t*, *J* = 1.9, 4 H); 4.88 (*s*, 4 H); 1.44 (*s*, 36 H); 1.43 (*s*, 36 H); the OH resonances are missing. Both H–C(8) and H–C(9) split into *doublets* probably as a consequence of atropisomerism. ^{13}C-NMR ($CDCl_3$, 75 MHz): 154.89; 150.99; 150.12; 149.93; 148.51; 143.37; 141.71; 138.98; 133.89; 133.70; 132.88; 132.25; 132.17; 131.82; 131.75; 131.62; 131.54; 129.65; 128.36; 128.26; 126.77; 126.02; 123.33; 121.20; 119.57; 65.45; 34.98; 31.69; four additional peaks due to atropisomerism. HR-FT-ICR-MALDI-MS (DHB): 1906.7648 (M^+, $C_{110}H_{114}N_8O_2Zn_2^+$; calc. 1906.7658).

*(μ3-[15,15″-Bis[3-(hydroxymethyl)phenyl]-10,10′,10″,20,20′,20″-hexakis[3,5-di(*tert*-butyl)phenyl]-5,5′:15′,5″-terporphyrinato(6−)-κN21,κN22,κN23,κN24:κN21′,κN22′,κN23′,κN24′:κN21″,κN22″,κN23″,κN24″])trizinc(II)* (**31**; 37 mg, 60% from **25**). Red solid. M.p. >300°. UV/VIS ($CHCl_3$): λ_{max} 420 (246700), 478 (216700), 572 (90000), 616 (sh, 41300). IR (neat): 2958*m*, 1590*m*, 1520*w*, 1475*m*, 1426*m*, 1392*w*, 1362*m*, 1321*m*, 1286*m*, 1247*m*, 1205*w*, 1168*w*, 1067*m*, 1031*w*, 993*s*, 928*s*, 899*w*, 881*w*, 843*w*, 821*m*, 793*s*, 723*m*, 714*m*, 663*w*. ^{1}H-NMR ($CDCl_3$, 300 MHz): 9.05 (*d*, *J* = 4.7, 4 H); 9.01 (*d*, *J* = 4.7, 4 H); 8.79 (*d*, *J* = 4.7, 4 H); 8.74 (*d*, *J* = 4.7, 4 H); 8.29–8.26 (*m*, *J* = 4.7, 8 H); 8.23 (*d*, *J* = 4.7, 2 H); 8.21 (*d*, *J* = 4.7, 2 H); 8.12 (*d*, *J* = 2.1, 8 H); 8.08 (*d*, *J* = 1.5, 4 H); 7.81–7.80 (*m*, 4 H); 7.73 (*t*, *J* = 2.1, 4 H); 7.56 (*t*, *J* = 1.5, 2 H); 5.01 (*s*, 4 H); 1.47 (*s*, 72 H); 1.35 (*s*, 36 H); the OH resonances are missing. ^{13}C-NMR ($CDCl_3$, 125 MHz): 154.95; 154.82; 151.04; 150.57; 150.17; 149.96; 148.54; 148.44; 143.39; 141.75; 141.59; 139.06; 134.00; 133.94; 133.71; 132.93; 132.35; 132.20; 132.13; 131.84; 131.72; 129.66; 129.46;

128.40; 128.31; 126.81; 126.07; 123.36; 121.25; 120.81; 120.75; 120.21; 119.64; 65.51; 35.15; 35.17; 31.72; 31.61. HR-FT-ICR-MALDI-MS (DHB): 2458.0921 ($[M-H]^+$, $C_{158}H_{163}N_{12}O_2Zn_3^+$; calc. 2458.0903).

*(μ_4-[15,15‴-Bis[3-(hydroxymethyl)phenyl]-10,10′,10″,10‴,20,20′,20″,20‴-octakis[3,5-di(*tert*-butyl)phenyl]-5,5′:15′,5″:15″,5‴-quaterporphyrinato(8−)-κN^{21},κN^{22},κN^{23},κN^{24}:κN$^{21'}$,κN$^{22'}$,κN$^{23'}$,κN$^{24'}$:κN$^{21''}$,κN$^{22''}$,κN$^{23''}$,κN$^{24''}$:κN$^{21'''}$,κN$^{22'''}$,κN$^{23'''}$,κN$^{24'''}$])tetrazinc(II)* (**32**; 27 mg, 55% from **26**). Red solid. M.p. >300°. IR (neat): 2961*m*, 1591*m*, 1520*w*, 1476*m*, 1423*m*, 1393*w*, 1362*m*, 1320*m*, 1287*m*, 1261*m*, 1207*w*, 1067*m* (br.), 996*s* (br.), 929*m*, 900*w*, 882*w*, 823*m*, 795*s*, 726*m*, 714*m*, 668*m*. UV/VIS ($CHCl_3$): λ_{max} 309 (28571), 419 (159821), 487 (164285), 576 (51786), 619 (sh, 12500). ^{1}H-NMR ($CDCl_3/CS_2$ 1:1, 500 MHz): 9.05 (*d*, *J* = 4.7, 4 H); 9.01 (*d*, *J* = 4.7, 4 H); 8.82 (*d*, *J* = 4.7, 4 H); 8.84 (*d*, *J* = 4.7, 4 H); 8.77 (*d*, *J* = 4.7, 2 H); 8.76 (*d*, *J* = 4.7, 2 H); 8.34 (*d*, *J* = 4.7, 4 H); 8.29 (*d*, *J* = 4.7, 4 H); 8.28–8.27 (*m*, 4 H); 8.24–8.23 (*m*, 4 H); 8.14 (*d*, *J* = 1.9, 8 H); 8.13 (*d*, *J* = 1.9, 8 H); 8.01–7.79 (*m*, 4 H); 7.74 (*t*, *J* = 1.9, 4 H); 7.63 (*t*, *J* = 1.9, 4 H); 4.96 (*s*, 4 H); 1.50 (*s*, 72 H); 1.49 (*s*, 72 H); the OH resonances are missing. ^{13}C-NMR ($CDCl_3/CS_2$ 1:1, 125 MHz): 154.89; 154.81; 154.78; 151.01; 150.58; 150.16; 149.94; 148.47; 148.38; 143.35; 141.75; 141.66; 139.05; 134.06; 133.01; 133.75; 132.92; 132.35; 132.22; 132.14; 131.87; 129.68; 129.47; 126.83; 125.99; 124.09; 123.36; 121.24; 120.81; 120.77; 120.24; 120.20; 119.64; 65.51; 34.95; 34.86; 31.72; 31.63. HR-FT-ICR-MALDI-MS (DCTB): 3207.4252 (M^+, $C_{206}H_{214}N_{16}O_2Zn_4^+$; calc. 3207.4297).

General Procedure for the Acylation of Oligoporphyrin-alcohols **30**–**32** *with Ethyl 3-Chloro-3-oxopropanoate.* To an oven-dried 50-ml round-bottomed flask charged with the appropriate alcohol derivative (1.5×10^{-2} mmol) and Et_3N (*ca.* 9 µl, 6.0×10^{-2} mmol) in dry CH_2Cl_2 (5 ml), $ClCOCH_2CO_2Et$ (*ca.* 6.0 µl, 6.0×10^{-2} mmol) was added at 0°, and the mixture was stirred for 30 min at 0°, then for 1 h at 25°. When all starting material had disappeared, the reaction was quenched with H_2O, and the mixture was diluted with $CHCl_3$ (10 ml). The org. layer was washed with H_2O (3×50 ml) and sat. aq. NaCl soln. (3×50 ml), dried (Na_2SO_4), and the solvent was evaporated *in vacuo*. FC (SiO_2; cyclohexane/CH_2Cl_2 1:1. 1% (*v*/*v*) Et_3N) and precipitation from MeOH upon dropwise addition of H_2O afforded the desired bis-malonate derivative.

*{µ-[15,15′-Bis(3-{[(3-ethoxy-3-oxopropanoyl)oxy]methyl}phenyl)-10,10′,20,20′-tetrakis[3,5-di(*tert*-butyl)phenyl]-5,5′-biporphyrinato(2−)-κN^{21},κN^{22},κN^{23},κN^{24}:κN$^{21'}$,κN$^{22'}$,κN$^{23'}$,κN$^{24'}$]}dizinc(II)* (**33**; 19.4 mg, 67% from **30**). Red solid. M.p. >300°. UV/VIS (PhMe): λ_{max} 306 (24800), 419 (184800), 458 (192600), 560 (48200), 604 (sh, 6090). IR (neat): 2958*s*, 2929*s*, 2857*m*, 1671*m*, 1590*m*, 1522*w*, 1463*m*, 1421*w*, 1370*m*, 1339*w*, 1289*s*, 1268*s*, 1217*m*, 1072*s* (br.), 998*s*, 950*m*, 900*w*, 889*w*, 850*m*, 848*m*, 800*s*, 779*m*, 713*m*, 667*w*. ^{1}H-NMR ($CDCl_3$, 300 MHz): 8.93 (*d*, *J* = 4.8, 4 H); 8.89 (*d*, *J* = 4.8, 4 H); 8.71 (*d*, *J* = 4.7, 4 H); 8.30–8.28 (*m*, 4 H); 8.71–8.12 (*m*, J_1 = 4.7, J_2 = 1.8, 12 H); 7.82–7.80 (*m*, 4 H); 7.71 (*t*, *J* = 1.8, 4 H); 5.54 (*s*, 4 H); 4.15 (*q*, *J* = 7.2, 4 H); 3.52 (*s*, 4 H); 1.44 (*s*, 72 H); 1.17 (*t*, *J* = 7.2, 6 H). ^{13}C-NMR ($CDCl_3$, 155 MHz): 166.61; 166.43; 154.91; 150.97; 150.14; 149.83; 148.48; 145.47; 143.56; 143.15; 141.74; 134.37; 133.98; 133.88; 133.68; 132.20; 131.67; 129.60; 127.24; 126.82; 123.32; 120.74; 120.65; 119.67; 67.40; 61.59; 41.75; 34.97; 31.67; 14.01. HR-FT-ICR-MALDI-MS (DHB): 1934.8350 (M^+, $C_{120}H_{126}N_8O_8Zn_2^+$; calc. 1934.8276).

*{µ$_3$-[15,15″-Bis(3-{[(3-ethoxy-3-oxopropanoyl)oxy]methyl}phenyl)-10,10′,10″,20,20′,20″-hexakis[3,5-di(*tert*-butyl)phenyl]-5,5′:15′,5″-terporphyrinato(6−)-κN^{21},κN^{22},κN^{23},κN^{24}:κN$^{21'}$,κN$^{22'}$,κN$^{23'}$,κN$^{24'}$:κN$^{21''}$,κN$^{22''}$,κN$^{23''}$,κN$^{24''}$]}trizinc(II)* (**34**; 29 mg, 71% from **31**). Red solid. M.p. >300°. UV/VIS (PhMe): λ_{max} 308 (34800), 417 (249000), 478 (232800), 567 (78400), 615 (sh, 8080). IR (neat): 2957*m*, 1590*m*, 1676*m*, 1523*w*, 1478*m*, 1429*m*, 1400*w*, 1369*m*, 1321*m*, 1296*m*, 1240*m*, 1215*w*, 1158*w*, 1076*m*, 1020*w*, 997*s*, 958*s*, 899*w*, 891*w*, 853*w*, 831*m*, 793*s*, 713*m*, 734*m*, 683*w*. ^{1}H-NMR ($CDCl_3$, 500 MHz): 9.05 (*d*, *J* = 4.7, 4 H); 9.01 (*d*, *J* = 4.7, 4 H); 8.78 (*d*, *J* = 4.6, 4 H); 8.74 (*d*, *J* = 4.6, 4 H); 8.31–8.28 (*m*, 4 H); 8.26 (*d*, *J* = 4.6, 4 H); 8.22–8.19 (*m*, 4 H); 8.12 (*d*, *J* = 1.7, 8 H); 8.08 (*d*, *J* = 1.5, 4 H); 7.81–7.80 (*m*, 4 H); 7.73 (*t*, *J* = 1.7, 4 H); 7.59 (*t*, *J* = 1.5, 2 H); 5.55 (*s*, 4 H); 4.15 (*q*, *J* = 7.2, 4 H); 3.52 (*s*, 4 H); 1.47 (*s*, 72 H); 1.34 (*s*, 36 H); 1.17 (*t*, *J* = 7.2, 6 H). ^{13}C-NMR ($CDCl_3$, 125 MHz): 166.61; 166.43; 154.94; 154.81; 151.04; 150.57; 150.20; 149.88; 148.54; 148.43; 143.48; 141.69; 141.55; 134.37; 133.97 (2×); 133.73; 132.36; 132.27; 132.14; 131.76; 130.86; 129.61; 126.86; 124.07; 123.42; 120.84; 120.79; 120.15; 119.71; 67.39; 61.59; 41.75; 34.99; 34.88; 31.59; 31.44; 14.14. HR-FT-ICR-MALDI-MS (DHB): 2681.1522 (M^+, $C_{168}H_{176}N_{12}O_8Zn_3^+$; calc. 2681.1603).

*{μ_4-[15,15‴-Bis(3-{[(3-ethoxy-3-oxopropanoyl)oxy]methyl}phenyl)-10,10′,10″,10‴,20,20′,20″,20‴-octakis[3,5-di(*tert*-butyl)phenyl]-5,5′:15′,5″:15″,5‴-quarterporphyrinato(8−)-κN^{21},κN^{22},κN^{23},κN^{24}:κN$^{21'}$,κN$^{22'}$,κN$^{23'}$,κN$^{24'}$:κN$^{21''}$,κN$^{22''}$,κN$^{23''}$,κN$^{24''}$:κN$^{21'''}$,κN$^{22'''}$,κN$^{23'''}$,κN$^{24'''}$]}tetrazinc(II)* (**35**; 30 mg, 70% from **32**). Red solid. M.p. >300°. UV/VIS ($CHCl_3$): λ_{max} 419 (297900), 487 (255300), 576 (106400), 619 (sh, 25400). IR (neat): 2960*m*, 1591*m*, 1523*w*, 1476*m*, 1392*w*, 1362*m*, 1319*m*, 1276*m*, 1260*m*, 1208*w*, 1068*m* (br.), 998*s*, 929*m*, 899*w*, 882*w*, 824*m*, 793*s*, 764*m*, 750*m*, 726*m*, 714*m*, 662*m*. ^{1}H-NMR ($CDCl_3/CS_2$ 3:1, 500 MHz): 9.06 (*d*, *J* = 4.6, 4 H); 9.02 (*d*, *J* = 4.6, 4 H); 8.82 (*d*, *J* = 4.7, 4 H); 8.80 (*d*, *J* = 4.7, 4 H); 8.77 (*d*, *J* = 4.7, 4 H); 8.35–8.32 (*m*, 8 H); 8.30 (*d*, *J* = 4.7, 4 H); 8.24 (*m*, 4 H); 8.14 (*d*, *J* = 1.8, 8 H); 8.13 (*d*, *J* = 1.8, 8 H); 8.01–7.79 (*m*, 4 H); 7.74 (*t*, *J* = 1.8, 4 H); 7.63 (*t*, *J* = 1.8, 4 H); 5.56 (*s*, 4 H); 4.17 (*q*, *J* = 7.5, 4 H); 3.52 (*s*, 4 H); 1.50 (*s*, 72 H); 1.49 (*s*, 72 H); 1.19 (*t*, *J* = 7.5, 6 H).

^{13}C-NMR ($CDCl_3/CS_2$ 3:1, 125 MHz): 166.50; 166.31; 154.91; 154.82; 154.78; 151.03; 150.60; 150.21; 149.88; 148.50; 148.41; 143.46; 141.69; 141.62; 134.39; 134.03 (× 3); 133.74; 132.39; 132.31; 132.22; 132.17; 131.80; 129.64; 129.22; 127.27; 126.89; 124.11; 123.43; 120.84; 120.81; 120.78; 120.24; 120.14; 119.74; 67.37; 61.57; 41.70; 34.96; 34.87; 31.71; 31.63; 14.04; two peaks are missing probably due to overlap. HR-FT-ICR-MALDI-MS (DCTB): 3427.4800 (M^+, $C_{216}H_{226}N_{16}O_8Zn_4^+$; calc. 3427.4930).

General Procedure for the Bingel *Cyclopropanation of C_{60} with Bis-malonates* **33**–**35**. To an oven-dried 200-ml round-bottomed flask charged with a soln. of the appropiate bis-malonate (1.5×10^{-2} mmol), C_{60} (43 mg, 6.0×10^{-2} mmol), and I_2 (7.5 mg, 3×10^{-2} mmol) in deoxygenated PhMe (50 ml), DBU (6 µl, 0.29 mmol) was added dropwise at 0°. After 1.5 h, the mixture was filtered through a short plug (SiO_2; PhMe). The brown-red fraction was purified by FC (SiO_2; cyclohexane/PhMe 8:2 → PhMe, 1% (*v*/*v*) Et_3N), and the solvent was evaporated *in vacuo*. Precipitation of the chromatographic fraction from $CHCl_3$ upon addition of MeOH afforded the desired fullerene–porphyrin derivatives as powder.

*{µ-[15,15′-Bis{3-[({[3′-(ethoxycarbonyl)-3′*H*-cyclopropa[1,9](C$_{60}$-I$_h$)[5,6]fullerene-3′-yl]carbonyl}oxy)methyl]phenyl}-10,10′,20,20′-tetrakis[3,5-di(*tert*-butyl)phenyl]-5,5′-biporphyrinato(4−)-κN^{21},κN^{22},κN^{23},κN^{24}:κN$^{21'}$,κN$^{22'}$,κN$^{23'}$,κN$^{24'}$]}dizinc(II)* (**4**; 28 mg, 55% from **33**). Brown solid. M.p. >300°. UV/VIS ($CHCl_3$): λ_{max} 259 (227000), 329 (56900), 422 (374000), 549 (18800). IR (neat): 2961*s*, 1748*s*, 1591*m*, 1524*w*, 1463*m*, 1427*m*, 1384*w*, 1362*m*, 1289*m*, 1266*m*, 1230*s*, 1204*s*, 1184*m*, 1095*m*, 1061*m*, 1000*s*, 931*m*, 882*m*, 848*w*, 824*m*, 794*m*, 780*m*. Fluorescence ($CHCl_3$; λ_{exc} = 422 nm): λ_{max} 596, 644. ^{1}H-NMR ($C_6D_5CD_3$, 300 MHz): 9.19 (*d*, *J* = 4.5, 2 H); 9.14 (*d*, *J* = 4.5, 2 H); 9.04 (*d*, *J* = 4.8, 2 H); 8.96 (*d*, *J* = 4.5 2 H); 8.92 (*d*, *J* = 4.8, 2 H); 8.53 (*d*, *J* = 4.5, 2 H); 8.43–8.48 (*m*, 8 H); 8.28–8.35 (*m*, 6 H); 8.18 (*m*, 2 H); 7.90 (*t*, *J* = 1.8, 2 H); 7.79 (*t*, *J* = 1.8, 2 H); 7.51 (*m*, 2 H); 7.28–7.31 (*m*, 2 H); 5.60 (*s*, 4 H); 4.09 (*q*, *J* = 7.1, 4 H); 1.51 (*s*, 18 H); 1.50 (*s*, 18 H); 1.40 (*s*, 18 H); 1.38 (*s*, 18 H); 1.01 (*t*, *J* = 7.1, 6 H). ^{13}C-NMR ($CDCl_3$,125 MHz): 163.57; 163.36; 154.93; 154.86; 150.88; 150.03; 150.00; 149.61; 149.58; 148.66; 148.48; 148.44; 144.73 (2×); 144.53 (2×); 144.49; 144.47; 144.37; 144.22 (2×); 144.17; 144.10; 144.07; 143.64; 143.56; 143.50; 143.49; 143.44; 143.31; 143.29; 143.11; 143.07; 142.74; 142.54; 142.49; 142.29; 142.25; 142.23; 142.17; 141.92; 141.85; 141.83; 141.67; 141.63; 141.45; 141.42; 141.40; 141.32; 141.30; 141.28; 140.68; 140.59; 140.32; 140.08; 140.03; 139.68; 139.63; 139.30; 139.28; 139.13; 139.06; 137.05; 137.01; 134.69; 133.89 (2×); 133.39; 133.25; 132.48; 132.33; 132.24; 132.09; 131.88; 131.82; 129.92; 129.76; 129.48; 126.90; 125.67; 123.54; 123.31; 120.85; 120.70; 119.70; 70.95; 68.21; 63.53; 52.18; 35.09; 35.06; 34.96; 34.94; 31.87; 31.86; 31.73; 31.69; 14.27. HR-FT-ICR-MALDI-MS (DCTB): 3370.7940 (M^+, $C_{240}H_{122}N_8O_8Zn_2^+$; calc. 3370.7963).

*{µ$_3$-[15,15″-Bis{3-[({[3′-(ethoxycarbonyl)-3′*H*-cyclopropa[1,9](C$_{60}$-I$_h$)[5,6]fullerene-3′-yl]carbonyl}oxy)methyl]phenyl}-10,10′,10″,20,20′,20″-hexakis[3,5di(*tert*-butyl)phenyl]-5,5′:15′,5″-terporphyrinato(6−)-κN^{21},κN^{22},κN^{23},κN^{24}:κN$^{21'}$,κN$^{22'}$,κN$^{23'}$,κN$^{24'}$:κN$^{21''}$,κN$^{22''}$,κN$^{23''}$,κN$^{24''}$]}trizinc(II)* (**5**; 10 mg, 60% from **34**). Brown solid. M.p. >300°. UV/VIS ($CHCl_3$): λ_{max} 259 (202000), 327 (78400), 423 (167000), 481 (180000), 574 (56800). IR (neat): 2961*s*, 1748*s*, 1591*m*, 1524*w*, 1463*m*, 1427*m*, 1384*w*, 1362*m*, 1289*m*, 1266*m*, 1230*s*, 1204*s*, 1184*m*, 1095*m*, 1061*m*, 1000*s*, 931*m*, 882*m*, 848*w*, 824*m*, 794*m*, 780*m*. Fluorescence ($CHCl_3$; λ_{exc} = 422 nm): λ_{max} 634. ^{1}H-NMR ($C_6D_5CD_3$, 300 MHz): 9.38 (*d*, *J* = 4.9, 1 H(*syn*), 1 H(*anti*)); 9.27 (*d*, *J* = 4.9, 1 H(*syn*), 1 H(*anti*)); 9.07 (*d*, *J* = 5.1, 4 H(*syn*), 4 H(*anti*)); 9.04 (*d*, *J* = 4.5, 1 H(*syn*), 1 H(*anti*)); 8.90–8.95 (*m*, 10 H(*syn*), 10 H(*anti*)); 8.65 (*d*, *J* = 4.8, 1 H(*syn*), 1 H(*anti*)); 8.59 (*d*, *J* = 4.5, 1 H(*syn*), 1 H(*anti*)); 8.58 (*d*, *J* = 4.5, 1 H(*syn*), 1 H(*anti*)); 8.50–5.52 (*m*, 6 H(*syn*), 4 H(*anti*)); 8.45 (*s*, 2 H(*syn*), 2 H(*anti*)); 8.37 (*s*, 4 H(*syn*), 8 H(*anti*)); 8.32–8.34 (*m*, 2 H(*syn*), 2 H(*anti*)); 8.25 (*d*, *J* = 1.5, 2 H(*syn*)); 8.20 (*s*, 4 H(*syn*), 4 H(*anti*)); 7.91 (*m*, 1 H(*syn*)); 7.82 (*m*, 4 H(*syn*), 4 H(*anti*)); 7.80 (*m*, 2 H(*anti*)) 7.69 (*m*, 1 H(*syn*)); 7.49–7.54 (*m*, 2 H(*syn*), 2 H(*anti*)); 7.30–7.32 (*m*, 2 H(*syn*), 2 H(*anti*)); 5.61 (*s*, 4 H(*syn*), 4 H(*anti*)); 4.18 (*q*, *J* = 7.2, 4 H(*syn*), 4 H(*anti*)); 1.49 (*s*, 18 H(*syn*)); 1.43 (*s*, 36 H(*syn*), 36 H(*anti*)); 1.41 (*s*, 36 H(*syn*), 36 H(*anti*)); 1.38 (*s*, 36 H(*anti*)); 1.26 (*s*, 18 H(*syn*)); 1.01 (*t*, *J* = 7.2, 6 H(*syn*), 6 H(*anti*)). ^{13}C-NMR ($C_6D_5CD_3$, 125 MHz): 163.57; 163.36; 154.92; 154.80; 150.93; 150.68; 150.61; 150.54; 150.03; 149.64; 148.86; 148.64; 148.49; 148.45; 148.40; 144.75; 144.57; 144.55; 144.52; 144.46; 144.38; 144.24; 144.22; 144.19; 144.12; 144.10; 143.64; 143.51; 143.31; 143.10; 143.09; 142.55; 142.49; 142.28; 142.21; 142.18; 142.02; 141.90; 141.89; 141.74; 141.52; 141.46; 141.38; 141.29; 140.66; 140.32; 140.28; 140.05; 139.66; 139.63; 139.30; 139.11; 139.09; 137.02; 134.75; 133.98; 133.91; 133.38; 133.32; 132.32; 132.10; 132.00; 131.87; 130.55; 129.98; 129.45; 129.39; 129.35; 128.85; 127.20; 126.87; 125.66; 124.63; 124.26; 123.89; 123.38; 120.80; 120.72; 120.19; 119.78; 70.95; 68.20; 63.52; 52.18; 35.16 (*syn*); 35.02 (*syn*); 34.99 (*anti*); 34.97 (*anti*); 34.87 (*syn*); 31.95 (*syn*); 31.76 (*anti*); 31.71 (*syn* and *anti*); 31.57 (*syn*); 14.26. HR-FT-ICR-MALDI-MS (DCTB): 4117.1200 (M^+, $C_{288}H_{172}N_{12}O_8Zn_3^+$; calc. 4117.1290).

*[µ$_4$-(15,15‴-Bis{3-[({[3′-(ethoxycarbonyl)-3′*H*-cyclopropa[1,9](C$_{60}$-I$_h$)[5,6]fullerene-3′-yl]carbonyl}oxy)methyl]phenyl}-10,10′,10″,10‴,20,20′,20″,20‴-octakis[3,5-di(*tert*-butyl)phenyl]-5,5′:15′,5″:15″,5‴-quaterporphyrinato(8−)-κN^{21},κN^{22},κN^{23},κN^{24}:κN$^{21'}$,κN$^{22'}$,κN$^{23'}$,κN$^{24'}$:κN$^{21''}$,κN$^{22''}$,κN$^{23''}$,κN$^{24''}$:κN$^{21'''}$,κN$^{22'''}$,κN$^{23'''}$,κN$^{24'''}$)]tetrazinc(II)* (**6**; 11 mg, 45% from **35**). Brown solid. M.p. >300°. UV/VIS ($CHCl_3$): λ_{max} 258 (224000), 327 (86900),

420 (218000), 489 (242000), 576 (93200). IR (neat): 2960*m*, 1591*m*, 1523*w*, 1476*m*, 1392*w*, 1362*m*, 1319*m*, 1276*m*, 1260*m*, 1208*w*, 1068*m* (br.), 998*s*, 929*m*, 899*w*, 882*w*, 824*m*, 793*s*, 764*m*, 750*m*, 726*m*, 714*m*, 662*m*. Fluorescence ($CHCl_3$; λ_{exc} = 422 nm) λ_{max} 634. ^{1}H-NMR ($CDCl_3$, 300 MHz): 8.99 (*d*, *J* = 4.5, 2 H); 8.92–8.93 (*m*, 10 H); 8.83 (*d*, *J* = 4.5, 2 H); 8.73–8.77 (*m*, 6 H); 8.45–8.48 (*m*, 2 H); 8.36–8.40 (*m*, 4 H); 8.22–8.29 (*m*, 18 H); 8.12 (*m*, 4 H); 7.91–7.86 (*m*, 2 H); 7.79–7.82 (*m*, 6 H); 7.69–7.71 (*m*, 6 H); 7.62 (*m*, 2 H); 6.02 (*s*, 4 H); 4.53 (*m*, 4 H); 1.48 (br. *s*, 78 H) 1.37–1.40 (*m*, 72 H). ^{13}C-NMR ($CDCl_3$, 125 MHz): 163.27; 163.05; 154.81; 154.74; 154.70; 154.78; 150.84; 150.57; 150.53; 150.49; 149.99; 148.50; 148.36; 148.31; 144.78; 144.61; 144.55; 144.52; 144.46; 144.33; 144.26; 144.24; 144.16; 144.13; 143.69; 143.64; 143.61; 143.26; 143.64; 143.39; 143.36; 142.82; 142.59; 142.51; 142.35; 142.04; 142.01; 141.78; 141.70; 141.61; 141.59; 141.47; 141.31; 140.86; 140.64; 140.14; 139.93; 139.34; 139.22; 137.30; 134.15; 134.04; 134.02; 133.52; 133.34; 132.30; 132.29; 132.27; 132.24; 132.08 (2×); 131.81; 129.93; 129.53; 129.47; 126.89; 124.26; 124.01; 123.32; 120.77; 120.69; 120.60; 120.23; 120.12; 119.74; 70.98; 68.21; 63.38; 52.08; 34.89; 34.85; 34.78; 31.74; 31.73; 31.68; 31.60; 14.28; some peaks are missing probably due to overlap. HR-FT-ICR-MALDI-MS (DCTB): 4864.4307 (MH^+, $C_{336}H_{223}N_{16}O_8Zn_4^+$; calc. 4864.4701).

*(μ-[15-[3-(Hydroxymethyl)phenyl]-10,10′,20,20′-tetrakis[3,5-di(*tert*-butyl)phenyl]-5,5′-biporphyrinato(4−)-*κ*N^{21},*κ*N^{22},*κ*N^{23},*κ*N^{24}:*κ*N$^{21'}$,*κ*N$^{22'}$,*κ*N$^{23'}$,*κ*N$^{24'}$])dizinc(II)* (**36**). Compound **36** was synthesized as described for **20**. The intermediates between the first and the third step were not purified and were submitted as crude mixture to the next conversion. *Step I:* **21** (300 mg, 0.20 mmol), I_2 (50 mg, 0.20 mmol), $CHCl_3$/pyridine 30:1 (30 ml), and $AgPF_6$ (50 mg, 0.20 mmol) in MeCN (3 ml); *Step II:* **19** (229 mg, 0.33 mmol), $[Pd(Ph_3P)_4]$ (10 mg, 0.022 mmol), Cs_2CO_3 (563 mg, 1.60 mmol), and three drops of H_2O in PhMe (7 ml); *Step III:* THF (10 ml), several drops of a 1M soln. of Bu_4NF in THF. FC (SiO_2; cyclohexane/CH_2Cl_2 1:1, 1% (*v*/*v*) Et_3N) and precipitation from $CHCl_3$ upon addition of MeOH/H_2O 9:1 afforded **36** (128 mg, 40% from **21**). Red solid. M.p. >300°. UV/VIS ($CHCl_3$): λ_{max} 306 (23000), 421 (174300), 457 (156300), 563 (34500). IR (neat): 2960*m*, 2866*w*, 1590*m*, 1520*w*, 1475*w*, 1422*w*, 1392*w*, 1361*m*, 1321*w*, 1287*m*, 1261*m*, 1247*m*, 1208*m* (br.), 1155*w* (br.), 1062*m* br, 995*s*, 928*m*, 900*w*, 882*m*, 849*w*, 821*m*, 817*s*, 714*s*, 700*m*, 661*w*. ^{1}H-NMR (500 MHz, $CDCl_3$): 10.31 (*s*, 1 H); 9.42 (*d*, *J* = 4.5, 2 H); 9.12 (*d*, *J* = 4.5, 2 H); 8.96–8.90 (*m*, 4 H); 8.69–8.62 (*m*, 4 H); 8.17–8.09 (*m*, 2 H); 8.08–8.01 (*m*, 12 H); 7.70–7.61 (*m*, 6 H); 4.84 (*d*, *J* = 5.6, 2 H); 1.70 (*t*, *J* = 5.6, 1 H); 1.39 (*s*, 72 H). ^{13}C-NMR ($CDCl_3$; 125 MHz): 154.92; 154.53; 151.01; 150.22; 150.12; 150.07; 149.93; 149.79; 148.60; 149.62; 148.52; 143.34; 141.67; 141.58; 139.01; 133.92; 133.70; 133.84; 132.90; 132.80; 132.25 (2×); 132.18; 131.83; 131.72; 129.73; 129.65; 126.80; 126.06; 123.48; 123.37; 122.82; 121.23; 120.82; 120.77; 119.83; 119.68; 106.51; 65.48; 35.01; 34.98; 31.71; 31.68. HR-FT-ICR-MALDI-MS (DCTB): 1718.7517 (M^+, $C_{103}H_{108}N_8OZn_2^+$; calc. 1718.7534).

*{μ-[15-(3-[[(3-Ethoxy-3-oxopropanoyl)oxy]methyl]phenyl)-10,10′,20,20′-tetrakis[3,5-di(*tert*-butyl)phenyl]-5,5′-biporphyrinato(4−)-*κ*N^{21},*κ*N^{22},*κ*N^{23},*κ*N^{24}:*κ*N$^{21'}$,*κ*N$^{22'}$,*κ*N$^{23'}$,*κ*N$^{24'}$]}dizinc(II)* (**37**). Compound **37** was synthesized as described for **9**. Compound **36** (128 mg, 8.0 10^{-2} mmol), Et_3N (30 μl, 1.6×10^{-1} mmol), and $ClCOCH_2CO_2Et$ (30 μl, 1.6 10^{-1} mmol) in CH_2Cl_2 (15 ml). After workup, **37** (123 mg, 90%) was obtained as red solid. M.p. >300°. IR (neat): 2959*s*, 2931*s*, 2871*m*, 1725*s*, 1592*m*, 1521*w*, 1461*m*, 1424*w*, 1383*w*, 1363*m*, 1287*s*, 1270*s*, 1208*m*, 1124*s*, 1072*s*, 1038*w*, 994*s*, 928*m*, 900*w*, 882*w*, 823*m*, 794*m*, 737*s*, 716*m*, 704*m*. ^{1}H-NMR ($CDCl_3$, 300 MHz): 10.42 (*s*, 1 H); 9.52 (*d*, *J* = 4.5, 2 H); 9.22 (*d*, *J* = 4.5, 2 H); 9.06 (*d*, *J* = 4.6, 2 H); 9.02 (*d*, *J* = 4.6, 2 H); 8.80 (*d*, *J* = 4.6, 2 H); 8.73 (*d*, *J* = 4.6, 2 H); 8.34–8.32 (*m*, 2 H); 8.22–8.18 (*m*, 4 H); 8.15–8.13 (*m*, *J* = 1.8, 4 H); 8.11 (*d*, *J* = 1.8, 4 H); 7.84–7.82 (*m*, 2 H); 7.74 (*t*, *J* = 1.8, 2 H); 7.72 (*t*, *J* = 1.8, 2 H); 5.55 (*s*, 2 H); 4.16 (*q*, *J* = 7.0, 2 H); 3.52 (*s*, 2 H); 1.48 (*s*, 36 H); 1.46 (*s*, 36 H); 1.18 (*t*, *J* = 7.0, 3 H). ^{13}C-NMR ($CDCl_3$, 75 MHz): 166.44; 166.26; 154.72; 154.33; 150.83; 149.99; 149.88; 149.70; 149.62; 148.43; 148.37; 143.28; 141.46; 141.40; 134.23; 133.84; 133.57; 132.70; 132.16; 131.64; 129.62; 128.92; 128.11; 127.19; 126.76; 123.31; 122.72; 120.71; 119.67; 67.40; 61.63; 41.79; 35.08; 35.05; 31.78; 31.76; 14.04. HR-FT-ICR-MALDI-MS (DCTB): 1718.7517 (M^+, $C_{108}H_{114}N_8O_4Zn_2^+$; calc. 1718.7534).

*[μ-(15-{3-[({[3′-(Ethoxycarbonyl)-3′*H*-cyclopropa[1,9](*C_{60}*-I*$_h$*)[5,6]fullerene-3′-yl]carbonyl}oxy)methyl]-phenyl}-10,10′,20,20′-tetrakis[3,5-di(*tert*-butyl)phenyl]-5,5′-biporphyrinato(4−)-*κ*N^{21},*κ*N^{22},*κ*N^{23},*κ*N^{24}:*κ*N$^{21'}$,*κ*N$^{22'}$,*κ*N$^{23'}$,*κ*N$^{24'}$)]dizinc(II)* (**7**). Compound **7** was synthesized as described for **3**. Compound **36** (70 mg, 5.0 × 10^{-2} mmol), C_{60} (72 mg, 0.1 mmol), I_2 (13 mg, 5.5×10^{-2} mmol), and DBU (8 μl, 0.15 mmol) in PhMe (100 ml). After workup, **7** (49 mg, 40%) was obtained as brown solid. M.p. >300°. UV/VIS ($CHCl_3$): λ_{max} 260 (241800), 328 (62900), 422 (180800), 458 (186700), 563 (41300). IR (neat): 2957*s*, 1748*s*, 1590*m*, 1521*w*, 1462*m*, 1426*w*, 1392*w*, 1362*m*, 1319*w*, 1289*m*, 1265*m*, 1228*s*, 1204*s*, 1184*s*, 1096*w*, 1061*s*, 1038*w*, 996*s*, 928*m*, 900*m*, 882*m*, 850*m*, 824*m*, 793*s*, 756*m*, 728*m*, 714*s*, 667*w*. ^{1}H-NMR (500 MHz, $CDCl_3$): 10.42 (*s*, 1 H); 9.54 (*d*, *J* = 4.5, 1 H); 9.51 (*d*, *J* = 4.5, 1 H); 9.29 (*d*, *J* = 4.5, 1 H); 9.20 (*d*, *J* = 4.5, 1 H); 8.98 (*d*, *J* = 4.5, 1 H); 8.91 (*s*, 4 H); 8.78 (*d*, *J* = 4.6, 1 H); 8.65 (*d*, *J* = 4.7, 1 H); 8.44 (*d*, *J* = 6.5, 1 H); 8.28 (*s*, 1 H); 8.22–8.21(*m*, 3 H); 8.18 (*d*, *J* = 4.7, 1 H); 8.16 (*t*, 2 H); 8.12 (*d*, *J* = 1.8, 2 H); 8.10 (*d*, *J* = 4.7, 2 H); 7.87 (*m*, *J* = 7.6, 1 H); 7.80 (*t*, *J* = 1.8, 2 H); 7.92 (*t*, *J* = 1.8, 2 H); 7.72 (*t*, *J* = 1.8, 2 H); 7.65 (*t*, *J* = 1.8, 2 H); 6.00 (*s*, 2 H); 4.53 (*q*, *J* = 7.1, 2 H); 1.56 (*s*, 18 H); 1.46 (*s*, 18 H); 1.44 (*s*,

18 H); 1.36 (*s*, 18 H); 0.89 (*t*, *J* = 7.1, 3 H). ^{13}C-NMR ($CDCl_3$, 75 MHz): 163.52; 163.31; 154.85; 154.47; 151.01; 150.96; 150.86; 150.02; 149.94; 149.73; 149.58; 148.62; 148.55; 148.43; 148.40; 144.70; 144.51; 144.48; 144.45; 144.34; 144.20; 144.15; 144.08; 144.05; 143.57; 143.48; 143.46; 143.27; 143.06; 142.51; 142.48; 142.23; 142.16; 142.86; 141.63; 142.52; 141.48; 141.42; 141.35; 141.34; 141.26; 140.62; 140.27; 140.02; 139.63; 139.26; 139.06; 137.00; 134.62; 133.89; 133.34; 132.76; 132.29; 132.19; 131.82; 131.68 (2×); 130.19; 129.69; 129.40; 129.33; 126.85 (2×); 123.33; 123.06; 122.73; 120.87; 120.72 (3×); 120.68; 119.79; 119.76; 122.72; 120.71; 119.67; 70.92; 68.15; 63.42; 52.14; 35.10; 34.96; 34.92; 34.90; 31.90; 31.84; 31.69; 31.67; 31.64; 14.23. HR-FT-ICR-MALDI-MS (DCTB): 2437.7376 (M^+, $C_{168}H_{112}N_8O_4Zn_2^+$; calc. 2437.7406).

(μ-{15-(3-Cyanophenyl)-10,10′,20,20′-tetrakis[3,5-di(tert-*butyl)phenyl]-5,5′-biporphyrinato(4−)-*κ*N^{21},*κ*N^{22},*κ*N^{23},*κ*N^{24}:*κ*N$^{21'}$,*κ*N$^{22'}$,*κ*N$^{23'}$,*κ*N$^{24'}$})dizinc(II)* (**40**) *and (μ-{15,15′-Bis(3-cyanophenyl)-10,10′,20,20′-tetrakis[3,5-di*(tert-*butyl)phenyl]-5,5′-biporphyrinato(4−)-*κ*N^{21},*κ*N^{22},*κ*N^{23},*κ*N^{24}:*κ*N$^{21'}$,*κ*N$^{22'}$,*κ*N$^{23'}$,*κ*N$^{24'}$})dizinc(II)* (**41**). To a N_2-flushed 50-ml round-bottomed flask charged with **24** (250 mg, 0.143 mmol) in dry PhMe (35 ml), **39** (225 mg, 0.857 mmol), [Pd(PPh_3)$_4$] (50 mg, 0.029 mmol), Cs_2CO_3 (810 mg, 2.29 mmol), and three drops of H_2O were added. The mixture was deoxygenated by three *freeze-pump-thaw* cycles with N_2 and stirred at 100° for 18 h. After cooling to 25°, the suspension was filtered through Celite, and the solvent was evaporated *in vacuo*. FC (SiO_2; cyclohexane/CH_2Cl_2 1:1, 1% (v/v) Et_3N) afforded three fractions corresponding to **21**, **40**, and **41**. Precipitation of the chromatographic fractions from $CHCl_3$ upon addition of MeOH/H_2O 9:1 afforded **21** (25 mg, 11%), **40** (50 mg, 20%), and **41** (167 mg, 69%).

Data of **40**. Red solid. M.p. >300°. UV/VIS ($CHCl_3$): λ_{max} 307 (33100), 421 (221600), 455 (209800), 515 (25400), 607 (9740). IR (neat): 2953*m*, 1590*m*, 1475*w*, 1410*w*, 1362*m*, 1296*m*, 1247*m*, 1220*w*, 1062*w*, 1046*w*, 994*s*, 916*m*, 897*w*, 882*w*, 846*m*, 804*s*, 759*w*, 738*m*, 714*s*, 688*m*, 636*w*. ^{1}H-NMR ($CDCl_3$, 300 MHz): 10.43 (*s*, 1 H); 9.53 (*d*, *J* = 4.5, 2 H); 9.22 (*d*, *J* = 4.5, 2 H); 9.09 (*d*, *J* = 4.5, 2 H); 8.91 (*d*, *J* = 4.5, 2 H); 8.80 (*d*, *J* = 4.5, 2 H); 8.74 (*d*, *J* = 4.5, 2 H); 8.63 (*s*, 1 H); 8.59 (*d*, *J* = 8.1, 1 H); 8.20–8.11 (*m*, 13 H); 7.94 (*t*, *J* = 8.1, 1 H); 7.75–7.72 (*m*, 4 H); 1.48 (*s*, 36 H); 1.46 (*s*, 36 H). ^{13}C-NMR ($CDCl_3$, 75 MHz): 154.87; 154.35; 150.94; 150.30; 149.92; 149.70; 149.20; 148.53; 148.49; 144.43; 141.43; 141.34; 138.02; 136.97; 134.12; 133.79; 132.77; 132.66; 132.37; 132.19; 131.72; 131.22; 131.00; 129.66; 129.55; 127.44; 123.69; 122.82; 120.85; 120.79; 119.48; 111.03; 106.58; 35.11; 31.82; 31.79; two extra peaks probably result from atropisomerism. HR-FT-ICR-MALDI-MS (DCTB): 1599.7077 (M^+, $C_{103}H_{105}N_9Zn_2^+$; calc. 1599.7062).

Data of **41**. Red solid. M.p. >300°. UV/VIS ($CHCl_3$): λ_{max} 309 (40000), 424 (245700), 461 (240000), 565 (54300), 611 (1530). IR (neat): 2960*m*, 2904*w*, 2868*w*, 2231*w*, 1806*w*, 1592*m*, 1522*w*, 1476*m*, 1425*w*, 1393*w*, 1362*m*, 1331*m*, 1288*m*, 1247*m*, 1220*w*, 1208*w*, 1170*w*, 1069*w*, 994*s*, 931*m*, 899*w*, 882*w*, 824*m*, 793*s*, 715*m*, 696*w*, 660*w*. ^{1}H-NMR ($CDCl_3$, 500 MHz): 9.00 (*d*, *J* = 4.7, 4 H); 8.81 (*d*, *J* = 4.7, 4 H); 8.66 (*d*, *J* = 4.7, 2 H); 8.67 (*d*, *J* = 4.7, 2 H); 8.54 (*t*, *J* = 1.3, 2 H); 8.49 (*dt*, *J* = 7.8, 1.3, 2 H); 8.08 (*d*, *J* = 4.7, 2 H); 8.06 (*d*, *J* = 4.7, 2 H); 8.05 (*dt*, *J* = 7.8, 1.3, 2 H); 8.02 (*d*, *J* = 1.9, 8 H); 7.85 (*t*, *J* = 7.8, 2 H); 7.64 (*t*, *J* = 1.9, 4 H); 1.38 (*s*, 36 H); 1.47 (*s*, 36 H). ^{13}C-NMR ($CDCl_3$, 125 MHz): 153.93; 153.91; 150.10; 149.41; 149.37; 148.36; 147.67 (2×); 147.59; 147.58; 143.51; 140.42; 140.39; 137.07; 136.03; 133.11; 133.08; 131.77; 131.75; 131.51; 131.47; 130.28; 130.09; 128.72; 128.60; 126.49; 122.80; 122.76; 119.91; 118.89; 118.07; 117.13; 110.10; 33.97; 33.96; 30.65 (2×). HR-FT-ICR-MALDI-MS (DCTB): 1696.7336 (M^+, $C_{110}H_{108}N_{10}Zn_2^+$; calc. 1696.7330).

{5,15-Bis[3,5-di(tert-*butyl)phenyl]-10-(3-cyanophenyl)porphyrinato(2−)-*κ*N^{21},*κ*N^{22},*κ*N^{23},*κ*N^{24}}zinc(II)* (**42**). To a N_2-flushed 50-ml round-bottomed flask charged with **15** (764 mg, 0.9 mmol) in dry PhMe (200 ml), **39** (525 mg, 2.29 mmol), [Pd(PPh_3)$_4$] (105 mg, 0.090 mmol), Cs_2CO_3 (2.030 g, 11.50 mmol), and three drops of H_2O were added. The mixture was then deoxygenated by three *freeze-pump-thaw* cycles with N_2 and stirred at 100° for 18 h. After cooling to 25°, the mixture was filtered through *Celite*, and the solvent was evaporated *in vacuo*. FC (SiO_2; cyclohexane/CH_2Cl_2 1:1, 1% (*v*/*v*) Et_3N) afforded two fractions corresponding to **14** and **42**. Precipitation of the chromatographic fractions from $CHCl_3$ upon addition of MeOH/H_2O 9:1 afforded **14** (147 mg, 23%) and **42** (494 mg, 67%). Red solid. M.p. >300°. UV/VIS ($CHCl_3$): λ_{max} 351 (5070), 421 (176700), 549 (7960). IR (neat): 2954*m*, 2230*w*, 1590*m*, 1523*w*, 1476*m*, 1424*w*, 1392*w*, 1382*w*, 1361*w*, 1330*w*, 1292*m*, 1246*m*, 1221*w*, 1208*w*, 1062*m*, 996*s*, 928*m*, 899*m*, 883*m*, 848*m*, 818*m*, 780*s*, 754*m*, 718*s*, 698*s*, 658*w*, 614*w*. ^{1}H-NMR ($CDCl_3$, 300 MHz): 10.33 (*s*, 1 H); 9.46 (*d*, *J* = 4.6, 2 H); 9.21 (*d*, *J* = 4.6, 2 H); 9.12 (*d*, *J* = 5.2, 2 H); 8.86 (*d*, *J* = 5.2, 2 H); 8.53 (*s*, 1 H); 8.50 (*d*, *J* = 3.8, 1 H); 8.15 (*d*, *J* = 2.1, 4 H); 8.08 (*d*, *J* = 3.8, 1 H); 7.86 (*m*, *J* = 2.1, 3 H); 1.59 (*s*, 36 H). ^{13}C-NMR ($CDCl_3$, 75 MHz): 150.62; 150.36; 149.85; 148.86; 148.63; 148.55; 144.40; 141.28; 137.91; 136.84; 133.06; 132.66; 131.84; 131.10; 130.88; 129.85; 129.73; 127.28; 122.34; 120.87; 110.87; 106.36; 35.15; 31.85. HR-FT-ICR-MALDI-MS (DCTB): 849.3733 (M^+, $C_{55}H_{55}N_5Zn^+$; calc. 849.3743). Anal. calc. for $C_{55}H_{55}N_4OZn$ · MeOH (883.49): C 76.13, H 6.73, N 6.93; found: C 76.16, H 7.67, N 6.86. X-Ray: see *Fig. 4*.

(μ-{10,10′-Bis(3-cyanophenyl)-5,5′,15,15′-tetrakis[3,5-di(tert-*butyl)phenyl]-18,18′:20,20′-dicyclo-2,2′-biporphyrinato(4−)-*κ*N^{21},*κ*N^{22},*κ*N^{23},*κ*N^{24}:*κ*N$^{21'}$,*κ*N$^{22'}$,*κ*N$^{23'}$,*κ*N$^{24'}$})dizinc(II)* (**38**). *Method A.* Sc(OTf)$_3$ (174 mg,

0.35 mmol) and DDQ (100 mg, 0.44 mmol) were added under N_2 to a soln. of **41** (150 mg, 0.088 mmol) in dry PhMe (150 ml). The mixture was heated to reflux for 30 min. After cooling to 25°, the mixture was diluted with pyridine (5 ml), washed with H_2O (3 × 100 ml) and sat. aq. NaCl soln. (3 × 100 ml), dried (Na_2SO_4), and the solvent was evaporated *in vacuo*. The compound was purified by repeated FC (SiO_2; CH_2Cl_2, 1% (*v*/*v*) Et_3N and Al_2O_3; cyclohexane/CH_2Cl_2 98:2, 1% (*v*/*v*) Et_3N). Precipitation from $CHCl_3$ by dropwise addition of hexane afforded **38** (150 mg; quant. yield).

Method B. $Sc(OTf)_3$ (400 mg, 0.81 mmol) and DDQ (200 mg, 0.88 mmol) were added under N_2 to a soln. of **42** (246 mg, 0.29 mmol) in dry PhMe (150 ml). The mixture was heated to reflux for 30 min. After workup (see above), **38** (220 mg, 89%) was obtained. Dark blue powder. M.p. > 300°. UV/VIS ($CHCl_3$): λ_{max} 422 (163100), 464 (59400), 565 (146400), 955 (20500), 1087 (33400). UV/VIS (PhMe): λ_{max} 422 (136000), 460 (45700), 565 (112200), 583 (114700), 649 (23600), 818 (6200), 923 (17900), 1053 (30600). IR (neat): 2961*m*, 2238*w*, 1593*m*, 1476*s*, 1393*w*, 1363*m*, 1345*w*, 1300*m*, 1266*w*, 1247*m*, 1225*w*, 1199*s*, 1074*w*, 1023*m*, 1001*m*, 943*s*, 900*m*, 881*m*, 826*m*, 791*s*, 724*m*, 716*m*, 696*m*, 658*w*. ^{1}H-NMR (500 MHz, $CDCl_3$): 8.09 (*s*, 2 H); 8.03–8.05 (*d*, *J* = 7.8, 2 H); 7.89 (*d*, *J* = 7.8, 2 H); 7.73 (*d*, *J* = 4.7, 4 H); 7.70 (*t*, *J* = 7.8, 2 H); 7.66–7.64 (*m*, 12 H); 7.55 (*d*, *J* = 4.7, 4 H); 7.36 (*s*, 4 H); 1.46 (*s*, 72 H). ^{13}C-NMR ($CDCl_3$, 125 MHz): 154.22; 154.01; 153.70; 152.12; 149.03; 149.01; 142.73; 139.67; 136.74; 135.99; 135.69; 131.99; 131.30; 130.32; 128.35; 128.24; 128.06; 127.86; 126.72; 121.77; 121.07; 117.40; 111.55; 35.00; 31.74. HR-FT-ICR-MALDI-MS (DCTB): 1692.7013 (M^+, $C_{110}H_{104}N_{10}Zn_2^+$; calc. 1692.7007).

*(μ-{10,10′-Bis(3-formylphenyl)-5,5′,15,15′-tetrakis[3,5-di(*tert*-butyl)phenyl]-18,18′:20,20′-dicyclo-2,2′-biporphyrinato(4−)-κN^{21},κN^{22},κN^{23},κN^{24}:κN$^{21'}$,κN$^{22'}$,κN$^{23'}$,κN$^{24'}$}) dizinc(II)* (**43**). To a soln. of **38** (130 mg, 0.077 mmol) in dry CH_2Cl_2 (50 ml), DIBAL-H in hexane (1M, 0.7 ml, 0.7 mmol) was added dropwise at −70°. The cooling bath was removed after 2 h, and the mixture was stirred overnight in the dark at 25°. The reaction was quenched with MeOH, and the org. phase was washed with 1M HCl (3 × 50 ml), H_2O (3 × 50 ml), and sat. aq. NaCl soln. (50 ml), dried (Na_2SO_4), and evaporated *in vacuo*. The resulting solid was purified by repeated FC (SiO_2; CH_2Cl_2/THF 99:1, 1% (*v*/*v*) Et_3N). Precipitation from $CHCl_3$ by dropwise addition of hexane afforded **43** (122 mg, 94%). Dark blue powder. M.p. > 300°. UV/VIS ($CHCl_3$): λ_{max} 419 (160400), 465 (56600), 565 (141600), 950 (17400), 1077 (33400). IR (neat): 2953*m*, 2867*m*, 1806*w*, 1698*w*, 1679*w*, 1593*m*, 1476*m*, 1427*m*, 1392*w*, 1362*m*, 1345*w*, 1299*m*, 1247*m*, 1225*w*, 1200*s*, 1156*m*, 1076*w*, 1023*m*, 1000*m*, 943*m*, 900*m*, 881*m*, 826*m*, 791*s*, 714*m*, 696*w*, 660*w*. ^{1}H-NMR (300 MHz, $CDCl_3$): 10.14 (*s*, 2 H); 8.29 (*s*, 2 H); 8.09 (*m*, 2 H); 7.74 (*m*, 2 H); 7.69–7.65 (*m*, 18 H); 7.57 (*m*, 4 H); 7.32 (*s*, 4 H); 1.46 (*s*, 72 H). ^{13}C-NMR ($CDCl_3$, 75 MHz): 192.68; 154.41; 154.12; 153.90; 152.61; 149.18; 142.66; 140.03; 138.49; 136.16; 135.58; 134.06; 132.01; 130.82; 128.81; 128.55; 128.17; 127.96; 126.81; 123.26; 121.23; 117.53; 35.17; 31.90. HR-FT-ICR-MALDI-MS (DCTB): 1702.7028 (M^+, $C_{110}H_{106}N_8O_2Zn_2^+$; calc. 1702.7011).

*(μ-{10,10′-Bis[3-(hydroxymethyl)phenyl]-5,5′,15,15′-tetrakis[3,5-di(*tert*-butyl)phenyl]-18,18′:20,20′-dicyclo-2,2′-biporphyrinato(4−)-κN^{21},κN^{22},κN^{23},κN^{24}:κN$^{21'}$,κN$^{22'}$,κN$^{23'}$,κN$^{24'}$}) dizinc(II)* (**44**). To a soln. of **43** (122 mg, 0.072 mmol) in dry CH_2Cl_2 (30 ml), DIBAL-H in hexane (1M, 0.7 ml, 0.7 mmol) was added dropwise at −70°. The cooling bath was removed after 2 h, and the mixture was stirred overnight in the dark at 25°. The reaction was quenched with MeOH, and the org. phase was washed with 1M HCl (3 × 50 ml), H_2O (3 × 50 ml), and sat. aq. NaCl soln. (3 × 50 ml). The org. layer was dried (Na_2SO_4), and the solvent was evaporated *in vacuo*. FC (SiO_2; CH_2Cl_2/THF 99:3, 1% (*v*/*v*) Et_3N) and precipitation from $CHCl_3$ by dropwise addition of hexane provided **44** (112 mg, 55%). Black powder. Intermediate **44** was characterized only by ^{1}H-NMR and HR-FT-ICR-MALDI-MS due to its instability in solution. ^{1}H-NMR ($CDCl_3$, 300 MHz): 7.65–7.48 (*m*, 28 H); 7.32 (*s*, 4 H); 4.64 (*s*, 4 H); 1.45 (*s*, 72 H); the OH resonances are missing. HR-FT-ICR-MALDI-MS (DCTB): 1706.7341 (M^+, $C_{110}H_{110}N_8O_2Zn_2^+$; calc. 1706.7324).

*{μ-[10,10′-Bis(3-{[(3-ethoxy-3-oxopropanoyl)oxy]methyl}phenyl)-5,5′,15,15′-tetrakis[3,5-di(*tert*-butyl)-phenyl]-18,18′:20,20′-dicyclo-2,2′-biporphyrinato(4−)-κN^{21},κN^{22},κN^{23},κN^{24}:κN$^{21'}$,κN$^{22'}$,κN$^{23'}$,κN$^{24'}$]}dizinc(II)* (**45**). To a mixture of **44** (30 mg, 0.018 mmol) and Et_3N (1 ml) in CH_2Cl_2 (7 ml), $ClCOCH_2CO_2Et$ (0.1 ml, 0.78 mmol) was added dropwise at 0°. After 15 min, the mixture was allowed to warm to 25° and stirred for 16 h. The mixture was diluted with $CHCl_3$, and the org. phase was washed with H_2O (3 × 20 ml) and sat. aq. NaCl soln. (3 × 20 ml), dried (Na_2SO_4), and the solvent was evaporated *in vacuo*. Repeated FC (SiO_2; CH_2Cl_2/THF 97:3, 1% (*v*/*v*) Et_3N) and precipitation from $CHCl_3$ upon dropwise addition of MeOH afforded **45** (30 mg, 88%). Dark blue powder. M.p. > 300°. UV/VIS ($CHCl_3$): λ_{max} 418 (159400), 464 (48400), 567 (140300), 950 (31400), 1073 (33400). UV/VIS (PhMe): λ_{max} 420 (133800), 460 (48100), 565 (111000), 583 (117200), 649 (23500), 818 (6500), 923 (17900), 1053 (31300). IR (neat): 2960*m*, 1739*m*, 1657*w*, 1592*m*, 1552*w*, 1478*m*, 1426*m*, 1392*w*, 1363*m*, 1298*m*, 1248*m*, 1202*m*, 1144*m*, 1094*m*, 1030*m*, 943*m*, 900*w*, 882*w*, 822*m*, 794*s*, 716*m*, 661*w*. ^{1}H-NMR ($CDCl_3$, 300 MHz): 7.79–7.55 (*m*, 28 H); 7.35 (*s*, 4 H); 5.35 (*s*, 4 H); 4.13 (*q*, *J* = 3.3, 4 H); 3.44 (*s*, 4 H); 1.45 (*s*, 72 H); 1.16 (*t*, *J* = 3.3, 6 H). ^{13}C-NMR ($CDCl_3$, 75 MHz): 166.73 (2×); 159.35; 159.35; 154.28; 153.97;

153.82; 152.88; 149.11; 141.87; 140.09; 136.04; 134.47; 132.87; 132.47; 131.75; 131.23; 128.50; 127.83; 127.62; 126.66; 124.667; 121.17; 67.34; 61.82; 41.87; 35.15; 31.90; 14.22. HR-FT-ICR-MALDI-MS (DCTB): 1934.7989 (M^+, $C_{120}H_{122}N_8O_8Zn_2^+$; calc. 1934.7969).

*[μ-(10,10′-Bis[3-[([3′-(ethoxycarbonyl)-3′*H*-cyclopropa[1,9](C$_{60}$-I$_h$)[5,6]fulleren-3′-yl]carbonyl}oxy)methyl]phenyl]-5,5′,15,15′-tetrakis[3,5-di(*tert*-butyl)phenyl]-18,18′:20,20′-dicyclo-2,2′-biporphyrinato(4 −)-κN^{21},κN^{22},κN^{23},κN^{24}:κN$^{21'}$,κN$^{22'}$,κN$^{23'}$,κN$^{24'}$)]dizinc(II)* (**8**). A soln. of **45** (35 mg, 0.018 mmol) and C_{60} (29 mg, 0.040 mmol) in dry PhMe (30 ml) was deoxygenated by bubbling N_2 through for 20 min. I_2 (10 mg, 0.04 mmol) and DBU (0.035 ml, 0.12 mmol) were then added at 0° in the dark. The reaction was monitored by TLC (SiO_2; PhMe). When all of **45** was consumed, the mixture was quickly filtered through a short plug (Al_2O_3; $CHCl_3$). Purification of the product was achieved *via* prep. size-exclusion chromatography (*Bio-Rad Bio-Beads S-X1*) with PhMe as eluent. Repeated precipitations from $CHCl_3$ upon addition of hexane and extensive washing of the precipitate with hexane, MeOH, and Et_2O provided **8** (25 mg, 41%). M.p. >300°. UV/VIS ($CHCl_3$): λ_{max} 259 (241200), 329 (89600), 424 (106300), 581 (106700), 1084 (26200). UV/VIS (PhMe): λ_{max} 332 (121900), 423 (124300), 461 (50300), 568 (112400), 584 (123400), 656 (25600), 814 (7300), 931 (19500), 1063 (34200). IR (neat): 2958*m*, 1749*m*, 1591*w*, 1477*m*, 1363*m*, 1230*s*, 1203*s*, 1095*w*, 1001*m*, 943*m*, 882*w*, 826*w*, 714*m*, 661*w*. ^{1}H-NMR (500 MHz, $CDCl_3$): 7.83–7.46 (*m*, 28 H); 7.25 (*s*, 4 H); 5.73 (*s*, 4 H); 4.47 (*m*, 4 H); 1.40–1.54 (*m*, 78 H). ^{13}C-NMR ($CDCl_3$, 125.75 MHz): 163.57; 163.42; 154.06; 153.57; 153.45; 152.43; 148.80; 144.78–127.39 broad signals of fullerene and porphyrin C(sp^2)-atoms; 126.40; 124.31; 120.98; 117.12; 70.86; 68.35; 63.46; 52.74; 34.87; 31.70; 14.22. HR-FT-ICR-MALDI-MS (DCTB): 3371.7749 (M^+, $C_{240}H_{118}N_8O_8Zn_2^+$; calc. 3371.7698).

*{5,15-Bis(3-cyanophenyl)-10,20-bis[3,5-di(*tert*-butyl)phenyl]porphyrinato(2 −)-κN^{21},κN^{22},κN^{23},κN^{24}}zinc(II)* (**46**). Compound **46** was synthesized as described for **42**. Compound **16** (380 mg, 0.38 mmol), dry PhMe (100 ml), **39** (525 mg, 2.29 mmol), [Pd(PPh_3)$_4$] (105 mg, 0.090 mmol), Cs_2CO_3 (2030 mg, 11.50 mmol), and three drops of H_2O. After workup, **46** (238 mg, 66%) was obtained. Red solid. M.p. >300°. UV/VIS ($CHCl_3$): λ_{max} 427 (204200), 555 (7560). IR (neat): 2964*m*, 2235*w*, 1593*m*, 1476*w*, 1392*w*, 1362*w*, 1338*w*, 1292*w*, 1247*w*, 1206*w*, 1069*w*, 1004*s*, 922*w*, 900*w*, 882*m*, 819*m*, 803*m*, 797*s*, 757*m*, 730*w*, 716*s*, 699*m*, 666*w*, 614*w*. ^{1}H-NMR ($CDCl_3$, 300 MHz): 9.05 (*d*, *J* = 4.3, 4 H); 8.83 (*d*, *J* = 4.3, 4 H); 8.49 (*m*, 4 H); 8.09 (*s*, 4 H); 791–7.82 (*m*, 6 H); 1.54 (*s*, 36 H). ^{13}C-NMR ($CDCl_3$, 75 MHz): 150.74; 149.56; 148.74; 148.66; 144.12; 141.19; 137.92; 136.88; 133.03; 131.24; 129.80; 127.43; 123.31; 121.02; 118.95; 118.00; 111.04; 35.17; 31.85. HR-FT-ICR-MALDI-MS (DCTB): 950.4001 (M^+, $C_{62}H_{58}N_6Zn^+$; calc. 950.4010). X-Ray: see *Fig. 6*.

*{5,15-Bis[3,5-di(*tert*-butyl)phenyl]-10,20-bis[3-(hydroxymethyl)phenyl]porphyrinato(2 −)-κN^{21},κN^{22},κN^{23},κN^{24}}zinc(II)* (**47**). To a 250-ml round-bottomed flask charged with a crude mixture of **15** and **16** (200 mg, **15**/**16** *ca.* 1:1) in dry PhMe (15 ml), **19** (120 mg, 0.35 mmol), [Pd(Ph_3P)$_4$] (23 mg, 2×10^{-2} mmol), and Cs_2CO_3 (644 mg, 1.83 mmol) were added. The mixture was deoxygenated by bubbling N_2 through for 30 min and then heated to reflux for 18 h. After cooling to 25°, the suspension was filtered through *Celite* and SiO_2 (cyclohexane/CH_2Cl_2 1:1), and the solvent was evaporated *in vacuo*. The crude mixture was charged in a 50-ml round-bottomed flask with THF (15 ml) together with several drops of a 1M soln. of Bu_4NF in THF at 0°. The soln. was stirred for 30 min at 0° and 1 h at 25°. When all starting material was consumed, the mixture was diluted with $CHCl_3$ (10 ml) and quenched with H_2O. The org. layer was washed with H_2O (3 × 50 ml) and sat. aq. NaCl soln. (3 × 50 ml), dried (Na_2SO_4), and the solvent was evaporated *in vacuo*. FC (SiO_2; cyclohexane/CH_2Cl_2 1:1) afforded three fractions corresponding to **14**, **20**, and **47**. Precipitation of the chromatographic fractions from $CHCl_3$ upon addition of MeOH/H_2O 9:1 afforded **20** (160 mg) and **47** (154 mg). Red solid. M.p. >300°. UV/VIS ($CHCl_3$): λ_{max} 304 (12100), 419 (449000), 546 (17000). IR (neat): 2963*m*, 1592*m*, 1475*m*, 1423*m*, 1392*w*, 1363*m*, 1337*m*, 1289*w*, 1247*m*, 1207*m*, 1069*w*, 1042*m*, 1001*s*, 931*m*, 901*m*, 882*m*, 847*w*, 823*m*, 792*s*, 776*s*, 717*s*, 668*m*. ^{1}H-NMR ($CDCl_3$, 300 MHz): 8.99 (*d*, *J* = 4.6, 4 H); 8.89 (*d*, *J* = 4.6, 4 H); 8.14–8.04 (*m*, *J* = 1.8, 8 H); 7.80 (*t*, *J* = 1.8, 2 H); 7.70–7.63 (*m*, 4 H); 4.67 (br. *s*, 4 H); 1.53 (*s*, 36 H); the OH resonances are missing. ^{13}C-NMR ($CDCl_3$, 75 MHz): 150.31; 149.96; 148.43; 143.28; 142.18; 139.53; 133.32; 132.86; 131.99; 131.70; 129.82; 126.39; 125.70; 122.09; 120.64; 120.56; 64.71; 35.01; 31.72. HR-FT-ICR-MALDI-MS (DHB): 960.4306 (100, M^+, $C_{62}H_{64}N_4O_2Zn^+$; calc. 960.4315). Anal. calc. for $C_{62}H_{64}N_4O_2Zn$ (962.60): C 77.20, H 6.90, N 5.81; found: C 76.98, H 6.79, N 5.74. X-Ray: see *Fig. 7*.

X-Ray Crystal Structures. Crystallographic data (excluding structure factors) for the structures reported in this paper have been deposited with the *Cambridge Crystallographic Data Centre* (*CCDC*). Copies of the data can be obtained, free of charge, on application to the *CCDC*, 12 Union Road, Cambridge CB2 1EZ UK (fax: +44 (1223) 336 033; e-mail:deposit@ccdc.cam.ac.uk).

Compound **21**. Crystal data at 223 K for $C_{96}H_{102}N_8Zn_2 \cdot 5$ MeOH (M_r = 1658.81): triclinic, space group $P\bar{1}$ (no. 2), D_c = 1.169 g cm^{-3}, Z = 2, a = 14.2737(3) Å, b = 16.5177(3) Å, c = 21.3353(4) Å, α = 70.85(1)°, β = 82.64(1)°, γ = 88.98(1)°, V = 4711.1(4) Å^3. *Bruker-Nonius Kappa-CCD* diffractometer, MoK_α radiation, λ =

0.7107 Å. A dark-red crystal obtained by evaporation of a MeOH soln. (linear dimensions *ca.* $0.2 \times 0.1 \times 0.08$ mm) was mounted at low temp. to prevent evaporation of enclosed solvents. The structure was solved by direct methods (SIR92) [45] and refined by full-matrix least-squares analysis (SHELXL-97) [46], using an isotropic extinction correction, and $w = 1/[\sigma^2(F_o^2) + (0.107P)^2 + 15.945P]$, where $P = (F_o^2 + 2F_c^2)/3$. The Me_3C-group at C(95) is disordered over two orientations. For C(98), C(99), and C(100), two sets of atomic parameters were refined with population parameters of 0.6 and 0.4 resp. In *Fig. 2*, only one orientation is shown for clarity. In addition, one of the five solvent molecules included in the crystal packing is also disordered. All heavy atoms were refined anisotropically (H-atoms of the ordered skeleton isotropically, whereby H-positions are based on stereochemical considerations). Final $R(F) = 0.081$, $wR(F^2) = 0.202$ for 1156 parameters and 11623 reflections with $I > 2\sigma(I)$ and $4.42 < \theta < 25.01°$ (corresponding *R*-values based on all 16236 reflections are 0.114 and 0.225, resp.). CCDC-259270.

Compound **42**. Crystal data at 173 K for $C_{55}H_{55}N_5Zn \cdot MeOH \cdot CHCl_3$ ($M_r = 1002.82$): monoclinic, space group $P2_1/n$ (no. 4), $D_c = 1.236$ g cm^{-3}, $Z = 4$, $a = 21.8235(8)$ Å, $b = 10.1234(5)$ Å, $c = 24.4990(9)$ Å, $\beta = 95.526(1)°$, $V = 5387.4(3)$ Å^3. *Bruker-Nonius Kappa-CCD* diffractometer, MoK_α radiation, $\lambda = 0.7107$ Å. A dark-red crystal, obtained by evaporation of a MeOH/$CHCl_3$ soln. (linear dimensions *ca.* $0.15 \times 0.13 \times 0.1$ mm) was mounted at low temp. to prevent evaporation of enclosed solvents. The structure was solved by direct methods (SIR92) [45] and refined by full-matrix least-squares analysis (SHELXL-97) [46], using an isotropic extinction correction, and $w = 1/[\sigma^2(F_o^2) + (0.090P)^2 + 19.305P]$, where $P = (F_o^2 + 2F_c^2)/3$. All heavy atoms were refined anisotropically (H-atoms isotropically, whereby H-positions are based on stereochemical considerations). Final $R(F) = 0.096$, $wR(F^2)^= 0.220$ for 661 parameters and 5874 reflections with $I > 2\sigma(I)$ and $1.31 < \theta$ 24.99° (corresponding *R*-values based on all 9370 reflections are 0.153 and 0.253, resp.). CCDC-259271.

Compound **47**. Crystal data at 203(2) K for 1.5 $C_{62}H_{66}N_4O_2Zn \cdot 4$ MeOH ($M_r = 1575.01$): triclinic, space group $P\bar{1}$ (no. 2), $D_c = 1.137$ g cm^{-3}, $Z = 2$, $a = 10.6155(4)$ Å, $b = 19.3518(8)$ Å, $c = 22.8967(9)$ Å, $\alpha = 93.007(2)°$, $\beta = 101.018(2)°$, $\gamma = 93.451(2)°$, $V = 4598.7(3)$ Å^3. *Bruker-Nonius Kappa-CCD* diffractometer, MoK_α radiation, $\lambda = 0.7107$ Å. A dark-red crystal obtained by evaporation of a MeOH soln. (linear dimensions *ca.* $0.2 \times 0.18 \times 0.14$ mm) was mounted at low temp. to prevent evaporation of enclosed solvents. The structure was solved by direct methods (SIR92) [45] and refined by full-matrix least-squares analysis (SHELXL-97) [46], using an isotropic extinction correction, and $w = 1/[\sigma^2(F_o^2) + (0.183P)^2 + 13.488P]$, where $P = (F_o^2 + 2F_c^2)/3$. There are two independent molecules in the asymmetric unit. One is in general position (molecule A), the other sits on an inversion center (molecule B with (′) primed atoms, see *Fig. 7*). The subunits C(45)–O(46) and C(61)–C(62) until O(68) of molecule A are disordered. The disorder could be resolved partly for O(46), and C(67)–O(68), *i.e.*, two sets of atomic parameters were refined with population parameters of 0.7, 0.3, and 0.5, 0.5, resp. In *Fig. 7*, only one orientation is shown for clarity. In addition, two of the four solvent molecules included in the crystal packing are also disordered over two orientations. All heavy atoms were refined anisotropically, except C(63) until C(68), and those of the disordered solvents. H-Atoms of the ordered skeleton were refined isotropically, whereby H-positions are based on stereochemical considerations. Final $R(F) = 0.107$, $wR(F^2) = 0.274$ for 1001 parameters and 8798 reflections with $I > 2\sigma(I)$ and $1.06 < \theta < 22.97°$ (corresponding *R*-values based on all 12191 reflections are 0.143 and 0.318, resp.). CCDC-259272.

REFERENCES

[1] D. Holten, D. F. Bocian, J. S. Lindsey, *Acc. Chem. Res.* **2002**, *35*, 57; D. Gust, T. A. Moore, A. L. Moore, *Acc. Chem. Res.* **2001**, *34*, 40; A. K. Burrell, D. L. Officer, P. G. Plieger, D. C. W. Reid, *Chem. Rev.* **2001**, *101*, 2751; D. Gust, T. A. Moore, A. L. Moore, *Pure Appl. Chem.* **1998**, *70*, 2189.

[2] H. Imahori, N. V. Tkachenko, V. Vehmanen, K. Tamaki, H. Lemmetyinen, Y. Sakata, S. Fukuzumi, *J. Phys. Chem. A* **2001**, *105*, 1750.

[3] D. M. Guldi, M. Prato, *Acc. Chem. Res.* **2000**, *33*, 695; J.-F. Nierengarten, J.-F. Eckert, D. Felder, J.-F. Nicoud, N. Armaroli, G. Marconi, V. Vicinelli, C. Boudon, J.-P. Gisselbrecht, M. Gross, G. Hadziioannou, V. Krasnikov, L. Ouali, L. Echegoyen, S.-G. Liu, *Carbon* **2000**, *38*, 1587; J. F. Nierengarten, N. Armaroli, G. Accorsi, Y. Rio, J.-F. Eckert, *Chem.–Eur. J.* **2003**, *9*, 37.

[4] S. K. Khan, A. M. Oliver, M. N. Paddon-Row, Y. Rubin, *J. Am. Chem. Soc.* **1993**, *115*, 4919.

[5] P. A. Liddell, J. P. Sumida, A. N. Macpherson, L. Noss, G. R. Seely, K. N. Clark, A. L. Moore, T. A. Moore, D. Gust, *Photochem. Photobiol.* **1994**, *60*, 537.

[6] D. Gust, T. A. Moore, A. L. Moore, D. Kuciauskas, P. A. Liddell, B. D. Halbert, *J. Photochem. Photobiol. B* **1998**, *43*, 209; H. Imahori, *Org. Biomol. Chem.* **2004**, *2*, 1425; H. Imahori, *J. Phys. Chem. B* **2004**, *108*, 6130;

N. Armaroli, in 'Fullerenes: from synthesis to optoelectronic properties', Eds. D. M. Guldi, N. Martin, Kluwer Academic Publishers, Dordrecht, 2002, p. 137; N. Armaroli, *Photochem. Photobiol. Sci.* **2003**, *2*, 73; D. M. Guldi, A. Hirsch, M. Scheloske, E. Dietel, A. Troisi, F. Zerbetto, M. Prato, *Chem.–Eur. J.* **2003**, *9*, 4968; S. D. Straight, J. Andréasson, G. Kodis, A. L. Moore, T. A. Moore, D. Gust, *J. Am. Chem. Soc.* **2005**, *127*, 2717.

[7] F. Diederich, C. O. Dietrich-Buchecker, J.-F. Nierengarten, J. P. Sauvage, *Chem. Commun.* **1995**, 781; N. Armaroli, F. Diederich, C. O. Dietrich-Buchecker, L. Flamigni, G. Marconi, J.-F. Nierengarten, J.-P. Sauvage, *Chem.–Eur. J.* **1998**, *4*, 406

[8] a) J.-P. Bourgeois, F. Diederich, L. Echegoyen, J.-F. Nierengarten, *Helv. Chim. Acta* **1998**, *81*, 1835; b) N. Armaroli, G. Marconi, L. Echegoyen, J.-P. Bourgeois, F. Diederich, *Chem.–Eur. J.* **2000**, *6*, 1629.

[9] D. Bonifazi, F. Diederich, *Chem. Commun.* **2002**, 2178.

[10] D. Bonifazi, M. Scholl, F. Y. Song, L. Echegoyen, G. Accorsi, N. Armaroli, F. Diederich, *Angew. Chem.* **2003**, *115*, 5116; *Angew. Chem., Int. Ed.* **2003**, *42*, 4966.

[11] A. Tsuda, A. Osuka, *Science* **2001**, *293*, 79.

[12] A. Tsuda, A. Osuka, *Adv. Mater.* **2002**, *14*, 75.

[13] A. Osuka, H. Shimidzu, *Angew. Chem.* **1997**, *109*, 93; *Angew. Chem., Int. Ed.* **1997**, *35*, 135; N. Aratani, A. Osuka, *Chem. Rec.* **2003**, *3*, 225.

[14] A. Tsuda, H. Furuta, A. Osuka, *Angew. Chem.* **2000**, *112*, 2649; *Angew. Chem., Int. Ed.* **2000**, *39*, 2549; A. Nakano, T. Yamazaki, Y. Nishimura, I. Yamazaki, A. Osuka, *Chem.–Eur. J.* **2000**, *2000*, 3254; N. Aratani, A. Osuka, Y. H. Kim, D. H. Jeong, D. Kim, *Angew. Chem.* **2000**, *112*, 1517; *Angew. Chem., Int. Ed.* **2000**, *39*, 1458.

[15] H. S. Cho, D. H. Jeong, S. Cho, D. Kim, Y. Matsuzaki, K. Tanaka, A. Tsuda, A. Osuka, *J. Am. Chem. Soc.* **2002**, *124*, 14642.

[16] H. S. Cho, H. Rhee, J. K. Song, C. K. Min, M. Takase, N. Aratani, S. Cho, A. Osuka, T. Joo, D. Kim, *J. Am. Chem. Soc.* **2003**, *125*, 5849.

[17] N. Aratani, A. Osuka, H. S. Cho, D. Kim, *J. Photochem. Photobiol. C: Photochem. Rev.* **2002**, *3*, 25; N. Aratani, H. S. Cho, T. K. Ahn, S. Cho, D. Kim, H. Sumi, A. Osuka, *J. Am. Chem. Soc.* **2003**, *125*, 9668; Y. H. Kim, D. H. Jeong, D. Kim, S. C. Jeoung, H. S. Cho, S. K. Kim, N. Aratani, A. Osuka, *J. Am. Chem. Soc.* **2001**, *123*, 76.

[18] D. Kim, A. Osuka, *J. Phys. Chem. A* **2003**, *107*, 8791.

[19] I. M. Blake, A. Krivokapic, M. Katterle, H. L. Anderson, *Chem. Commun.* **2002**, 1662; K. J. McEwan, P. A. Fleitz, J. E. Rogers, J. E. Slagle, D. G. McLean, H. Akdas, M. Katterle, I. M. Blake, H. L. Anderson, *Adv. Mater.* **2005**, *16*, 1933; H. Imahori, Y. Sekiguchi, Y. Kashiwagi, T. Sato, Y. Araki, O. Ito, H. Yamada, S. Fukuzumi, *Chem.–Eur. J.* **2004**, *10*, 3184.

[20] I. M. Blake, H. L. Anderson, J. L. Beljonne, J.-L. Brédas, W. Clegg, *J. Am. Chem. Soc.* **1998**, *120*, 10764; K. M. Smith, in 'Porphyrins and Metalloporphyrins', Ed. K. M. Smith, Elsevier, Amsterdam, 1978, p. 29; P. D. Rao, B. J. Littler, G. R. Geier, J. S. Lindsey, *J. Org. Chem.* **2000**, *65*, 1084; P. D. Rao, S. Dhanalekshmi, B. J. Littler, J. S. Lindsey, *J. Org. Chem.* **2000**, *65*, 7323; J. B. Paine III, in 'The Porphyrins', Vol. 1, Ed. D. Dolphin, Academic Press, New York, 1978, p. 101.

[21] A. Osuka, N. Tanabe, S. Nakajima, K. Maruyama, *J. Chem. Soc., Perkin Trans. 2* **1996**, 199; J. S. Lindsey, S. Prathapan, T. E. Johnson, R. W. Wagner, *Tetrahedron* **1994**, *50*, 8941.

[22] G. P. Arsenault, E. Bullock, S. F. MacDonald, *J. Am. Chem. Soc.* **1960**, *82*, 4384; T. D. Lash, *Chem.–Eur. J.* **1996**, *2*, 1197; C.-H. Lee, J. S. Lindsey, *Tetrahedron* **1994**, *50*, 11427; B. Felber, F. Diederich, *Helv. Chim. Acta.* **2005**, *88*, 120.

[23] M. O. Senge, W. W. Kalisch, I. Bischoff, *Chem.–Eur. J.* **2000**, *6*, 2721; P. Weyermann, J. P. Gisselbrecht, C. Boudon, F. Diederich, M. Gross, *Angew. Chem.* **1999**, *111*, 3400; *Angew. Chem., Int. Ed.* **1999**, *38*, 3215; A. G. Hyslop, M. A. Kellett, P. M. Iovine, M. J. Therien, *J. Am. Chem. Soc.* **1998**, *120*, 12676.

[24] P. Weyermann, F. Diederich, J. P. Gisselbrecht, C. Boudon, M. Gross, *Helv. Chim. Acta* **2002**, *85*, 571.

[25] B. J. Littler, M. A. Miller, C.-H. Hung, R. W. Wagner, D. F. O'Shea, P. D. Boyle, J. S. Lindsey, *J. Org. Chem.* **1999**, *64*, 1391.

[26] P. J. Skinner, A. G. Cheetham, A. Beeby, V. Gramlich, F. Diederich, *Helv. Chim. Acta* **2001**, *84*, 2146.

[27] S. G. DiMagno, V. S.-Y. Lin, M. J. Therien, *J. Am. Chem. Soc.* **1993**, *115*, 2513.

[28] D. P. Arnold, R. C. Bott, H. Eldridge, F. M. Elms, G. Smith, M. Zojaji, *Aust. J. Chem.* **1997**, *50*, 495.

[29] A. Nakano, H. Shimidzu, A. Osuka, *Tetrahedron Lett.* **1998**, *39*, 9489.

[30] A. Suzuki, *J. Organomet. Chem.* **1999**, *576*, 147; N. Miyaura, in 'Metal-Catalyzed Cross-Coupling Reactions', Vol. 1, 2nd edn., Eds. A. de Meijere, F. Diederich, Wiley-VCH, 2004, p. 41.

[31] C. A. Hunter, J. K. M. Sanders, *J. Am. Chem. Soc.* **1990**, *112*, 5525.
[32] M. Nakash, Z. Clyde-Watson, N. Feeder, S. J. Teat, J. K. M. Sanders, *Chem.–Eur. J.* **2000**, *6*, 2112.
[33] L. Sebo, F. Diederich, V. Gramlich, *Helv. Chim. Acta* **2000**, *83*, 93.
[34] D. Bonifazi, H. Spillmann, A. Kiebele, M. de Wild, P. Seiler, F. Cheng, H.-J. Guntherodt, T. Jung, F. Diederich, *Angew. Chem.* **2004**, *116*, 4863; *Angew. Chem., Int. Ed.* **2004**, *43*, 4759.
[35] M. O. Senge, M. Speck, A. Wiehe, H. Dieks, S. Aguirre, H. Kurreck, *Photochem. Photobiol.* **1999**, *70*, 206.
[36] D. V. Konarev, I. S. Neretin, Y. L. Slovokhotov, E. I. Yudanova, N. V. Drichko, Y. M. Shul'ga, B. P. Tarasov, L. L. Gumanov, A. S. Batsanov, J. A. K. Howard, R. N. Lyubovskaya, *Chem.–Eur. J.* **2001**, *7*, 2605; D. Sun, F. S. Tham, C. A. Reed, L. Chaker, P. D. W. Boyd, *J. Am. Chem. Soc.* **2002**, *124*, 6604; J.-Y. Zheng, K. Tashiro, Y. Hirabayashi, K. Kinbara, K. Saigo, T. Aida, S. Sakamoto, K. Yamaguchi, *Angew. Chem.* **2001**, *113*, 1909; *Angew. Chem., Int. Ed.* **2001**, *40*, 1857; D. M. Guldi, T. Da Ros, P. Braiuca, M. Prato, E. Alessio, *J. Mat. Chem.* **2002**, *12*, 2001.
[37] J. Sandström, 'Dynamic NMR Spectroscopy', Academic Press, London, 1982.
[38] S. S. Eaton, G. R. Eaton, *J. Am. Chem. Soc.* **1977**, *99*, 6594.
[39] A. Graja, I. Olejniczak, A. Bogucki, D. Bonifazi, F. Diederich, *Chem. Phys.* **2004**, *300*, 227.
[40] N. Armaroli, G. Accorsi, F. Song, A. Palkar, L. Echegoyen, D. Bonifazi, F. Diederich, *ChemPhysChem* **2005**, *6*, 732.
[41] A. Gilbert, J. Baggott, 'Essentials of Molecular Photochemistry', Blackwell Scientific Publications, Oxford, 1991, p. 111.
[42] N. Armaroli, G. Accorsi, D. Felder, J.-F. Nierengarten, *Chem.–Eur. J.* **2002**, *8*, 2314; N. Armaroli, G. Accorsi, J.-P. Gisselbrecht, M. Gross, V. Krasnikov, D. Tsamouras, G. Hadziioannou, M. J. Gomez-Escalonilla, F. Langa, J. F.-Eckert, J.-F. Nierengarten, *J. Mater. Chem.* **2002**, *12*, 2077.
[43] F. Wilkinson, W. P. Helman, A. B. Ross, *J. Phys. Chem. Ref. Data* **1995**, *24*, 663.
[44] Y. Rio, G. Accorsi, H. Nierengarten, C. Bourgogne, J.-M. Strub, A. Van Dorsselaer, N. Armaroli, J. F. Nierengarten, *Tetrahedron* **2003**, *59*, 3833.
[45] A. Altomare, G. Cascarano, C. Giacovazzo, A. Guagliardi, M. C. Burla, G. Polidori, M. Camalli, *J. Appl. Crystallogr.* **1994**, *27*, 435.
[46] G. M. Sheldrick, 'SHELXL-97 Program for the Refinement of Crystal Structures', University of Göttingen, Germany, 1997.

Received March 2, 2005